UNIL | Université de Lausanne
Faculté de biologie
et de médecine

Laboratoire de Biologie et Génétique des Tumeurs Cérébrales
Département des Neurosciences Cliniques, Service de Neurochirurgie
Centre Hospitalier Universitaire Vaudois (CHUV)

BET inhibitors: A novel epigenetic approach to tackle glioblastoma treatment resistance

Thèse de doctorat ès sciences de la vie (PhD)

présentée à la

Faculté de biologie et de médecine
de l'Université de Lausanne

par

Alessandro Tancredi

Master of Science in Experimental Biomedical Research
Université de Fribourg (Suisse, 2018)

Jury

Prof. Johanna Joyce, Présidente
Prof. Monika Hegi, Directrice de thèse
Prof. Francesco Bertoni, expert
Dr PD Olivier Dormond, expert

Lausanne 2022

UNIL | Université de Lausanne
Faculté de biologie et de médecine

Ecole Doctorale
Doctorat ès sciences de la vie

Imprimatur

Vu le rapport présenté par le jury d'examen, composé de

Président·e	Madame	Prof.	Johanna	**Joyce**
Directeur·trice de thèse	Madame	Prof.	Monika	**Hegi**
Expert·e·s	Monsieur	Prof.	Francesco	**Bertoni**
	Monsieur	Dr	Olivier	**Dormond**

le Conseil de Faculté autorise l'impression de la thèse de

Alessandro Tancredi

Master - Msc in experimental biomedical research, Université de Fribourg, Suisse

intitulée

BET inhibitors: A novel epigenetic approach to tackle glioblastoma treatment resistance

Lausanne, le 1 avril 2022

pour le Doyen
de la Faculté de biologie et de médecine

Joyce

Prof. Johanna Joyce

"We can only see a short distance ahead, but we can see plenty there that needs to be done."

Alan Turing, 1950.

ACKNOWLEDGEMENTS

First of all, I would like to express my profound and sincere gratitude to Prof. Monika Hegi for the opportunity and privilege to have worked with her. I am grateful for her constant guidance throughout my PhD, for sharing her tremendous knowledge in the field, and for her continuous financial support over the years. She transmitted to me her immense passion and commitment, together with discipline and resilience. Additionally, I would like to thank her for strongly encouraging inclusion, diversity, and equity in the lab - a beneficial, constructive, and valuable asset in a workplace.

Moreover, I would like to thank all lab members that contributed to this work. In particular, Olga Gusyatiner for her guidance, support, and preliminary work that initiated this project. Pierre Bady for his input on data analysis and for sharing his biostatistics expertise. Many thanks to Michelle Buri (Intern), Julia Laube and Rémy Lomazzi (Master students), and Davide Chiesi (PhD student) for their contribution to some experiments presented here and for creating a friendly and pleasant work environment.

Additionally, I would like to thank the many UNIL/CHUV facilities, labs, and individuals that assisted and contributed to this work. I would also like to express my gratitude to the jury members Prof Johanna Joyce, Prof Francesco Bertoni, and Dr Olivier Dormond for being part of the committee and their valuable scientific support.

On this unique occasion, I would like to especially thank my parents for their endless love and support, for educating me with solid principles, valuing integrity and morality above everything else, and allowing me to independently find my own path in life. Thanks also to my little brother for always being present and supportive.

With a deep sense of gratitude, I would also like to thank my boyfriend for being extraordinarily supportive, caring and loving. His courage, resilience, determination, and optimism helped me reach this outstanding achievement and enrich my life constantly.

Last but not least, I would like to thank my friends, with whom I celebrated good times and significantly supported me during “less good” ones.

Thank you!

ABSTRACT

Bromodomain and extra-terminal tail (BET) proteins have been identified as potential epigenetic targets in different cancers, including glioblastoma (GBM), the most common and malignant primary brain tumor in adults. BET proteins are epigenetic modifier proteins that recognize acetylated lysines on histone tails and promote the signal downstream by linking the histone code to gene transcription.

Differential gene expression profiling of GBM-derived spheres in our laboratory revealed significant downregulation of cancer-relevant genes upon BET inhibitor (BETi) treatment. Interestingly, the O-6-methylguanine-DNA methyltransferase gene (*MGMT*) was among them. MGMT is a DNA repair enzyme whose function is to remove alkyl-groups from the O6-position of guanine, thereby blunting the treatment effect of alkylating drugs such as temozolomide. Hence, BETi mediated downregulation of MGMT expression may sensitize GBM patients with an unmethylated *MGMT* promoter to temozolomide treatment, which is part of the current standard of care.

We investigated the effect of BETi on MGMT expression and other clinically relevant DNA damage repair genes involved in GBM, and explored respective underlying mechanisms.

We observed that the use of BETi on GBM lines directly reduced MGMT expression and inhibited its induction, typically observed upon temozolomide treatment. Moreover, we reported that BETi treated GBM cells were significantly more sensitive to temozolomide treatment compared to single-agent therapy.

Therefore, the addition of BET-inhibitors in combination with the current standard of care may improve overall survival of GBM patients with an unmethylated *MGMT* promoter (about 45% of total GBM cases).

RÉSUMÉ

Les protéines bromodomain and extra-terminal tail (BET) sont une potentielle cible de thérapie épigénétique pour le traitement de divers types de cancers. Parmi les cancers investigués, le glioblastome (GBM) est chez les adultes la tumeur cérébrale primaire la plus commune et la plus maligne.

Les protéines BET sont considérées comme des protéines modifiant l'épigénome. En effet, de par leur capacité à reconnaître les lysines acétylées des résidus de queues d'histone et celle de promouvoir la signalisation transcriptionnelle en aval, elles permettent de tisser un lien entre l'encodage des histones et la transcription des gènes.

Grâce aux études menées par notre laboratoire sur des sphères dérivées de GBM, nous avons pu révéler par profilage d'expression génique différentielle que les inhibiteurs de BET (BETi) peuvent diminuer de manière significative l'expression de gènes liés au cancer. Parmi ceux-ci figure le gène de la O-6-méthylguanine-ADN méthyltransférase (*MGMT*), qui est une enzyme de réparation de l'ADN dont la fonction est de retirer les groupes alkyles de la position O6 de la guanine, ce qui atténue l'effet thérapeutique des médicaments alkylants tels que le témozolomide. Par conséquent, la réduction de l'expression de *MGMT* médiée par les BETi pourrait sensibiliser les patients atteints de GBM présentant un promoteur non méthylé de *MGMT* au traitement par témozolomide, lequel constitue le fondement du traitement standard actuel. Ainsi, nous avons étudié l'effet de BETi sur l'expression de *MGMT* et d'autres gènes cliniquement pertinents de réparation des dommages de l'ADN impliqués dans les GBM et avons exploré le mécanisme sous-jacent de ce type de composé. Au travers de cette étude, nous avons observé que l'utilisation de BETi sur des lignées cellulaires de GBM réduisait directement l'expression de *MGMT* et inhibait son induction habituellement observée lors de traitements au témozolomide. De plus, nous constatons que les cellules de GBM traitées par BETi sont significativement plus sensibles au traitement par temozolomide qu'au traitement en monothérapie.

Par conséquent, le recours aux inhibiteurs de BET en association avec le traitement standard actuel pourrait améliorer la survie globale des patients atteints de GBM dont le promoteur *MGMT* n'est pas méthylé (soit environ 45 % de l'ensemble des cas de GBM).

LIST OF ABBREVIATIONS

2HG	2-hydroxyglutarate
5-ALA	Five-aminolevulinic acid
AEs	Adverse events
APCs	Antigen-presenting cells
BBB	Blood-Brain Barrier
BD1 and BD2	Bromodomain motifs
BER	Base Excision Repair
BET	Bromodomain and extra-terminal tail proteins
BETi	Bromodomain and extra-terminal tail proteins inhibitors
CCLE	The Cancer Cell Line Encyclopedia
CNS	Central Nervous System
CR	Complete response
CTD	Carboxyl-terminus domain
DNMTi	DNA methylation inhibitors
DOX	Doxycycline
DSB	Double-strand breaks
EGFRamp	EGFR amplification
ET	Extraterminal domain
EZH2i	Enhancer of zeste homolog 2 inhibitors
FBS	Fetal Bovine Serum
FDA	Food and Drug Administration
gamma-H2AX	Phosphorylation of the histone H2AX
GBM	Glioblastoma
G-CIMP	Gliomas CpG Island Methylator Phenotype
GS	Patient-derived glioblastoma sphere
GTR	Gross total resection
H3K27me3	Trimethylation of Lys-27 in histone 3
H3K9	Histone H3 lysine 9
HADACs	Histone deacetylases
HDACi	Histone deadetylase inhibitors

HEXIM1	Hexamethylene Bisacetamide Inducible 1
HR	Homologous Recombination
IDH	Isocitrate dehydrogenase
IDHmt	Isocitrate dehydrogenase mutant
LB	Luria-Bertani
LGG	Low-grade glioma
MeCP2	Methyl-CpG binding protein 2
MGMT	O-6-methylguanine-DNA methyltransferase
miRNAs	microRNAs
MMR	Mismatch Repair
MRI	Magnetic resonance imaging
MSH2	MutS Homolog 2
MSH6	MutS Homolog 6
MTIC	5-(3-methyltriazen-1-yl) imidazole-4-carboxamide
mtIDHi	Inhibitors of mutant IDH
NHEJ	non-homologous end-joining
NMC	NUT midline carcinoma
ns	not significant
NUT	Nuclear protein in testis
O6BG	O^6-benzylguanine
OS	Overall Survival
P/E	promoter/enhancer
PD	Pharmacodynamic
PFS	Progression-free survival
PR	Partial response
PROTACs	Protein proteolysis-targeting chimera
P-TEFb	Positive transcription elongation factor b
pTERTmut	TERT gene promoter mutation
PTM	Post-translational modifications
PUMA	p53 upregulated modulator of apoptosis
Rb	Retinoblastoma
RNAP II	RNA polymerase II
RT	Radiotherapy

RT	Room temperature
RTKs	Receptor tyrosine kinases
SD	Stable disease
SD	Standard deviation
SRS	Stereotactic radiosurgery
STR	Subtotal resection
TMZ	Temozolomide
TTFields	Tumor Treating Fields
TUJ1	Beta-III tubulin
α-KG	Isocitrate to alpha-ketoglutarate

TABLE OF CONTENTS

TABLE OF FIGURES

LIST OF TABLES

1. INTRODUCTION

1.1 Classification of adult diffuse gliomas

Gliomas are the most common primary brain tumors in adults, accounting for almost 30% of all primary brain tumors and 80% of all malignant ones [9]. Traditionally, this highly heterogeneous group of tumors was classified based on histological evaluation. Gliomas can morphologically resemble astrocytes, oligodendrocytes, oligo-astrocytes, or ependymal cells; thus, they can be classified into astrocytomas, oligodendrogliomas, oligoastrocytomas, or ependymomas, respectively. However, in 2016 the fourth edition of the WHO Classification of Tumors of the Central Nervous System (CNS) [10] has conceptually updated the classification of gliomas, adding molecular parameters in addition to the classical histological examination to define gliomas subtypes better. Accordingly, gliomas are stratified based on anaplastic features, with WHO grade I gliomas indicating a low proliferative index. Most commonly, those exhibit clear tumor boundaries, are not invasive, and can be treated with surgical resection only. On the contrary, WHO grade II-IV diffuse gliomas include infiltrative, proliferative and malignant tumor entities. Common WHO grade II and III gliomas in adult patients include diffuse astrocytoma (WHO grade II) and anaplastic astrocytoma (WHO grade III), with a median overall survival (OS) of over 5 years and 3-5 years, respectively. WHO grade IV diffuse astrocytic glioma, or glioblastoma (GBM), is the most common primary brain cancer and the most frequent among gliomas, with an annual incidence of 3.19 cases per 100’000 persons in the United States. The median overall survival in adults is 15-17 months, with a 5-year survival of less than 5%. Essentially, all grade II/III lesions eventually progress to GBM [11].

In 2021, the fifth edition of the WHO Classification of Tumors of the Central Nervous System (CNS) [12] introduced significant changes that advanced the role of molecular diagnostics in CNS tumor classification, together with important updates for the molecular diagnosis and management of cancer patients with diffuse gliomas [5] in response to the constant and rapid changes in the neuro-oncology field (Figure 1.1). Gliomas can be further stratified according to the isocitrate dehydrogenase (*IDH*) mutation status. IDH is a critical enzyme in the Krebs cycle and plays a key role in energy metabolism. Mutations of IDH result in loss of the enzyme’s ability to catalyze the oxidative decarboxylation [13] of isocitrate to alpha-ketoglutarate (α-KG). This results in an accumulation of the oncometabolite 2-hydroxyglutarate (2HG) from the

abnormal conversion of α-ketoglutarate. Testing for IDH1/2 mutations is considered standard practice in neuro-oncology, as individuals with IDH-mutant gliomas show superior survival [14]. IDH-mutant low-grade gliomas (LGG), which mainly affect younger adults, can be divided based on the chromosome arms 1p/19q codeleted (oligodendroglioma) and non-codeleted (astrocytoma). Additionally, the latter displays nuclear ATRX loss and mutations in *TP53*. According to the updated guidelines, GBM is now defined as IDH-wildtype WHO grade IV diffuse astrocytic glioma, which is characterized by EGFR amplification (EGFRamp), TERT promoter mutation (pTERTmut), and gain of chromosome 7 and loss of chromosome 10 (7+/10-). Conversely, IDH-mutant glioblastoma is now referred to as IDH-mutant astrocytoma, WHO grade 4. Moreover, an additional distinct marker of IDH-mutant astrocytoma, WHO grade 4, is the homozygous deletion of *CDKN2A/B* locus.

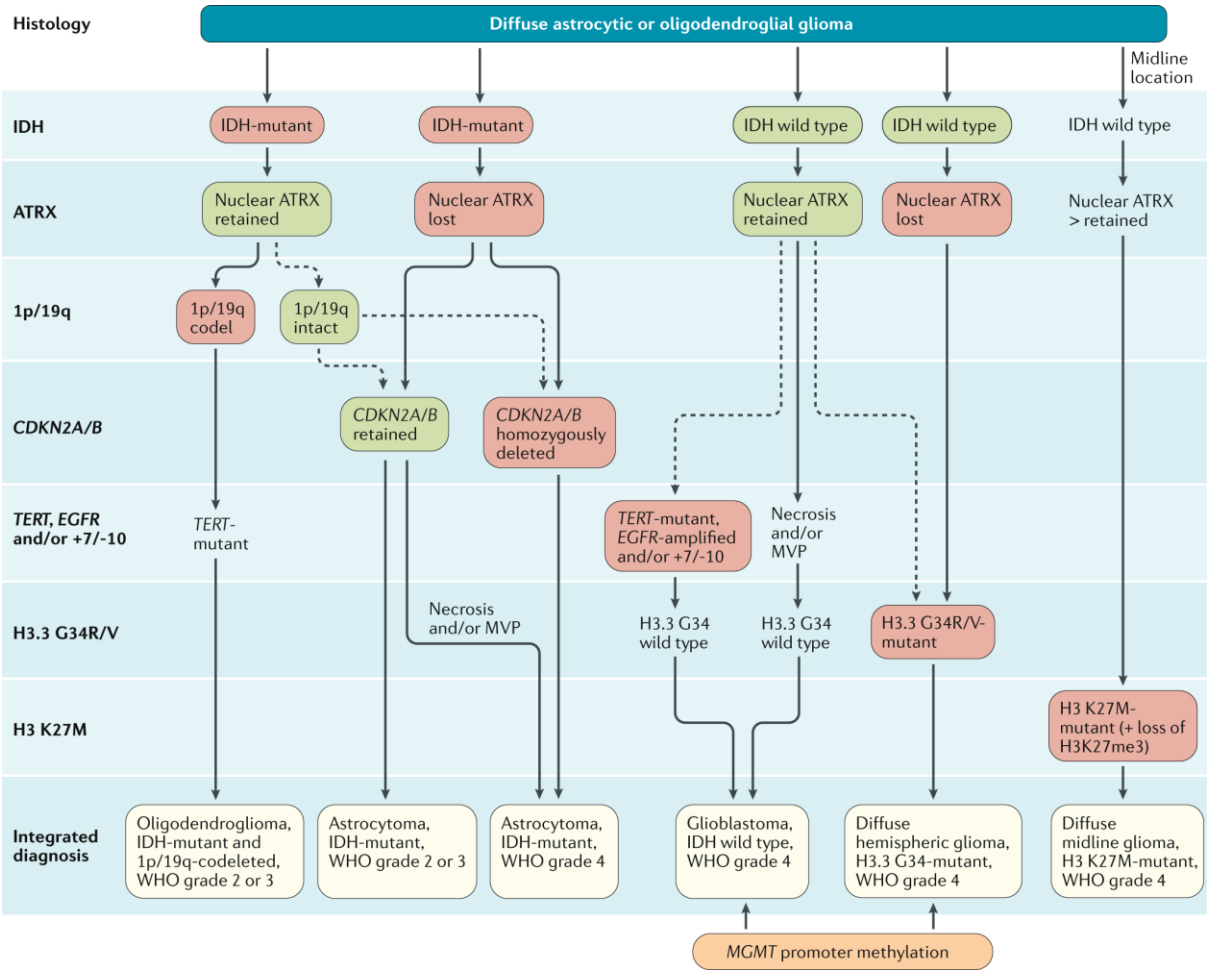

Figure 1. 1 Diagnostic algorithm for the integrated classification of the major diffuse gliomas of adulthood. Tissue biopsies from potential patients with diffuse gliomas are routinely assessed by immunohistochemistry to detect the presence of key relevant alterations. Each glioma subtype displays distinct molecular alterations. Figure taken from [5].

1.1.1 DNA methylation-based classification of gliomas

The current WHO classification of central nervous system (CNS) tumors and the recent updates extensively reflect the critical complexity of brain tumors, which can greatly differ both biologically and clinically. In 2018, Capper and others [2] proposed a novel and unique approach for DNA methylation-based CNS tumor classification, which may significantly improve and support diagnostic precision compared to classic techniques only. Genome-wide DNA methylation profiles of more than 70 different tumor entities were used to generate a CNS tumor reference cohort consisting of 2'801 samples to identify specific DNA methylation classes within and between tumor entities. This approach led to the identification of 82 CNS tumor classes characterized by distinct DNA methylation profiles (Figure 1.2). Interestingly, this approach has convincingly shown that DNA methylation profiles are highly sensitive and reproducible for the subclassification of CNS tumor entities that were previously reported to be homogeneous, and resulted in a change of diagnosis in up to 12% of selected cases. Therefore, implementing DNA methylation-based classification for CNS tumors combined with classical histology and molecular classification improves diagnostic accuracy and subsequent treatment decisions.

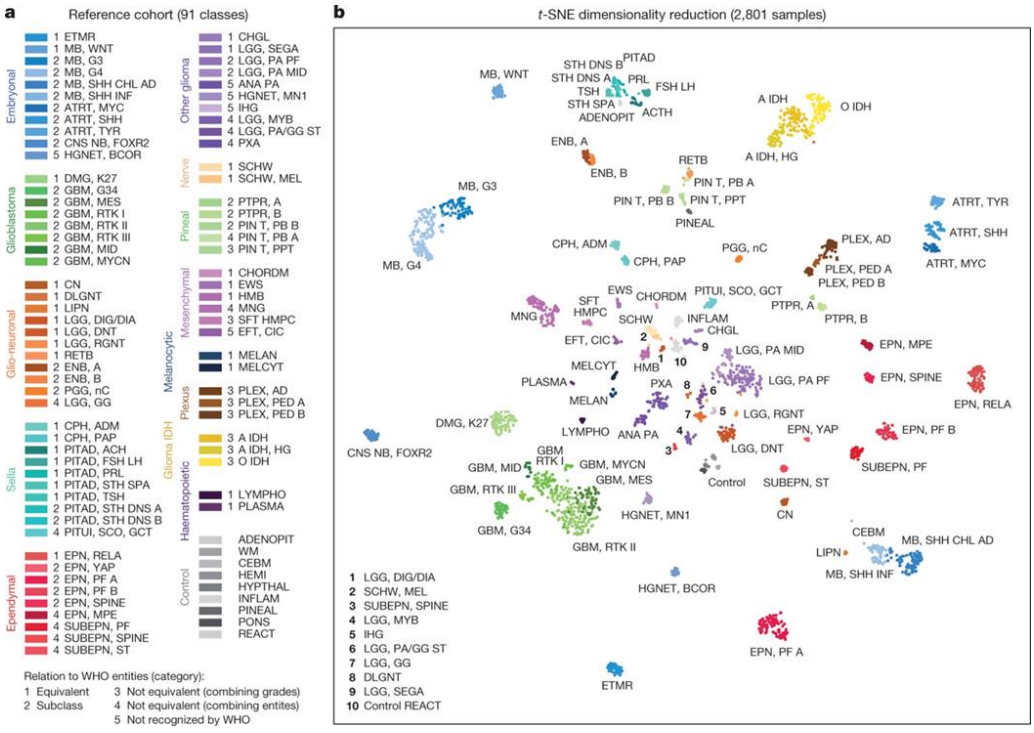

Figure 1. 2 DNA methylation-based CNS tumor reference cohort. Visual representation of the 82 CNS tumors methylation classes in the reference cohort. Figure taken from [2].

1.2 Molecular characterization and classification of glioblastoma

In 2010, Verhaak and others [15] proposed gene expression-based molecular classification of clinically relevant subtypes of glioblastoma, characterized by abnormalities in PDGFRA/IDH1 (Proneural), EGFR (Classical), and NF1 (Mesenchymal). Accordingly, each GBM subtype may be associated with different survival, and patients may require a subtype-specific treatment approach. Aggressive standard therapy, including radiotherapy (RT) and temozolomide (TMZ), did not benefit Proneuronal GBM patients, whereas those with a Classical and Mesenchymal subtype tend to benefit from the standard of care. However, others [16, 17] have demonstrated that multiple molecular subtypes coexist within the same tumor (Figure 1.3), and the Neural subtype is non-tumor specific [3]. Moreover, over 50% of GBM recurrences exhibit expression-based subtype change [18]. In conclusion, GBM molecular stratification adds essential implications in the understanding of GBM pathology; however, its clinical implications are still controversial.

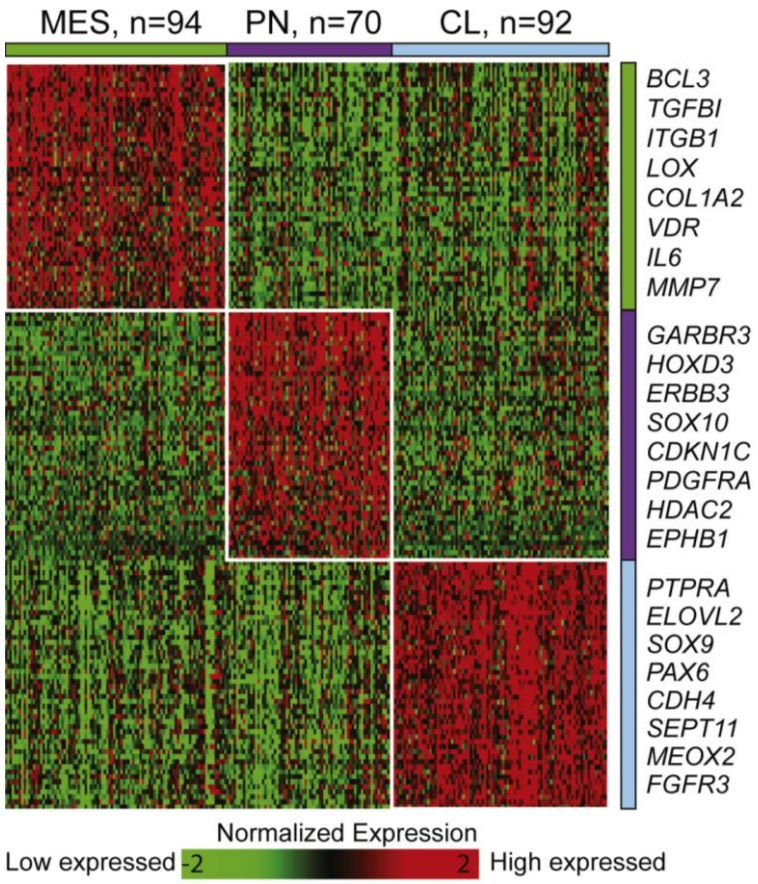

Figure 1. 3 Gene expression and genomic alterations across glioblastoma subtypes. Different genomic alterations define the type of glioblastoma, and 3 subtypes have been proposed. Taken from [3].

1.3 Clinical management of glioblastoma

Maximal safe resection followed by combined chemoradiation therapy with the alkylating agent TMZ is the current standard of care for newly diagnosed GBM patients since 2005 [19]. At recurrence, there is no standard of care.

1.3.1 Surgical resection

Surgical removal has long been the backbone therapy for patients diagnosed with GBM, and the first-ever reported resection of a primary brain tumor was performed by Dr. Rickman J. Godlee in 1884 [20]. When feasible, gross total resection (GTR) is generally recommended over subtotal resection (STR) and biopsy, as multiple studies have suggested that it may benefit survival outcomes and progression-free survival (PFS) in patients [21-23]. Moreover, the implementation of fluorescence-guided surgery with five-aminolevulinic acid (5-ALA) improved PFS [24]. At recurrence, the role of surgical resection remains controversial, as some clinical investigations indicated that it might improve survival and quality of life [25-27], whereas others did not [28, 29]. However, no randomized trials were specifically designed for this purpose [30].

1.3.2 Radiotherapy

Radiotherapy, as surgical resection, has been implemented in the treatment regimen for GBM patients for long to control tumor growth and recurrence. Typically, conventional RT following surgery is delivered at 60Gy in 2-Gy fractions over 6 weeks, in combination with the alkylating agent TMZ [19]. The benefit of using RT at recurrence is currently debated. However, stereotactic radiosurgery (SRS) and short-course hypofractionated stereotactic RT may improve outcomes in selected cases [31].

1.3.3 Temozolomide

In 2005, Stupp and others demonstrated that TMZ in combination with conventional RT significantly improves median overall survival in GBM patients from 12.1 to 14.6 months, compared to RT alone [19, 32]. As a result, TMZ has become the standard first-line systemic chemotherapy and part of the current standard of care. Commonly, it is administered at 75 mg/m^2 daily during RT, followed by 6 cycles of TMZ alone at 150-200 mg/m^2 on days 1-5 every 28 days. Most patients experience recurrence within 6 months following concomitant chemoradiation and adjuvant chemotherapy. GBM progression is most often monitored by magnetic resonance imaging (MRI).

1.3.4 Tumour Treating Fields and supportive care

Tumour Treating Fields (TTFields) is a locoregional antimitotic therapy that delivers low-intensity alternating electric fields, interfering with cancer cells division. TTFields were proven to significantly improve PFS and OS in newly diagnosed GBM patients combined with adjuvant TMZ [33]. Median PFS was 6.7 months in patients treated with TTFields in combination with TMZ and 4.0 months in the TMZ treatment alone group. Median OS was 20.9 months vs 16.0 months in the combinatorial treatment group vs TMZ alone group, respectively. Therefore, TTFields can be offered as a valid therapeutic option in willing and eligible patients. Seizures and peritumoral vasogenic edema are frequently observed in GBM patients [34, 35]. As such, antiepileptic and corticosteroids therapy are often required as supportive care.

1.3.5 Future directions: Targeted therapies and immunotherapies

The urgent need for better therapeutic options in GBM led to major efforts exploring alternative precision oncology approaches. However, GBM unique biological aspects represent a substantial challenge difficult to overcome [30].

Typically, GBM is a multiple pathway disease hard to control with targeted therapies. Most clinical trials focused on frequently altered cellular pathways, such as the phosphoinositide 3-kinase (PI3K)/protein kinase B (AKT)/mammalian target of rapamycin (mTOR), the epidermal growth factor receptor (EGFR) gene amplification or mutation, and the p53 and the retinoblastoma (RB) pathways. However, none showed improved survival [36], primarily due to insufficient blood-brain barrier (BBB) permeability, rescue mechanisms, poor tolerability, and challenging targeted drug design.

Microenvironmental targets have also been explored in clinical settings for GBM, focusing on angiogenesis, immune checkpoint blockade, CAR T cells therapy, oncolytic viral therapy, and vaccine therapy. However, most studies failed to improve survival in late clinical development [36, 37]. Most notably, multiple studies on the VEGF antibody, bevacizumab, have demonstrated prolonged progression-free survival; however, it did not improve overall survival [38-40]. Moreover, studies on the PD-1 inhibitor, nivolumab, showed favorable tolerability; however, they failed to improve survival in GBM patients [41-44].

Although current clinical data from immunotherapy and targeted therapy in GBM did not improve survival in GBM patients, some promising outcomes have been achieved [45], providing solid and consistent insights that these “cold” tumors might shift to a “hot “ state, potentially guiding the way to effective immunotherapy to implement in the current standard of care for GBM patients [37].

1.4 O6-Methylguanine-DNA Methyltransferase (MGMT)

1.4.1 Function of MGMT

The *MGMT* gene is located on chromosome 10q26 and encodes a DNA repair enzyme whose function is to remove alkyl-groups from the O6-position of guanine [46, 47] in a one-step transfer reaction, where the alkyl group is transferred from the DNA to a cysteine residue of MGMT. This stoichiometric reaction inactivates MGMT permanently and restores DNA. The inactivated alkylated MGMT undergoes degradation via ubiquitination [48].

1.4.2 Regulation of MGMT expression

Aberrant hypermethylation of *MGMT* promoter is detected in about 40% of colorectal cancer and glioma, and in 25% of non-small cell lung carcinomas, lymphomas, and head and neck carcinomas [49]. However, it is debated which and how many CpG sites must be methylated to silence *MGMT* successfully [50-52]. Methylation can also affect *MGMT* gene body, regulating *MGMT* expression independently from the promoter methylation status. Accordingly, gene body methylation has been linked with increased sensitivity to TMZ treatment [53].

MGMT expression may also be regulated by histone modifications such as acetylation and methylation, and aberrant transcription factors. For instance, increased methylation levels of histone H3 lysine 9 (H3K9) and methyl-CpG binding protein 2 (MeCP2) to the *MGMT* promoter region was linked with gene silencing [54, 55].

Interestingly, regulation of *MGMT* expression can also be dictated by specific microRNAs (miRNAs), which target mRNA sequences and cause both translation repression and mRNA degradation [56]. Known miRNAs involved in MGMT translational repression include miR-181b [57, 58], miR-181d [58], miR221 and miR-222 [59], miR-767-3p and miR-684 [60]. Up to date, none of them have been linked with increased TMZ sensitivity in GBM patients.

Moreover, the role of distal enhancer regions has also been linked with the regulation of *MGMT* expression. Notably, the methylation of a promoter/enhancer (P/E) region that includes a promoter and a 59 bp cis-acting enhancer element spanning the first exon–intron of *MGMT* gene has been associated with *MGMT* expression silencing [61]. However, there are some discrepancies between MGMT protein expression and

methylation phenotype at the P/E region, as some samples were found to express high levels of MGMT even with a confirmed promoter methylation status [62], supporting the idea of multiple regulatory mechanisms dictating *MGMT* expression.
In 2018, a study led by Chen and others [63] described the discovery of a novel enhancer of *MGMT* located between the promoter of Ki67 and *MGMT*. The study has shown that TMZ treatment forces the activation of the enhancer in GBM lines with minimal *MGMT* expression, resulting in increased *MGMT* expression and resistance to TMZ treatment, despite promoter methylation.

1.5 Clinical implications of *MGMT* methylation status in GBM

Hegi and colleagues [6] have shown in 2005 that the benefit from TMZ treatment is largely determined by *MGMT* promoter methylation status (Figure 1.4). Patients with *MGMT* promoter unmethylated, which accounts for about 45% of total cases, do not profit from TMZ. Inversely, patients with *MGMT* promoter methylated tend to benefit from TMZ treatment. Therefore, *MGMT* promoter methylation is associated with a favorable outcome after TMZ chemotherapy in patients with newly diagnosed GBM. Thus, the *MGMT* promoter methylation status has become a frequently tested biomarker in GBM patients. Nevertheless, almost all patients experience tumor recurrence, leading to death.

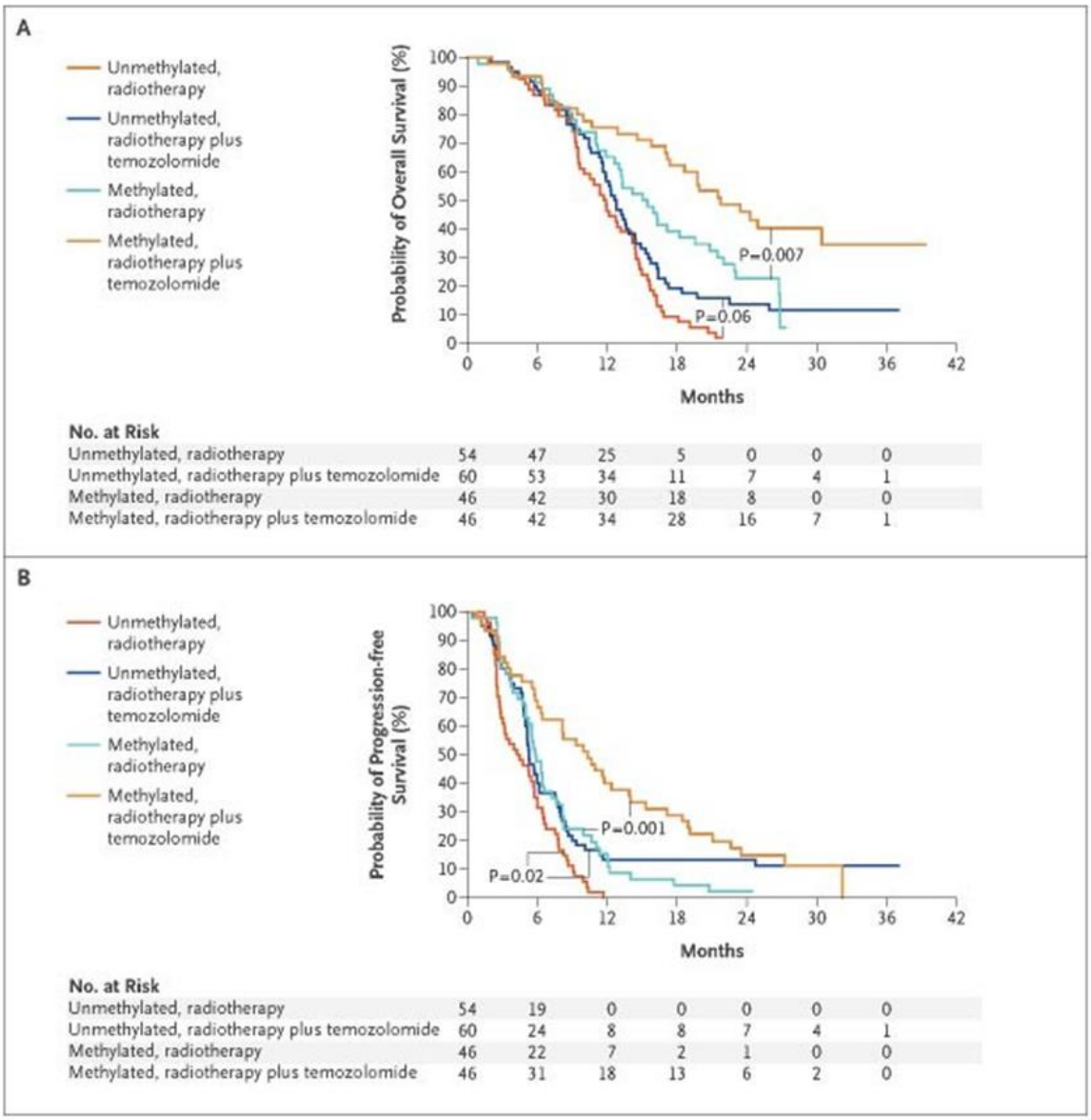

Figure 1. 4 Probability of OS and PFS according to *MGMT* promoter methylation status and randomization to TMZ plus RT or RT alone. Kaplan–Meier estimates for OS and PFS indicate that the group of patients with a methylated *MGMT* promoter significantly benefit form TMZ treatment compared to those with an unmethylated MGMT promoter. Figure taken from [6]

1.5.1 MGMT-mediated DNA repair

TMZ is a prodrug sold under the brand name Temodar [64], and it is given orally or via intravenous infusion. An imidazotetrazine derivative of the potent alkylating agent dacarbazine, TMZ is stable at rather acidic conditions (pH <5) but gets rapidly hydrolyzed at physiological pH (pH >7) to generate the active metabolite 5-(3-methyltriazen-1-yl) imidazole-4-carboxamide (MTIC) [65]. Following oral administration, TMZ is quickly and almost entirely absorbed in the small intestine and displays good penetration of the BBB due to its lipophilic nature and small molecular size of 194.151 g/mol. It has an elimination half-life of 1.8 hours. DNA alkylation upon TMZ treatment can occur at the N7 (80-85%) or the O^6 (5%) position of guanine, as well as the N3 (8-18%) position of adenine [66, 67]. DNA alkyl adducts are often effectively repaired by the base excision repair (BER) pathway. In GBM, the BER pathway is rarely compromised; therefore, it is associated with resistance to TMZ therapy and potential worse prognosis [68-70]. However, despite their preponderance, the most toxic and mutagenic lesion is the O^6MeG [67], which MGMT directly and efficiently repairs (Figure 1.5). Interestingly, most MGMT translocates from the cytoplasm to the nucleus upon alkylation [71].

The knowledge that MGMT deficient cells are vulnerable to alkylating agents compared to MGMT proficient cells was already demonstrated in multiple early studies [72, 73]. Therefore, the ability of a cell to repair O6-alkylguanine adducts strongly depends on the amount of MGMT molecules present and on the cell's capacity to induce MGMT expression upon alkylation. Notably, induction of MGMT expression in GBM xenografts is associated with TMZ resistance [74]. In the absence of MGMT, replication of DNA containing O6-alkylguanine adducts may result in futile cycles of DNA mismatch repair (MMR) pathway [75], which is critical for the repair of base mismatches generated by base deamination, methylation, oxidation, and replication errors [76].

1.5.2 The role of the DNA mismatch repair system

The O6meG/cytosine pair can cause the O6meG/thymine mismatch in the newly synthesize DNA strand after the first round of DNA replication. Naturally, guanine/thymine mismatches are recognized by the heterodimer MutSα, which incorporates MSH2 with MSH6 [77]. However, as the alkyl-group from the O6-position remains on the parental strand, the MMR system cannot successfully process and repair the lesion, leading to futile MMR cycles. This event can generate a collapsed replication fork [78], resulting in DNA double-strand break (DSB) that may lead to G2/M cell cycle arrest. Eventually, DSBs can be repaired by downstream homologous recombination (HR) and non-homologous end joining (NHEJ) repair pathways. However, excessive DSBs accumulation caused by O^6MeG lesions can rapidly saturate those systems [79].

DNA DSBs are described as the ultimate cytotoxic lesion in the O^6MeG repair cascade, leading to cell death. Activation of DNA damage response and cell death pathways occurs mostly once cells have undergo two DNA replication cycles [80].

Notably, multiple studies have demonstrated that a compromised MMR system generates resistance to TMZ treatment in GBM. For example, it was shown that MSH6 mutations occur in 41% of recurrent GBM cases, resulting in acquired TMZ resistance [81, 82]. Moreover, preclinical studies [83, 84] have confirmed that loss of MSH2 and MSH6 renders GBM cells TMZ resistant, independently of *MGMT* promoter methylation status.

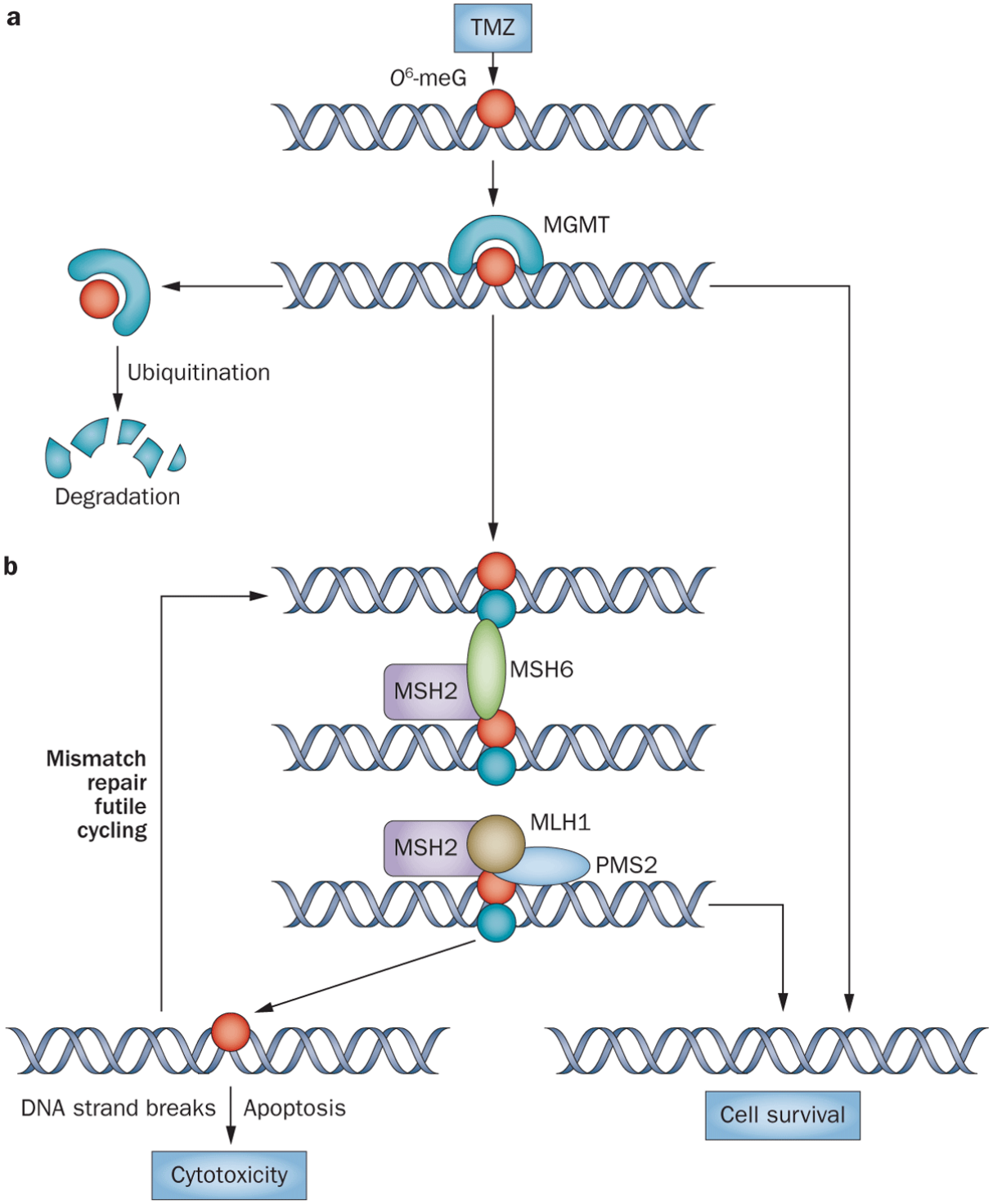

Figure 1. 5 MGMT-mediated repair cascade upon TMZ. The use of TMZ causes multiple DNA lesions, including the O^{6}MeG lesion. The latter can be repaired by the repair enzyme MGMT, restoring DNA. Figure taken from [4]

1.5.3 Clinical approaches to overcome MGMT-mediated TMZ resistance in GBM

A number of clinical studies have tried to overcome TMZ resistance found in GBM patients with an unmethylated *MGMT* promoter. For example, a dose-intensive TMZ treatment compared to standard TMZ treatment in patients with newly diagnosed GBM was performed in the RTOG0525 randomized phase III trial [85]. The study hypothesized that a higher dose regimen would enhance the alkylating effect of TMZ, sensitizing MGMT-unmethylated tumors. However, this study failed to demonstrate improved efficacy of intensified TMZ maintenance regimen in newly diagnosed GBM patients compared to standard protocol, regardless of *MGMT* promoter methylation status.

Another approach to counteract TMZ resistance in GBM patients with MGMT-unmethylated tumors was reported in a phase II trial [86], where patients with recurrent or progressive disease were treated with O6-benzylguanine (O6BG), a selective inhibitor of MGMT. However, the study reported no significant restoration of TMZ sensitivity; thus, no improved survival compared to TMZ alone. Moreover, the main limitation in systemic administration of O6BG in combination with TMZ was the high dose-related toxicity to the hematopoietic system.

Chemotoxicity on blood and bone marrow cells of GBM patients treated with O6BG and TMZ caused severe myelosuppression, which largely limited dose escalation and clinical efficacy. Early *in vivo* studies [87] suggested that the overexpression of O6BG-resistant MGMT protected hematopoietic cells from the combination of O6BG and TMZ. Subsequently, Adair *et al*., [88] demonstrated extended survival of chemoresistant GBM patients following gene therapy using mutant MGMT–modified hematopoietic stem and progenitor cells. After bone marrow transplant, patients tolerated better dose-intensified chemotherapy than those without gene-modified bone marrow transplant.

Thus, these studies demonstrated efficient hematoprotection following mutant MGMT gene therapy, potentially maximizing dose escalation and clinical efficacy.

1.6 Epigenetics determinants and classification of glioma

1.6.1 Epigenetic regulations in normal cells

Epigenetics is the study of phenotype changes without altering the DNA sequences. Every cell in the body shares the same genome; thus, they are genetically identical [89]. However, every cell expresses only a limited and distinct set of genes that define the cell type. Therefore, cells need to differentiate into phenotypically different types of cells [90] to sustain the normal functioning of the human body. These modifications occur at different genomic regions and are mostly modulated by regulatory mechanisms, such as DNA methylation and histone proteins modifications [91].

DNA methylation is commonly found in eukaryotes and plays a crucial role in regulating transcription. Methylation in the nitrogenous bases is a common epigenetic alteration typically found in the heterochromatin, modulating gene expression. Cytosine residues are more frequently subjected to methylation compared to other bases. Additionally, such modifications are most commonly found in regions with a high frequency of CpG sites [92], known as CpGs islands. These islands frequently overlap with promoter regions, regulating gene expression.

Post-translational histone proteins modifications mostly include acetylation, methylation, phosphorylation, ubiquitination, SUMOylation, deimination, crotonylation, citrullination and ADP-ribosylation [93, 94]. Modifier enzymes responsible for such modifications are referred to as epigenetic writers. As epigenetic modifications are often temporary [95], epigenetic erasers are responsible for removing histone proteins modifications. For example, histone deacetylases (HDACs) are well known epigenetic erasers responsible for removing acetyl groups from histones.

1.6.2 Disruption of epigenetic regulation in cancer

Cancer cells are well known for featuring major genetic mutations, as well as a profoundly altered epigenetic landscape [96]. The cancer epigenome is mostly characterized by significant global changes in DNA methylation and histone modifications, particularly in CpG islands regions, which play a fundamental role in the cancer multi-step process of growth and progression.

Aberrant DNA methylation profiles in cancer cells are the most extensively investigated epigenetic changes in cancer research [97], primarily focusing on CpG island promoter regions. Interestingly, tumor cells methylome can be both characterized by hypo- and hypermethylation events [98]. Hypomethylation changes contribute to severe genomic instability and frequent activation of normally silenced oncogenes [99]. For example, hypomethylation of the *MDR1* gene was associated with MDR1-overexpressing multidrug-resistant cancer cells [100-102]. Conversely, hypermethylation events in promoters have been strongly implicated in the inactivation of tumor suppressor genes, a hallmark in cancer [103]. Notably, Greger and others [104] first suggested that aberrant hypermethylation patterns of the tumor suppressor gene Retinoblastoma (*Rb*) was associated with development in some retinoblastoma tumors.

Dysregulated post-translational modifications (PTM) of histones have been strongly implicated in the abnormal expression of target genes in cancer [105]. Multiple genomic studies [106] have provided relevant evidence that many types of cancer display profound dysregulation patterns of chromatin modifiers. However, most literature in cancer research has focused on aberrant histone methylation, acetylation, and phosphorylation profiles.

1.6.3 Epigenetic classification of gliomas

The epigenetic landscape of gliomas is characterized by significant mutations in chromatin modifier genes [8]. Accordingly, gliomas can be classified based on characteristic epigenetic alterations (Figure 1.6). The most glioma-relevant epigenetic alterations include mutations in *IDH1* or *IDH2* genes in LGG, histone 3 mutations in pediatric high-grade gliomas linked with distinct DNA methylation patterns, and *MGMT* promoter methylation in GBM. Those epigenetic subtypes of gliomas display distinct clinical features, and an appropriate subclassification plays a pivotal role in treatment

strategies. *IDH1* or *IDH2* genes point mutation (IDHmt) is a distinct feature for LGG. Those can be further divided based on the chromosome arms 1p/19q codeleted (oligodendroglioma) and non-codeleted (astrocytoma).

Interestingly, IDHmt LGG displays a characteristic DNA hypermethylation profile that significantly differs from IDHwt glioma, known as Gliomas CpG Island Methylator Phenotype (G-CIMP) [107]. Histone 3 mutations in pediatric high-grade gliomas can be observed as H3K27M, which is characteristic for pediatric midline high-grade glioma, or as H3G34R/V mutation for hemispheric high-grade glioma. Those specific epigenetic alterations are often associated with distinct DNA methylation profiles [108]. *MGMT* promoter methylation status has become a frequently tested biomarker in GBM patients. Accordingly, MGMT promoter methylation is associated with a favorable outcome after TMZ chemotherapy in patients with newly diagnosed GBM [6].

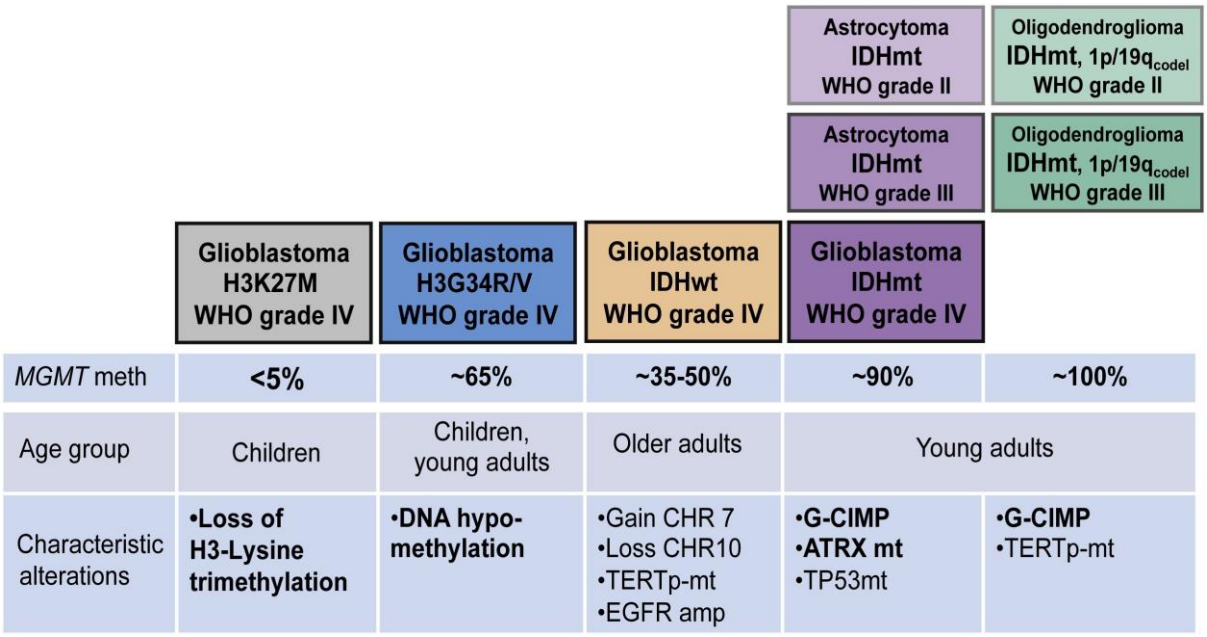

Figure 1. 6 Epigenetic and genetic subclassification of gliomas. Characteristic epigenetic and genetic alterations define the type of glioma. Figure taken from [8]

1.7 Therapeutic strategies targeting the glioma epigenome

Multiple approaches targeting the glioma epigenome have been proposed and are currently being investigated in clinical trials. For example, drugs targeting epigenetic modifiers that are currently under investigation include Histone deacetylase inhibitors (HDACi), Enhancer of zeste homolog 2 inhibitors (EZH2i), DNA methylation inhibitors (DNMTi), Inhibitors of mutant IDH (mtIDHi) and Bromodomain and extra-terminal tail proteins inhibitors (BETi).

1.7.1 Histone deacetylase inhibitors (HDACi)

HDACi, such as Vorinostat, aim at reverse dysregulated target cancer-relevant genes expression by interfering with histone acetylation marks [109]. Generally, this approach leads to a hyperacetylation of histones, resulting in a global disruption of gene expression. For example, the HDACi Vorinostat has shown radiosensitizing properties in preclinical settings [110, 111]. Moreover, multiple clinical trials [112-114] have shown that Vorinostat has good tolerability in newly diagnosed or recurrent GBM patients, but no primary efficacy endpoint was met. However, molecular signatures changes may facilitate patients selection in the future.

1.7.2 Enhancer of zeste homolog 2 inhibitors (EZH2i)

EZH2 is an enzymatic catalytic subunit of polycomb repressive complex 2 (PRC2), which is responsible for the modulation of downstream target genes expression by trimethylation of Lys-27 in histone 3 (H3K27me3). Interestingly, the EZH2 is overexpressed in multiple cancers [115], including gliomas, and its expression was associated with poor prognosis [116, 117]. In pediatric glioma with H3K27M mutation, PRC2 is inhibited [118]; therefore, the use of EZH2i plays a promising role. The EZH2i Tazemetostat is currently being tested in The Pediatric MATCH Screening Trial NCT03155620, which includes pediatric gliomas with *EZH2* overexpression or loss of function mutations in *SMARCB1* or *SMARCA4*. Moreover, preclinical studies have shown [119] that EZH2i impair GBM cell proliferation and synergize with TMZ.

1.7.3 DNA methylation inhibitors (DNMTi)

Up to date, DNMTi displayed anti-cancer features in preclinical settings of IDHmt glioma [120, 121]; however, this was not successfully translated in patients. This may be the result of poorly clinically relevant DNMTi tested so far. Novel and more promising DNMTi [122, 123] are currently being tested. Nevertheless, the concept of a global demethylation in glioma patients is debated, as it can lead to the activation of previously silenced oncogenes, and can generate potential resistances to the current standard of care. For example, demethylation of the *MGMT* promoter in GBM patients may result in TMZ resistance.

1.7.4 Inhibitors of mutant IDH (mtIDHi)

mtIDHi aim at normalizing the function of α-ketoglutarate dependent enzymes by halting the production of 2HG. Therefore, this is of relevance in the context of IDHmt gliomas. However, the real benefit of mtIDHi in glioma patients is controversial. Some preclinical studies indicated that the use of mtIDHi significantly inhibited cell proliferation of IDHmt glioma cells [124], whereas others suggest that it promotes cell growth [120]. Moreover, attenuation of tumor growth in orthotopic tumor xenografts treated with mtIDHi was not significant [120, 125]. At the clinical level, a limited number of mostly phase I/II clinical trials [126-129] suggest that mtIDHi treatment in glioma patients displays good brain distribution, long half-life, favorable safety and tolerability profile, as well as long-term disease control and improved seizure control.

1.7.5 Bromodomain and extra-terminal tail proteins inhibitors (BETi)

Bromodomain and extra-terminal tail proteins inhibitors are another therapeutic option targeting the glioma epigenome and will be extensively discussed in the following chapter.

1.8 Bromodomain and extra-terminal tail (BET) proteins

BET proteins are epigenetic readers that recognize acetylated lysines on histone tails of relaxed chromatin and promote the signal downstream by linking the histone code to gene transcription [7]. The BET family protein consist of BRD2, BRD3, BRD4, and the testis-specific BRDT [130]. BET proteins share common structural characteristics, featuring dual, mutually related [131] bromodomain motifs (BD1 and BD2) arranged in tandem at the N-terminal end of the protein [132]. In addition to the bromodomain motifs, BET proteins include an extraterminal domain (ET) and a carboxyl-terminus domain (CTD), allowing chromatin remodeling via interaction with chromatin-modifying factors. For this reason, BET proteins modulate genes expression by acting as scaffold proteins (Fig.1.7), recruiting transcriptional complexes at promoters and enhancers of active genes. Superenhancer-associated transcripts are known to drive cell identity and to be highly cell-type specific [133, 134]. BRD4 is associated with a multiprotein complex (mediator complex) that facilitates the initiation of transcriptional activation [135]. Moreover, early investigations [136] have shown that BRD4 associates with the active form of positive transcription elongation factor b (P-TEFb), a complex that stimulates RNA polymerase II transcriptional elongation.

1.8.1 Small molecule inhibitors and degraders of BET proteins

This interaction can be targeted by small-molecule BET inhibitors that are currently in clinical development. BETi are a class of drugs [137] that specifically bind to both tandem domains of BET proteins and prevent their ability to interact with acetylated lysines on histones. Currently, most BETi are not BET subfamily specific. Up to date, over 40 BETi are known, and about 20 entered into clinical development. However, none has reached FDA approval yet [138].

Selective induced target protein degradation with proteolysis-targeting chimeras (PROTACs) emerged as an alternative strategy to BETi. However, although BET degraders demonstrated a more potent antitumor activity than BETi, the clinical potential of this technology is still largely limited by metabolic instability, low bioavailability, unfavorable physicochemical characteristics, and limited BBB penetration [139-142].

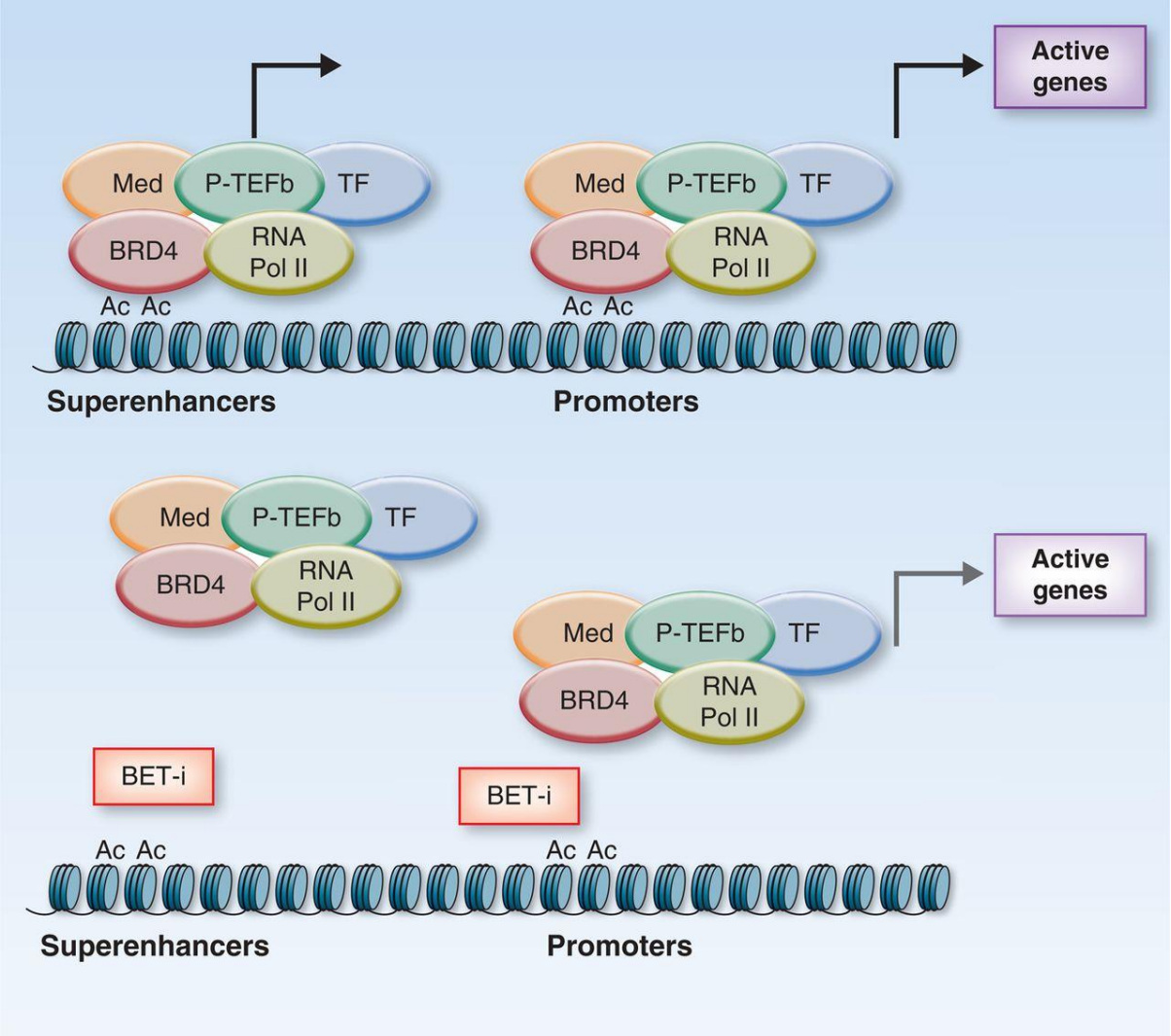

Figure 1. 7 Schematic representation of the mechanism of action of BET inhibitors. BET proteins recruit transcriptional complexes at both the promoter region and at enhancers of genes. BETi reduces BET proteins occupancy in those regions. Figure taken from [7].

1.9 The role of BET proteins in cancer

BET proteins have been identified as potential epigenetic targets in different cancers, including GBM. Studies have shown that BRD2 and BRD4 are often upregulated or translocated in various cancers [143, 144], underlying the pivotal role of BET proteins in human malignancies.

These proteins first emerged as clinically relevant therapeutic targets in hematological malignancies and NUT midline carcinoma (NMC). The latter is of particular interest as studies [145] have suggested that the driver event for this malignancy is determined

by the insertion of the coding region of nuclear protein in testis (NUT) into the 3' end of BRD4, creating the BRD4-NUT fusion gene.

BET-family members are implicated in the modulation of multiple oncogenes, such as *MYC, JUNB,* CCND1, and *CCNA1* [146-148]. Accordingly, silencing of BRD4 leads to a significant arrest in the S phase of the cell cycle in some cancers. Moreover, BETi has been shown to halt cell invasion and migration in breast cancer models via regulation of *Snail* [149], and induce apoptosis and cell cycle arrest in leukemia in via the inhibition of *C-MYC*, *BCL2* and *CDK6* [150]. BETi have also been reported to disrupt double-strand break repair and sensitize pancreatic cancer cells to PARP inhibitors [151].

The role of BET proteins have also been extensively investigated in hematological cancer models [138], with substantial data supporting the use of BETi as an anti-cancer treatment. For example, inhibition of the PD-1/PD-L1 axis by combining anti-PD-1 antibodies and BETi resulted in a synergistic response in mice bearing Myc-driven lymphomas [152]. Interestingly, several preclinical studies demonstrated that BET proteins also influence the tumor microenvironment. For example, BRD4 is involved in promoting the release of pro-inflammatory cytokines from macrophages [153], as well as cancer cells-secreted cytokines [154]. Moreover, the use of BETi alone showed enhanced T cell persistence [155] and positively impacted the anti-tumor activity of T-cells in non-small lung cancer by inhibiting *Foxp3*, *CTLA-4*, and *PD-1* expression when combined with HDACi [156]. The use of BETi in antigen-presenting cells (APCs) halted the release of IL-10 and IL-6 after LPS stimulation, decreased *PDL1* expression, and improved priming of naïve CD4+ T-cells [157]. As such, BET proteins likely provide a significant contribution in promoting cancer development and metastasis formation by modulating the tumor microenvironment [158].

Conversely, evidence from Veneziani and others [159] suggests that BETi reduce the anti-tumor effects of NK cell-based immunotherapy. Therefore, combinatorial treatment regimens with BETi in the context of immunotherapy must be carefully considered.

1.9.1 BET proteins implications in GBM

BET proteins are also of particular interest in the context of GBM. Multiple studies have demonstrated that BETi treatment in GBM resulted in G1 cell-cycle arrest, apoptosis, significant growth inhibition of orthotopic glioblastoma tumors, and increased survival [160-164]. Interestingly, there is a strong consistency among those different findings showing repression of *C-MYC* upon BETi in GBM.

Moreover, BETi synergized against MYCN-positive GBM when combined with Aurora Kinase A inhibitors [165], sensitized GBM cells to TMZ via p53 upregulated modulator of apoptosis (PUMA) induction [166] and, most recently, studies from Gusyatiner and others [167] revealed that BETi halted the expression of interferon-stimulated genes and synergized with HDAC inhibitors in GBM. Additionally, it also showed MYC repression via BETi.

1.10 Clinical trial with BETi

BETi emerged as a promising class of anti-cancer drugs. Multiple BETi are currently being investigated in clinical trials against solid and hematological cancers [7, 138, 158]. Interestingly, published clinical studies demonstrate a very heterogeneous clinical activity of BETi across cancer types.

1.10.1 Clinical activity of BETi in hematological malignancies

A study led by Amorim and others [168] on 33 patients with lymphoma and 12 with myeloma reported 2 complete responses (CR) and 1 partial response (PR) in lymphoma patients treated with BETi. Conversely, no responses were reported in multiple myeloid patients. Another study from Berthon and colleagues, which included a cohort of 41 leukemia patients [169], showed 3 PR to BETi, whereas 2 had a CR lasting up to 5 months. Moreover, investigations from Abramson and others [170] demonstrated BETi clinical activity in lymphoma patients, as 2 CR and 1 PR were reported from a cohort of 44 patients. More recent evidence of BETi clinical responses in hematological malignancies come from Falchook and colleagues [171], showing 1 CR and 3 PR in lymphoma patients, 1 CR in a leukemia patient, and 2 PR in myelofibrosis patients.

1.10.2 Clinical activity of BETi in solid tumors

Clinical responses to solid tumors have been reported in several studies. However, the clinical activity of BETi in solid tumors tends to be weaker than hematological cancers.

Published results from Stathis and others [172] reported 2 PR and 1 stable disease (SD) in patients with advanced-stage NMC with confirmed BRD4–NUT fusions, among 4 treated. Lewin and others [173] have shown that among 10 NMC patients treated with BETi, 3 PR was observed. However, no responses were reported for prostate and lung cancer patients. Additional investigations [174, 175] among 19 NMC patients treated with BETi have shown 4 PR, 8 SD, and 4 progression-free for over 6 months. Moreover, for the prostate cancer patient's cohort, 60% had SD, whereas 40% had progressive disease. More evidence of BETi clinical activity in solid tumors has been investigated by Falchook and others [171], reporting results on over 200 patients treated with BETi. They reported 48 SD among patients with different solid tumors and 1 PR in a breast cancer patient.

Other studies [176] have also shown promising BETi clinical activity in solid tumors, were among 67 patients they reported 1 CR, 1PR and 6 SD. Interestingly, the CR reported was observed in a grade 2 astrocytoma patient. In the latter study, the novel BETi CC-90010 was used to treat patients, showing high tolerance, long half-life, strong single-agent activity, and ability to cross the BBB.

1.10.3 Clinical activity of BETi in GBM

Hottinger and others [177] reported no evidence of antitumoral activity in a small phase IIa trial, including 12 GBM patients treated with the BETi OTX015, and the study was discontinued due to lack of clinical activity and high toxicity features.

Currently, a phase 1b, open-label, dose-finding study (NCT04324840) of CC-90010 in combination with TMZ with or without radiation therapy in subjects with newly diagnosed glioblastoma is ongoing to determine the safety and tolerability of the drug.

1.10.4 Toxicities associated with the use of BETi

Based on the reported clinical studies above cited, toxicities for this class of drugs appear to be rather common. Briefly, the most common adverse events (AEs) include fatigue, anemia, diarrhea, decreased appetite, dysgeusia, thrombocytopenia, nausea, and vomiting.

As such, it is fundamental to consider the role of pharmacodynamic (PD) biomarkers for BETi, as it may assist investigators in dose-escalation studies to avoid severe side effects [158]. Preclinical studies suggest that PD biomarkers allow the clinical monitoring of drug activity and enhance the optimization for clinical use. For instance, upregulation of HEXIM1 [178, 179] and CCR2 and CD180 downregulation [180] have been reported in patients treated with BETi.

1.11 Resistance mechanisms to BETi

Up to date, multiple mechanisms of resistance to BETi have been reported. Interestingly, none of them involves direct mutation of BET proteins. Instead, BETi resistance most probably arises from unspecific adaptations to drug pressure [181].

Most commonly, preclinical studies have reported resistance to BETi through reactivation of *MYC* expression in *MYC*-dependent cancers, such as activation of Wnt signaling [182, 183], modulation by *GLI2* [184], or phosphorylation of the BET protein BRD4 [185]. However, recent investigations [186] have shown that BRD4 phosphorylation can be independent of transcriptional activation of *MYC*. Additional studies have demonstrated that upregulation of BCL-2 family members [187], as well as *MCL1* upregulation [188] and activation of the AMPK-ULK1 pathway [189], confers resistance to BETi. Moreover, Saenz and colleagues [190] reported that the β-catenin-TCF7L2-JMJD6-c-Myc axis is also associated with BETi resistance. Interestingly, several investigations [191, 192] have associated the depletion of the PD biomarkers HEXIM1 with BETi resistance.

1.12 Hypothesis and project objectives

Single-agent therapies have not been successful in treating GBM, and limited therapeutic options are currently available. Therefore, smarter combination therapies are urgently needed.

BETi have shown promising antitumoral effect in various cancers, including GBM. Unpublished preliminary data from our laboratory have shown that BET proteins inhibition causes extensive and diverse changes in the DDR pathways. Interestingly, *MGMT* was rapidly and significantly downregulated upon BETi compared to control.

Therefore, we hypothesized that the addition of BETi in combination with the current standard of care might improve survival of GBM patients with an unmethylated *MGMT* promoter.

Project objectives:

I. Explore DDR genes modulation upon BETi.
II. Preclinical studies with BETi to characterize the *in vitro* modulation of *MGMT* and relevant DDR genes.
III. Explore the mechanistic specificity behind *MGMT* modulation upon BETi.
IV. Determine whether BETi modulates repair of TMZ-induced DNA damage.
V. Evaluate cell cycle profile changes upon BETi in combination with TMZ treatment.
VI. Investigate whether BETi sensitizes GBM to TMZ.

2. MATERIALS AND METHODS

2.1 Cell culture

Patient-derived glioblastoma sphere (GS) line LN-2683GS was established in our laboratory, molecularly characterized and authenticated [50, 167, 193-195]. GS line LN-4372GS was recently derived in our laboratory (authentication and characterization pending). The Lang Frederick Lab at MD Anderson kindly provided the GS line GSC-23luc (authenticated and characterized). Adherent cell lines LN-340 and LN-229 were established in our laboratory. T98G originates from ATCC. Adherent cell lines were molecularly characterized and authenticated [193, 195]. All lines were regularly tested mycoplasma-free (MycoAlert Kit Lonza, Cat. LT07-418).

GS lines were maintained under neural stem cell culture conditions in Dulbecco's modified Eagle medium/F12 (Life Technologies, Cat. 31331-028) containing B27 supplement (Invitrogen, Cat. 17504-001, 50X dilution), 20ng/mL of epidermal growth factor (EGF, PeproTech, Cat. AF-100-15-100) and 20ng/mL of fibroblast growth factor (FGF, PeproTech, Cat. AF-100-15/100-18B). Prior experimental set-ups, spheroids were washed with PBS (CHUV Pharmacy) and dissociated using the cell detachment solution Accutase (Life Technologies Cat. A11105-01 until 11/2021 or Innovative Cell Technologies, Inc Cat. AT104 from 11/2021) by gentle vortexing (average of 45s. Optimized for each GS line). Following dissociation, Accutase was inhibited with fresh neural stem cell complete medium (1:2 ratio). Single cells spheroids were filtered through a 40 µm cell strainer (Falcon, Cat. 352340) in fresh neural stem cell complete medium. Cells were counted with an automatic cell counter (EVE system) using the trypan blue exclusion assay (included with EVE system). For the regular maintenance of GS lines in culture, cells were kept at a density of 1 M per 9mL medium at 37°C, 5% CO_2.

LN-340, LN-229, and T98G were grown in Dulbecco's Modified Eagle Medium (DMEM Glutamax Gibco™ Cat. 61965-026) with 5% Fetal Bovine Serum (FBS) (Hyclone). Upon 80% vessel confluency, cells were dissociated via trypsinization (Trypsin, Invitrogen Cat. 25300-062) and maintained at 37°C, 5% CO_2. LN-229MGMT^{ind}_C12 was continuously maintained under 10µg/mL Blasticidin (Thermofisher, R21001). LN-

340shCTRL, LN-340shMSH6#1^{ind}_C8 and LN-340shMSH6#2 ^{ind} were continuously maintained under 5µg/mL Puromycine (P8833, Sigma).

2.2 Molecular Cloning

LN-229MGMT^{ind}_C12 is a human GBM cell line with a Tet-ON inducible system for *MGMT* derived from LN-229. Recipient vector pCW22 (kindly provided by Prof Joachim Linger, EPFL [196]). Donor vector pSV2MGMT (17) (kindly provided by Prof Bernd Kaina, UMC Mainz [197]). According to manufacturer's protocol, recipient vector and donor vectors were separately transformed into One Shot TOP10 Chemically Competent E. *Coli* (Thermofisher, C404010), using 100µg/mL Ampicillin (Chimbar, A0839,0025) for bacterial selection. Both vectors were separately amplified in Luria-Bertani (LB) liquid medium (10g Tryptone, 5g NaCl, 5g Yeast extract x liter of water) with Ampicillin and isolated by QIAGEN Plasmid Maxi Kit (QIAGEN, 12163). Part of the LB liquid medium was used to make a bacterial stock in 50% glycerol and stored at -80°C. pCW22 was digested with Sal-I and SBF-I to remove the Cas9 gene (4kb) from the trAT(Tet-ON)-containing plasmid (9.6kb).

Insert pSV2MGMT was PCR cloned in order to add restriction sites (sticky ends) Sal-I and Sbf-I. PCR products were run on a gel to confirm MGMT amplification. PCR cloned MGMT was digested with Sal-I and Sbf-I to generate compatible ends. Ligation of both isolated and digested pCW22 and PCR cloned *MGMT* cDNA was performed via LigaFast Rapid DNA Ligation System (Promega, M8221) at RT 2 hours (100ng total DNA/ reaction, ratio 1:3). Transfection of ligation product was performed into One Shot® TOP10 Chemically Competent E. coli using protocol from manufacture. Ampicillin-selected bacterial colonies were tested with PCR for *MGMT* presence, followed by DNA sequencing for validation. Plasmid pCW22MGMT was expanded in E.*coli* in LB medium followed by QIA plasmid miniprep kit (QIAGEN, 27104) for subsequent lentiviral production.

2.3 Production and delivery of lentiviral particles

2.5M HEK293T cells (kindly provided by Paolo Dotto's Lab, UNIL) were seeded in a 10cm petri dish with DMEM 10% FBS. 24 hours later, cells were transfected according to Lipofectamine™ 3000 Transfection Reagent Protocols (Thermofisher, L3000001). Briefly, 2.0mL tubes were prepared as follows: 1.5ml Optimem medium

(Lifetechnologies, 31985-062) and 41µl Lipofectamine 3000 were added to Tube A. 1.5mL Optimem medium, 35 µl P3000 Reagent and 18µg of DNA were added to Tube B. DNA was composed of 3 plasmids at 1:3:4 ratio, including the expression vector pCW22MGMT (4), the packaging vector pCMV9.74 (3) (Addgene, 22036), and the envelope vector pMD2.G (Addgene, 12259). Following 20 minutes of incubation at room temperature (RT), Tube A was mixed with Tube B and incubated at RT for 15 minutes. Medium from HEK293T was removed, and the transfection mixture was gently added to the cells. In addition, 2mL of Optimem medium was added to cover the cells completely. Following incubation at 37°C and 5% CO_2 for 6 hours, the transfection mixture was removed and cells were incubated again with DMEM 10% FBS for 48 hours. Target cells (LN-229) were seeded 24 hours prior viral transduction in order to be 80% confluent on the transduction day (1M cells in a 10cm petri dish)
After 48 hours, viral supernatant was harvested, filtered through a 0.22µM filter (Milan, SCGPT05RE), and complemented with 10µg/mL Polybrene Infection / Transfection Reagent (Sigma-Aldrich, TR-1003-G). Subsequently, the viral medium was added to the target cells. Following 24 hours of incubation, the medium was carefully removed and replaced with fresh DMEM 5% FBS. After an additional 24 hours, Blasticidin 10µg/mL was added to the medium to select successfully transduced cells.
For the production of LN-340shCTRL, LN-340shMSH6#1^{ind}_C8 and LN-340shMSH6#2^{ind}, we purchased a non-targeting TRIPZ shRNA designed with minimal homology to known mammalian genes (Horizon Discovery Ltd. Catalog ID:RHS4743) and TRIPZ Inducible Lentiviral shRNA targeting hMSH6 as E. coli glycerol stock cultures (Horizon Discovery Ltd. Clone Id: V2THS_258239 & Clone Id: V2THS_82749), respectively. Here, replication-incompetent lentiviral particles were produced according to the manufacturer's protocol (Dharmacon™ Trans-Lentiviral packaging kits, Cat. TLP5912).

Briefly, 2.5M HEK293T cells were seeded in a 10cm petri dish with DMEM 10% FBS. 24 hours later, 1 tube of transfer vector DNA, and Trans-Lentiviral Packaging Mix was prepared in a 15mL polystyrene tube, including 42µg lentiviral transfer vector DNA (shRNA) and 30µl Trans-Lentiviral packaging mix. Total volume 945µl (with sterile water). 105µl $CaCl_2$ was added to the diluted DNA. The tube was vortexed and 1050µl 2xHBSS was added to the DNA mixture. The solution was incubated at RT for 3

minutes, and added drop-wise to the cells following medium removal. Cells were incubated for 16 hours at 37°C with 5%CO_2. Subsequently, the transfection mix was removed and 14mL DMEM 5% FBS was added to the cells. After 48 hours, viral supernatant was harvested, filtered through a 0.22µM filter and complemented with 10µg/mL Polybrene Infection / Transfection Reagent. Subsequently, the viral medium was added to the target cells. Following 24 hours of incubation, the medium was carefully removed and replaced with fresh DMEM 5% FBS. After an additional 24 hours, Puromycin 5µg/mL was added to the medium to select for successfully transduced cells.

2.4 Generation of monoclonal populations

Single clone populations were generated according to Addgene protocol "Isolating a Monoclonal Cell Population by Limiting Dilution - Last Upload: August 1, 2016". Briefly, the general population of a target cell line was diluted at a concentration of 5 cells/mL in 10mL DMEM 10% FBS. This 5 cells/mL solution was used to seed 2 to 4 96-well plates. 100 µL of the 5 cells/mL solution was transferred into each well of a 96-well plate. Cells were incubated undisturbed at 37°C with 5% CO_2 for about 7-14 days. After 7 days, cells were scanned to observe colonies. If none, cells were incubated for additional 7 days. Wells with more than a single colony were discarded.

2.5 Doxycycline-inducible Tet-system validation

Following 14 days of antibiotics selection, the general population was in a multi-dose assay with Doxycycline (Sigma Aldrich, D9891-1G) in order to identify the optimal Doxycycline concentration for our experimental questions. Briefly, 1M cells were seeded in a 10cm petri dish, and treated with doxycycline 24 hours later. Cells were incubated for 48 hours, and pellets were harvested for RNA or protein analysis.

2.6 RNA Extraction and qRT-PCR

Total RNA was isolated from target cells with the ReliaPrep™ RNA cell miniprep system (Promega, cat. z6011). The quality and quantity of isolated RNA was determined by Nanodrop. DNAse treatment was performed prior cDNA synthesis with the RapidOut DNA Removal Kit (Thermo Fisher Scientific, cat. K2981). cDNA was

generated with the PrimeScript RT reagent kit (Takara, cat. RR037A), followed by real-time qPCR using the Kapa Sybr® Fast Universal qPCR kit (Kapa Biosystems, cat. KK4602) and the Rotor Gene 6000 real-time PCR system (Qiagen). qPCR conditions were programmed as follows: 95°C (100s) followed by 40 cycles at 95°C (3s) to 60°C (20s). Obtained expression levels were normalized to the housekeeping gene GAPDH. Primers were designed with the online software Primer3 or with the Universal Probe Library System Assay Design (Roche). Genes-specific primer sequences are described in Table 1 (Supplementary data).

2.7 Protein extraction and quantification

Target cells were collected by centrifugation (GS lines) or by mechanical collection (adherent lines) using Cell Lifters Costar (Vitaris AG, cat. 3008). Collected pellets were snap-frozen in liquid nitrogen for 5 minutes and stored at -80°C. Frozen pellets were lysed in RIPA Lysis and Extraction Buffer (Thermofisher, cat.89901) supplemented with Complete™, Mini Protease Inhibitor Cocktail (Sigma-Aldrich, cat. 4693124001) and PhosSTOP™ (Sigma-Aldrich, cat. 4906837001). Pellets were lysed by passing them 5 times through a 1mL 25G syringe with needle while on ice, followed by centrifugation at 15,000g for 15 minutes at 4°C to remove cellular debris. The supernatant was collected and protein quantification was performed in double using the Bradford Assay (Bio-Rad, Hercules, USA). Briefly, A standard curve was generated with Bovine Serum Albumin (BSA) (PanReac AppliChem, A1391,0100).

2.8 Western Blot

Western blot was performed with 20-40µg of protein extracts (generally 40µg) on SDS polyacrylamide gradient gel (Biorad, cat. 456-1086) at 120V for 2h30 at RT. Proteins were exposed and transferred to a nitrocellulose 0.45µm blotting membrane (Biorad, cat. 162-0115). Protein transfer was performed at 4°C (cold room) at 100V for 1h15. Equal loading was confirmed with Ponceau S Solution (Sigma-Aldrich, cat. P717D-1L). Membranes were blocked in 5% BSA or 5% non-fat skimmed milk at RT for 1h (according to antibody specifics). Blocked membranes were incubated overnight at 4°C with antibodies of interest: anti-α-Tubulin (Sigma, T5168, 1:10,000), anti- β-Actin Bioconcept, 8H10D10. 1:10,000), anti-MGMT (R&D systems, AF3794-SP, 1:4,000), anti-MSH6 (Cell Signaling, #5424S, 1:4,000), anti-MSH2 (Cell Signaling,

#2017S, 1:4,000). Membranes were washed 5 minutes x3 in TBS-T at RT, followed by incubation at RT for 1h with the following secondary antibodies (according to primary antibody specifics): anti-rabbit (Promega, W4011, 1:5,000), anti-mouse (Thermofisher, 31430, 1:5,000), anti-goat (Thermofisher, 31402, 1:5000).

2.9 ChIP-qPCR

ChIP-qPCR was largely performed following the iDeal ChIP-seq kit for Transcription Factors (Diagenode, cat. C01010170). Briefly, proteins from 20M T98G cells were cross-linked to DNA in a 15cm petri dish by adding fresh PFA (Lucerna, cat. 15714) to a final concentration of 1% for 15 minutes at RT. Fixation was quenched with Glycine for 5 minutes at RT. Fixed cells were then washed with cold PBS, and nuclei were extracted via cell membrane lysis. Using 1.5mL Bioruptor® Microtubes with caps (Diagenode, cat. C30010016), chromatin was sonicated at a concentration of 1.5M cells / 100µl complete Shearing buffer iS1b with Bioruptor Pico (Diagenode, Serial Number P-181503) for 12 cycles (30 seconds “ON”, 30 seconds “OFF”) in order to obtain fragments between 100bp and 600bps. The chromatin was briefly centrifuged for 15 seconds, and subsequently, the supernatant was centrifuged for 10 minutes at 4°C at 16,000g. An aliquot of 50µl of the supernatant was kept for shearing assessment, whereas the remaining part was maintained at -80°C for further immunoprecipitation.

Shearing assessment was performed by adding 50µl TE elution and RNAse A (Thermo Fisher Scientific, cat. EN0531) for 1 hour at 55°C. Subsequently, chromatin was decross-linked with proteinase K (Life Technologies, cat. AM2546) overnight at 65°C. DNA was extracted by adding one volume of phenol/chloroform/isoamyl alcohol (25/24/1) to the sample and mixed vigorously for 30s. Samples were centrifuged at RT for 5 minutes at 16,000g. The aqueous phase was carefully removed and transferred to a new tube. 2.5 volumes of ice-cold 100% ethanol, 0.5 volumes of sodium acetate and 1µl of GlycoBlue™ Coprecipitant (Invitrogen, cat. AM9515) were added to the samples and incubated at -80°C for 2 hours. Samples were centrifuged for 30 minutes at 4°C at 16,000g. The supernatant was carefully removed and the DNA pellet was washed with 300µl with 70% ethanol. Samples were centrifuged for 10 minutes at 4°C at 16,000g. The supernatant was carefeully removed, and the DNA pellet was air-dried. The pellet was dissolved in 30µl TE elution buffer and DNA was quantified with

the Qubit™ dsDNA HS Assay Kit (Thermofisher, cat. Q32851). 300-600ng of DNA were analyzed on a 1.5% agarose gel to determine fragment sizes. Samples with fragments between 100bp and 600bps were used for subsequent magnetic immunoprecipitation.

Previously frozen sheared chromatin pellets were incubated overnight at 4°C under constant rotation with the corresponding ChIP reaction mix. Each ChIP reaction mix is corresponds to 1 immunoprecipitation of interest: anti-BRD4 (Bethyl Laboratories Inc., A301-985A50, 2µg/IP), anti-RNAPII (Cell Signalling Technology, CST14958, 1µg/IP), anti-CTCF (Diagenode Kit, 2µg/IP), anti-IgG (Diagenode Kit, 1µg/IP). Subsequently, immunoprecipitated DNA was eluted, decross-linked, and purified according to protocol. DNA was quantified with Qubit™ dsDNA HS Assay Kit for quality control purposes only. Immunoprecipitated DNA and corresponding INPUT were analyzed by qPCR analysis with primers of interest (Table 2, supplementary data).

Finally, the relative amount of immunoprecipitated DNA compared to INPUT DNA (% of recovery) was calculated.

2.10 Immunofluorescence analysis

Target cells were seeded on an open µ-Slide (chambered coverslip) with 8 wells (Vitaris, 80826) at defined densities (normally between 2,500-3,000 cells/well). Cells were treated with JQ1 and Doxycycline for 5 days prior TMZ and O6BG treatments. Subsequently, cells were incubated for 48 hours at 37°C, 5% CO_2. Cells were fixed with 4% PFA (Lifetechnologies, cat. 28908) for 15 minutes at RT, followed by permeabilization with 0.3% Triton-X for 15 minutes at RT. Cells were blocked at RT for 1 hours in blocking buffer (5% Donkey Serum, 0.5% BSA, 0.3% Triton-x-100).

Cells were incubated overnight at 4°C with γ-H2AX (Cell signaling, 2577, 1:800 in blocking buffer). Secondary Alex Fluor 647 (Thermofisher, A31573, 1:300 in blocking buffer) was added to cells for RT. Image acquisition was performed with Zeiss LSM 880 Airyscan at 40x magnification with oil. Fifteen images per condition were acquired and further analyzed with the Cell Profiler software. γ-H2AX was represented as integrated intensity obtained from an optimized images acquisition software pipeline.

2.11 Cell cycle analysis

0.25M LN-340 cells were seeded on a 10cm petri dishes per condition. Following 5 days JQ1 treatment, cells were treated with TMZ and O6BG for 48 hours before washing with PBS and fixation with ice-cold 70% ethanol overnight at 4°C. Subsequently, cells pellets were washed with ice-cold PBS and treated with 1mL Propidium Iodide solution (20µg/mL final concentration) (Sigma-Aldrich, P4864-10mL) and RNAse A. Following at least 4 hours incubation at 4°C (protected from light), cells were filtered via a 5mL round-bottom polystyrene test tube with a cell strainer snap cap designed for flow cytometry applications. Stained and filtered cells were immediately processed with the Gallios II Beckman Coulter (Flow Cytometry Facility - University of Lausanne). Cell cycle distribution was analyzed with the FlowJo software.

2.12 Cell viability analysis

Target cells were seeded on a 48-well plate at cell line-specific concentrations (normally between 2,000 and 3,000 cells per well). Cells were treated for 5 days with JQ1 and Doxycycline, followed by a 96 hours treatment with TMZ and O6BG. Subsequently, cells were stained with the CyQUANT Direct Cell Proliferation Assay Kit (Thermoscientific, cat. C35011). Following 1 hours incubation at 37°C 5%CO_2, cells were scanned, and fluorescence was measured with the SpectraMax® M Series Multi-Mode Microplate Readers.

2.13 IC50 analysis

3,000 target cells were seeded on a 96-well plate. Cells were treated for 72 hours with a 1:2 serial dilution form 12.8µM. Ultra-high dose of JQ1 was considered 0% viability, whereas DMSO only was considered 100% viability. Subsequently, cells were stained with the CyQUANT Direct Cell Proliferation Assay Kit. Following 1 hours incubation at 37°C 5%CO_2, cells were scanned, and fluorescence was measured with the SpectraMax® M Series Multi-Mode Microplate Readers. IC50 values were calculated with Graphpad Prism.

2.14 Cell Morphology analysis

Target cells were seeded on a 48-well plate at cell line-specific concentrations (normally between 2,000 and 3,000 cells per well). Cells were treated with JQ1 and cell proliferation was followed. Images were taken every 2 hours for 5 days with the live-cell imaging system Incucyte Zoom.

2.15 Analysis of *MGMT* expression in glioma lines

MGMT expression in glioma lines was assessed via affymetrix expression data from The Cancer Cell Line Encyclopedia (CCLE) [198]. RNA expression values were normalized and the background was corrected with R package affy. Results are shown for the most variable probe 204880_at.

2.16 Statistical analysis

Statistical analysis of the experiments was executed using GraphPad Prism 9 Software. For statistical tests, Student t-test was performed to compare variables between two groups. Two-way ANOVA to compare variables between multiple groups. Statistical significance is defined according to p-values, indicated by the asterisk symbol (*). (*) $P< 0.05$, (**) $p< 0.01$, (***) means $p<0.001$. (****) means $p<0.0001$. Data are shown as mean values. Error bars represent Standard Deviation (SD), unless otherwise indicated.

3. RESULTS

3.1 BET protein inhibition extensively modulates the DNA damage response signaling pathways in glioblastoma

Previously published RNA-seq data from our laboratory [167] have shown significant and extensive transcriptome changes over time in the GBM sphere line LN-2683GS treated with the BETi JQ1, a potent, reversible, and selective BETi of the BET family of bromodomain proteins [199].

Therefore, we later analyzed *in silico* the effect of JQ1 on the DDR genes modulation from the same dataset. Interestingly, we observed profound and yet heterogeneous DDR genes responses to BETi compared to DMSO control. Accordingly, JQ1 treatment revealed the existence of 6 distinct DDR genes response patterns. Only genes significantly associated with the interaction between treatment and time have been considered (Figure 3.1A).

Importantly, our analysis revealed that *MGMT* expression changes upon BETi followed pattern 4, with a rapid and significant downregulation over time compared to control. Moreover, given the fundamental role of a fully functional MMR system in the MGMT-mediated DNA repair pathway, we also looked at the potential modulation of key genes involved in the MMR system, such as *MSH6* and *MSH2*. We observed that both *MSH6* and *MSH2* followed pattern 3, with rapid downregulation upon BETi at early time points (6h and 12h). However, their expression was quickly restored to baseline at 24h post-treatment with JQ1, suggesting that BETi does not compromise the MMR system (Figure 3.1B).

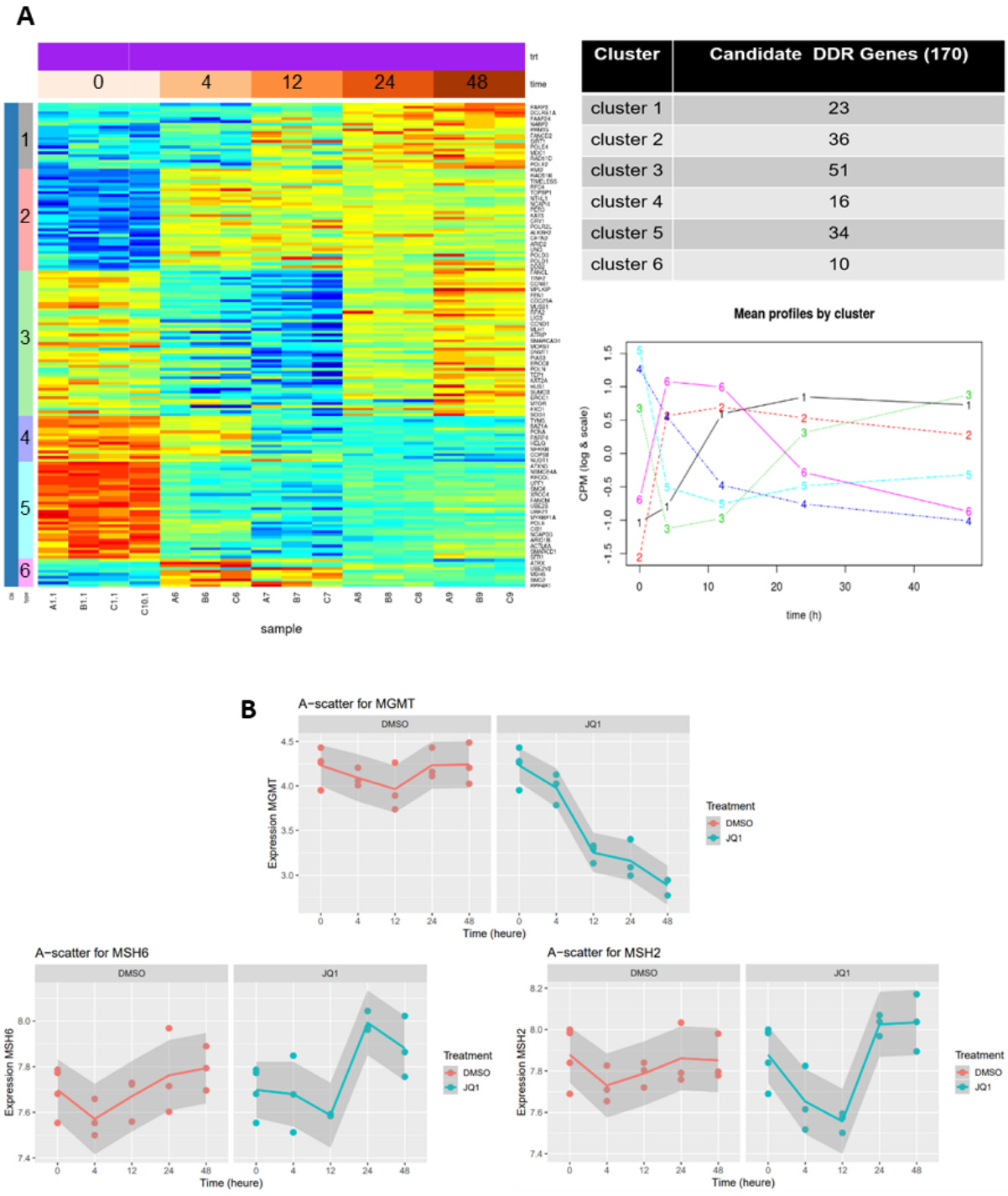

Cluster	Candidate DDR Genes (170)
cluster 1	23
cluster 2	36
cluster 3	51
cluster 4	16
cluster 5	34
cluster 6	10

Figure 3. 1 DDR genes response patterns upon BETi. (A) Heatmap and cluster profiles representation of the 6 response patterns of DDR genes from RNA-seq performed on LN-2683GS cells treated with 1 µM (+)-JQ1 or DMSO for 4, 12, 24, and 48 hours. The experiment includes 3 independent biological replicates. (B) Scatter plots showing *MGMT*, *MSH6* and *MSH2* expression changes upon BETi or DMSO over time were generated using the Fréchet distance measure.

3.2 BET protein inhibition reduces MGMT expression and halts its induction upon temozolomide treatment

Following the assessment of the different sensitivities (Figure S3.1A) and morphological changes (Figure S3.1B) of GBM cell lines in response to JQ1 treatment, we evaluated MGMT protein expression changes over time upon multiple JQ1 concentrations in highly MGMT positive lines (Figure S3.1C). We observed a significant downregulation of MGMT protein expression in multiple GBM models in a time- and dose-dependent fashion (Figure S3.1D). Interestingly, substantial protein expression changes were observed only after 72 hours of treatment, with the strongest effect after 120 hours.

Subsequently, we assessed relative *MGMT* expression changes upon BETi alone or combined with TMZ (Figure 3.2A). Our results confirmed that relative *MGMT* expression was strongly and rapidly downregulated upon JQ1 treatment over 5 days. Moreover, MGMT induction generally observed upon TMZ treatment alone was halted by BETi, and its expression level was kept significantly below baseline level, suggesting a maintenance of TMZ sensitivity in MGMT promoter unmethylated GBM lines. This behavior was also translated at the protein level (Figure 3.2B), and was consistent across different GBM lines tested, including GS lines (Figure S3.1E). Additionally, we regularly monitored relative Hexamethylene Bisacetamide Inducible 1 (*HEXIM1)* expression, a negative regulator of the P-TEFb [179]. Remarkably, *HEXIM1* was reported to be upregulated in a number of human malignancies upon BETi, such as neuroblastoma [200], diffuse large B cell lymphoma [201], and in GBM [160, 167]. Accordingly, *HEXIM1* was among the most upregulated genes upon JQ1 in the RNA-seq analysis performed in our laboratory [167]. As such, *HEXIM1* upregulation is considered a biomarker of BET proteins inhibition. Our results showed that *HEXIM1* was rapidly upregulated upon JQ1 treatment among all GBM lines tested, indicating the successful displacement of BET proteins on active enhancer and promoter regions.

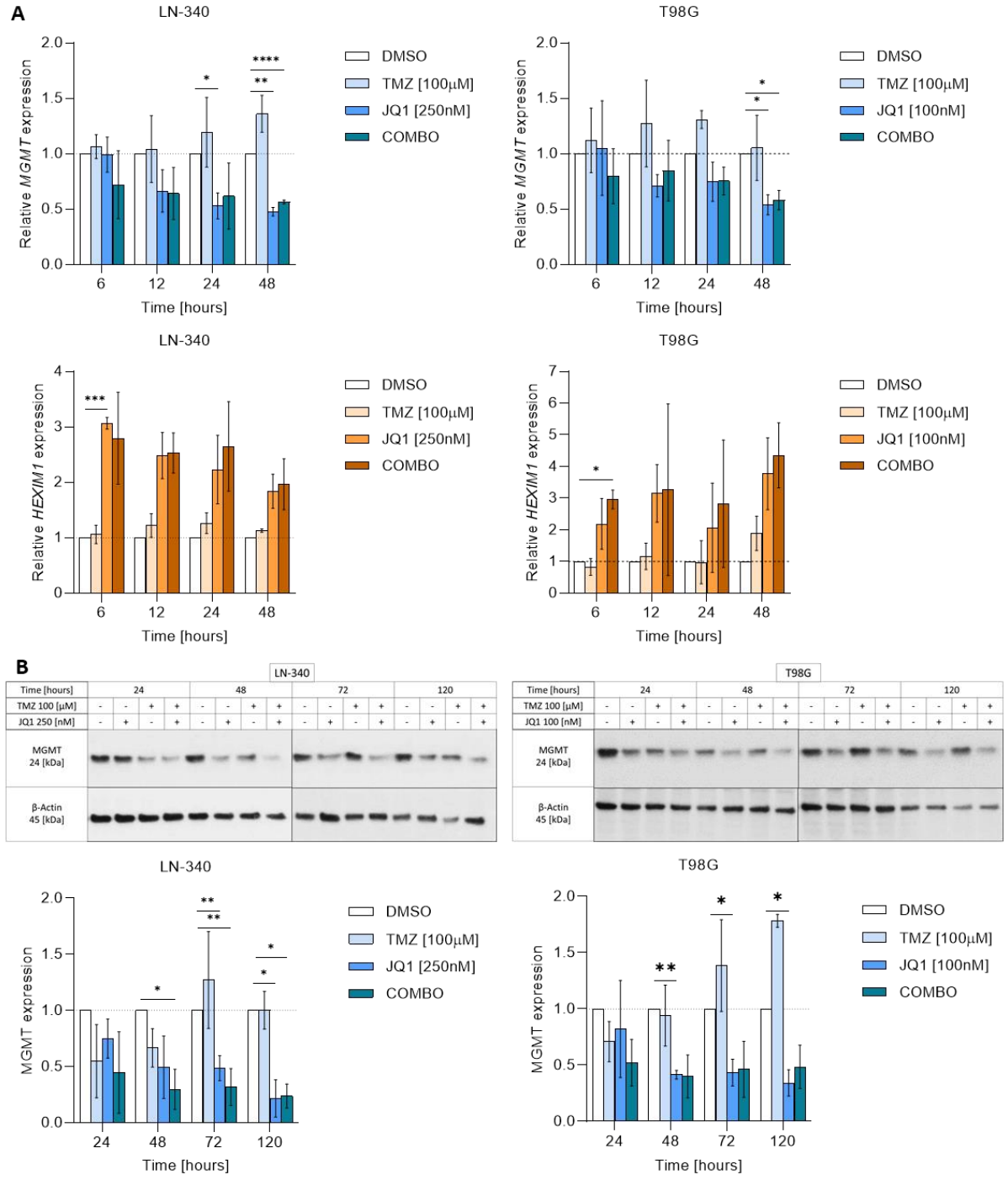

Figure 3. 2 BET protein inhibition reduces MGMT expression in GBM. (A) qRT-PCR analysis of relative *MGMT* and *HEXIM1* gene expression at 6, 12, 24 and 48 hours after treatment. Data represent 3 independent biological replicates. Data were normalized to the respective DMSO treatment for each time point (baseline). P-values were determined by two-way ANOVA test. Error bars are SD. * (p≤0.05), ** (P≤ 0.01), *** (P≤ 0.001) **** (P≤ 0.0001). (B) Protein expression analysis of MGMT and β-Actin (housekeeping) via western blot at 24, 48, 72 and 120 hours after treatment. 1 of 3 biological replicates is shown as representative figure. P-values were determined by two-way ANOVA test. Error bars are SD. * (p≤0.05), ** (P≤ 0.01), *** (P≤ 0.001) **** (P≤ 0.0001).

3.3 BET protein inhibition reduces BRD4 occupancy at the *MGMT* promoter region

To investigate whether *MGMT* expression is directly regulated through BRD4-mediated transcription, we performed ChIP-qPCR analysis for BRD4, a particularly well-studied member of the BET protein family. For this purpose, we treated the GBM cell line T98G for 2 hours with or without JQ1, and proceeded to evaluate BRD4 occupancy. Accordingly, we referred to previously tested *MGMT* promoter regions [1, 50], and specifically designed primers to investigate BRD4 occupancy to the *MGMT* promoter region F2 and F3, located within the promoter and the first exon CpG island (Figure 3.3A).

Data obtained thorugh ChIP-qPCR analysis demonstrated a robust and significant decrease in BRD4 occupancy to both MGMT promoter regions tested upon BETi, indicating a direct regulation of *MGMT* expression. Furthermore, we also evaluated RNA polymerase II (RNAP II) occupancy changes upon JQ1 treatment versus untreated (Figure 3.3B). Notably, Hogg and others [152] have revealed that BRD4 is rapidly recruited to the *CD274* locus, resulting in an increased H3K27Ac and RNAP II occupancy. Therefore, we considered RNAP II a biomarker for active DNA-directed mRNA synthesis. Interstingly, we detected a significant RNAP II occupancy decrease from both *MGMT* promoter regions tested, indicating an arrest in the *MGMT* transcription process.

The experiment also included negative (IgG) and positive (CTCF) control antibody to monitor the efficiency of each ChIP reaction, togheter with qPCR primer pairs for amplification of H19 imprinting control region and Myoglobin exon 2 as positive and a negative control target for CTCF, respectively. Accordingly, CTCF occupancy was highly detected for H19 but not in Myoglobin exon 2.

Overall, our results confirmed that *MGMT* synthesis is halted upon BETi due to the direct decrease in BRD4 occupancy at the promoter region.

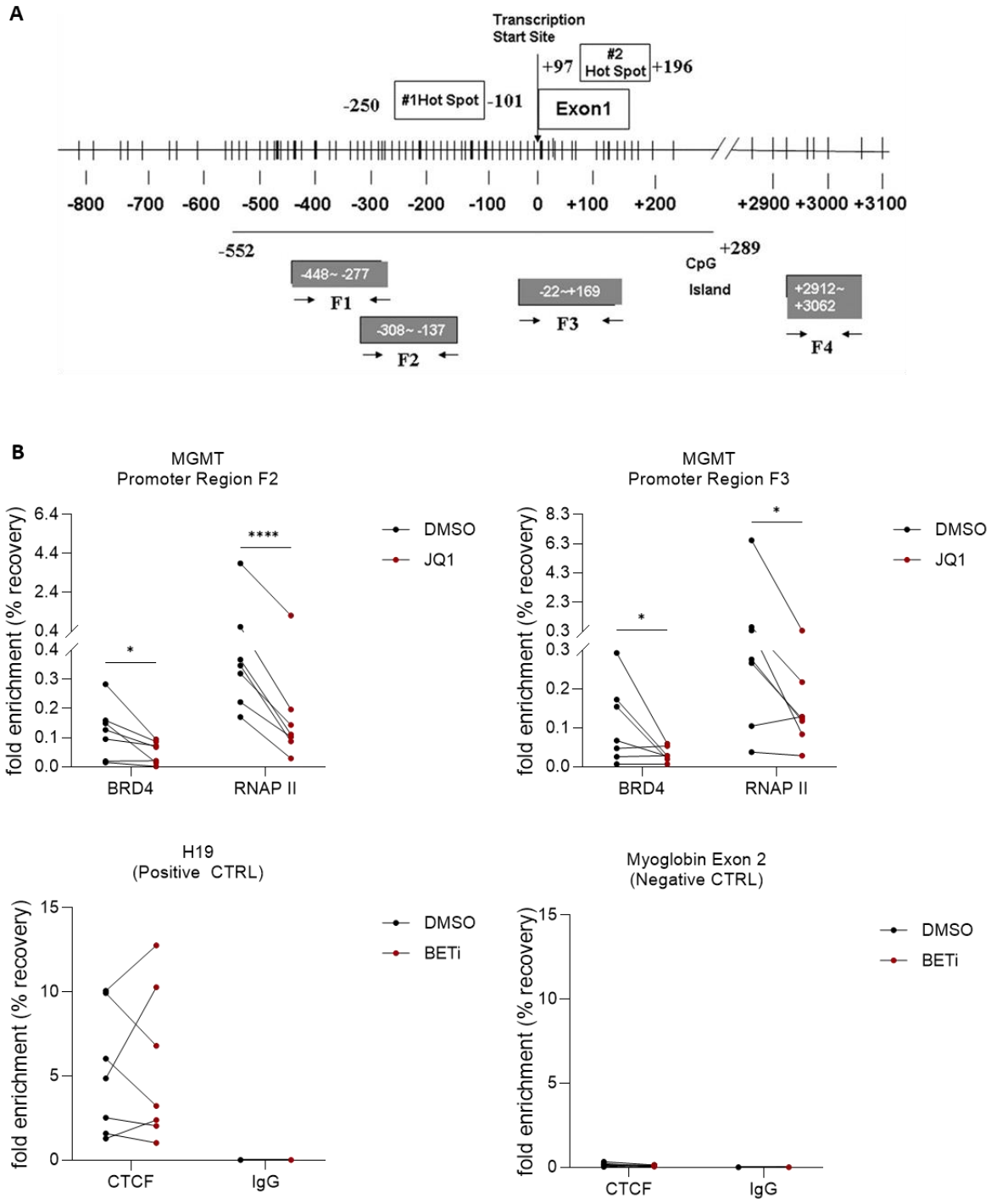

Figure 3. 3 BRD4 occupancy at the *MGMT* promoter region is reduced upon BETi. (A) Schematic representation of the CpG island of *MGMT* promoter [1]. Each CpG dinucleotide is represented with a vertical bar. F2 and F3 represent regions selected for ChIP-qPCR analysis. (B) T98G cells were treated for 2 hours with or without 1µM JQ1. BRD4 and RNAP II occupancy on both F2 and F3 regions are represented as enrichment (%input). Positive control CTCF and negative control IgG were included in the experiment alongside with qPCR primer pairs for amplification of H19 imprinting control region and Myoglobin exon 2 as positive and a negative control target for CTCF, respectively. The experiment includes 7 independent biological replicates. P-values were determined by Student t-test. * ($p<0.05$), **** ($p< P \leq 0.0001$).

3.4 BET protein inhibition modulates repair of TMZ-induced DNA damage

In light of the direct downregulation of *MGMT* upon BETi in GBM lines, we investigated the role of BET protein inhibition in modulating the TMZ-induced DNA damage response. We treated the MGMT expressing GBM line LN-340 with TMZ alone or in combination with BETi, and we monitored gamma-H2AX level as a marker to assess DNA double-strand breaks (DSBs). Endogenous or exogenous agents causing DSBs are always associated [202] with the phosphorylation of the histone H2AX (gamma-H2AX). This event is among the first steps that initiate the recruitment of DNA repair proteins.

Interestingly, we observed that LN-340 has a higher increase in gamma-H2AX levels in TMZ treatment combined with JQ1 compared to TMZ alone, indicating that depletion of MGMT upon JQ1 led to an increase in DSBs formation following TMZ treatment (Figure 3.4A). Moreover, we also treated GBM cells with the potent MGMT-specific inhibitor O^6-benzylguanine (O6BG) to show the extent of MGMT dependency in GBM cells. Indeed, LN-340 cells treated with O6BG in combination with TMZ showed a robust increase in DSBs rate compared to TMZ treatment alone. However, the use of O6BG in JQ1 treated cells did not further sensitize cells to TMZ, suggesting that MGMT protein levels were already low from BETi therapy.

Additionally, to support our findings on the BETi-directed regulation of *MGMT* expression and to confirm the key role of MGMT in conferring resistance to TMZ in GBM, we developed a doxycycline (dox)-inducible Tet-On system for MGMT in the GBM line LN-229 (Figure S3.2 A). Naturally, the latter does not express MGMT, and it is known to be highly sensitive to the use of TMZ [203-205]. Accordingly, we observed that LN-229MGMT^{ind}_C12 cells acquired a strong TMZ resistance phenotype upon MGMT induction via dox treatment. However, the use of O6BG significantly restored TMZ sensitivity. Furthermore, we investigated the role of BET protein inhibition in the dox-directed MGMT expression system. Notably, the use of JQ1 did not sensitize dox-treated LN-229MGMT^{ind}_C12 cells to TMZ treatment. As a matter of fact, MGMT expression in those cells is controlled by the dox-inducible Tet-On system only.

Therefore, BET protein inhibition did not influence MGMT expression or sensitivity to TMZ. Nevertheless, the pharmacological depletion of MGMT via O6BG treatment reversed the acquired TMZ resistance under dox again (Figure 3.4B).

Altogether, our data have shown that BETi induces more DNA DSBs in TMZ treated GBM compared to TMZ alone. Furthermore, our findings confirmed the pivotal role of MGMT in conferring resistance to TMZ in human GBM, and we observed that BET protein inhibition in the dox-induced MGMT model did not reverse MGMT-mediated TMZ resistance as in LN-340, where MGMT is endogenously expressed and directly regulated in part via BRD4.

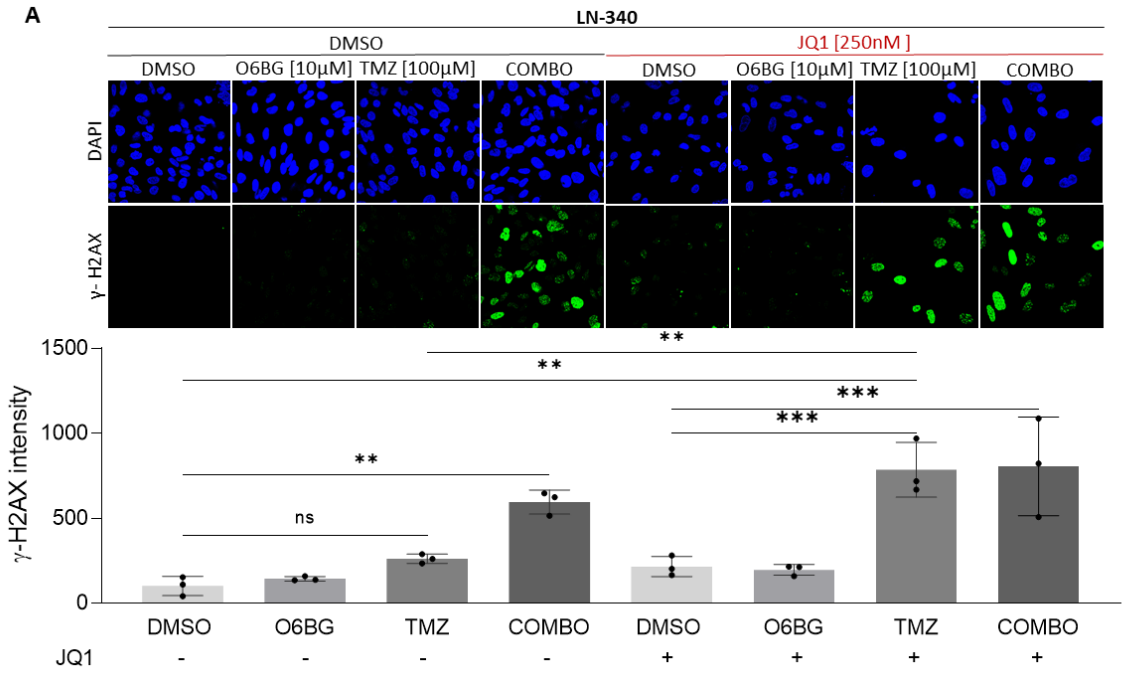

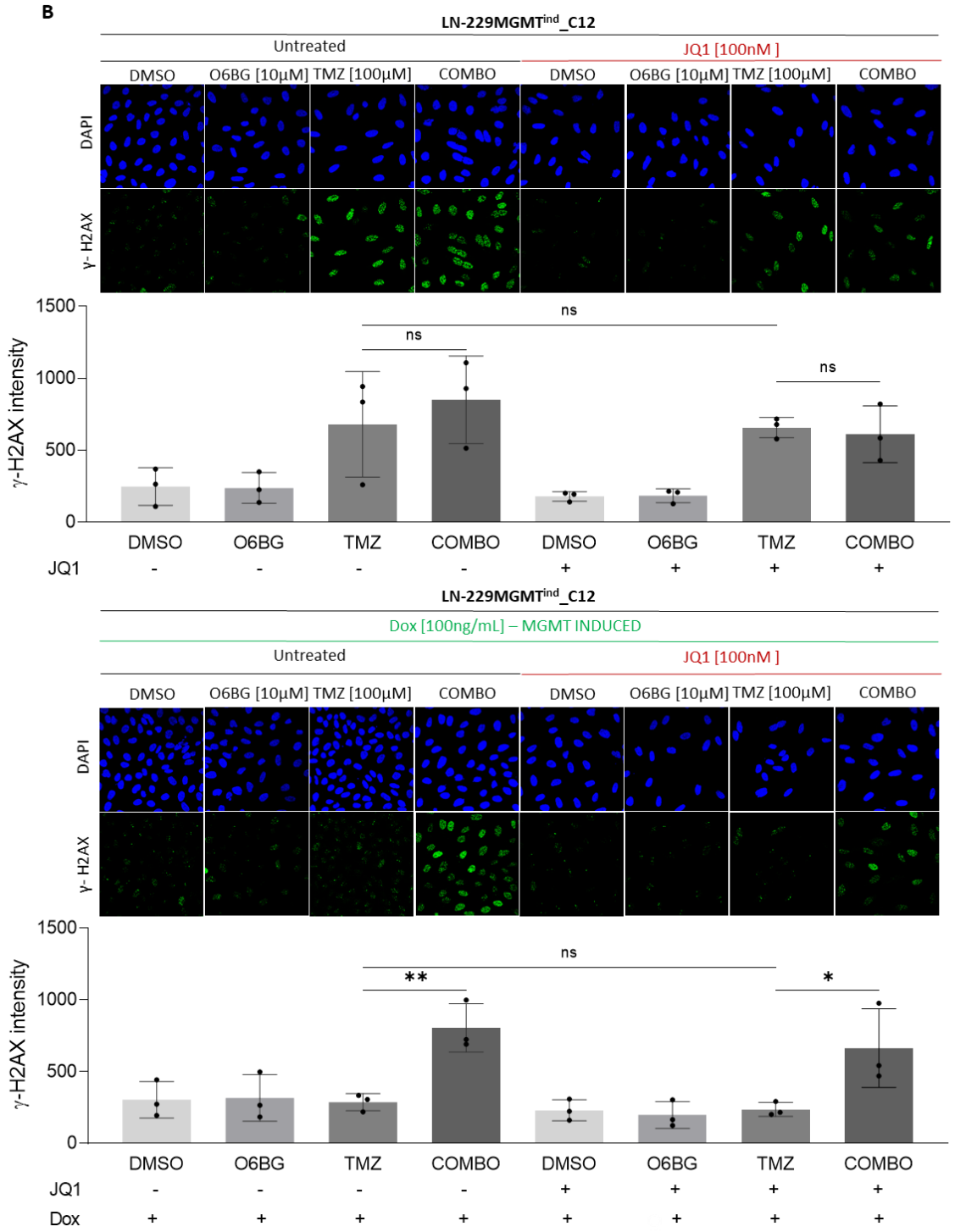

Figure 3. 4 BETi modulates repair of TMZ-induced DNA damage. (A) Mean gamma-H2AX integrated intensity analysis was performed on LN-340 and cells via immunofluorescence (IF). Cells were treated with JQ1 250nM for 5 days. On day 5, cells were treated with O6BG 10 µM together with TMZ 100µM. 2 additional TMZ treatments were given every 6 hours, for a total of 3 TMZ treatments on day 5. End-point was set at 48 hours after TMZ treatments. (B) Mean gamma-H2AX integrated intensity analysis was performed GBM line LN-229MGMTC12 via immunofluorescence (IF). Cells were treated with JQ1 100nM and doxycycline 100ng/mL for 5 days. On day 5, cells were treated with O6BG 10 µM together with TMZ 100µM. 2 additional TMZ treatments were given every 6 hours, for a total of 3 TMZ treatments on day 5. End-point was set at 48 hours after TMZ treatments. Data represent the mean from 3 independent biological experiments. P-values were determined by one-way ANOVA. * (p≤0.05), ** (p≤0.01), *** (P≤ 0.001). Error bars are SD.

3.5 BET protein inhibition increases S and G2/M phase cell cycle arrest in TMZ treated glioblastoma

In order to investigate the effect of BET protein inhibition on the cell cycle profile in TMZ treated GBM, we treated LN-340 cells with TMZ alone or in combination with BETi (Figure 3.5). We observed that TMZ alone did not alter the cell cycle profile compared to untreated. However, using O6BG in combination with TMZ had a strong impact in modulating the cell cycle profile of cells, with an increase in the S phase and G2/M phase cell cycle arrest. Interestingly, BETi was able to reverse TMZ resistance in LN-340 without the use of O6BG. We observed an increase in the S phase and G2/M phase cell cycle arrest in TMZ treatment following BETi compared to TMZ alone. Moreover, the use of O6BG in BETi treated cells did not have an additional impact on TMZ sensitivity.

Our results have shown that BETi induces more S and G2/M phase cell cycle arrest in TMZ treated GBM compared to TMZ treatment alone, which is consistent with our previous findings on the modulation of DNA DSBs.

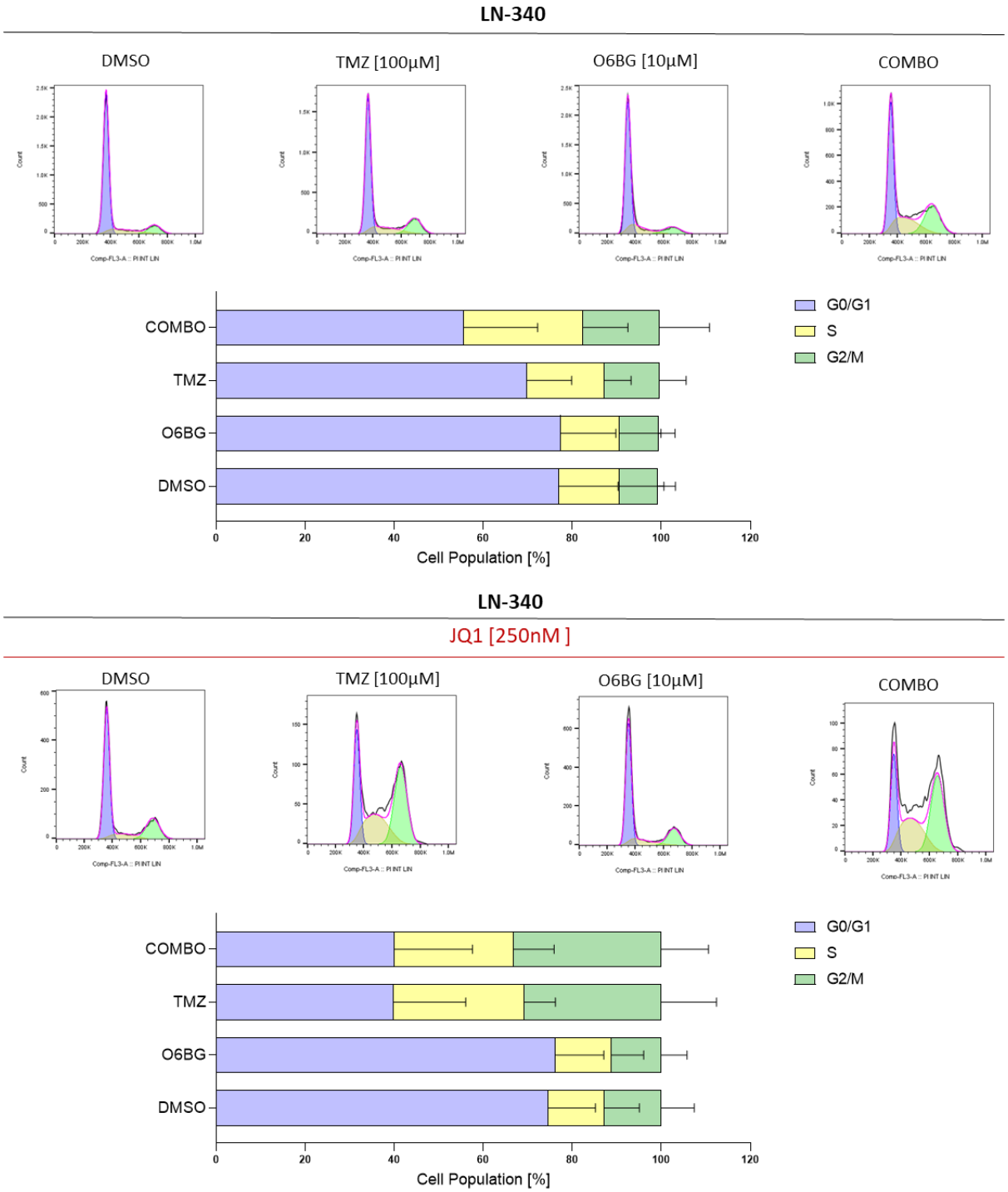

Figure 3. 5 BETi modulates the cell cycle profile in TMZ treated GBM. Analysis of the effect of BETi on the cell cycle profile of TMZ treated LN-340 cells was performed via DAPI staining and subsequent flow cytometry cell cycle analysis. Cells were treated with JQ1 250nM for 5 days. On day 5, cells were treated with O6BG 10 µM together with TMZ 100µM. 2 additional TMZ treatments were given every 6 hours, for a total of 3 TMZ treatments on day 5. The stacked bar charts represents the mean from 3 independent biological replicates. Error bars are SD.

3.6 BET protein inhibition impairs glioblastoma viability upon TMZ

Previous results on DNA DSBs rates and cell cycles profiles analysis suggested that the use of BETi might reduce MGMT-positive GBM viability to TMZ treatment. Consequently, we treated LN-340 and T98G with TMZ treatment alone or combined with BETi. We observed that TMZ alone had a modest impact in reducing cell viability in both lines; however, the addition of BETi in combination with TMZ had a significantly stronger cytotoxic effect on cells. Moreover, the use of O6BG had an essential role in increasing the sensitivity rate of GBM cells to TMZ treatment. However, the O6BG-driven effect was not observed in BETi treated cells, confirming the absence of MGMT in GBM under BETi treatment and the strong MGMT dependency in the context of TMZ-induced DNA repair in GBM (Figure 3.6A).

In order to further support the pivotal role of MGMT in GBM, we treated the previously described experimental model LN-229MGMT^{ind}_C12 inducible for MGMT. We reported that LN-229MGMT^{ind}_C12 was highly sensitive to TMZ treatment alone but became TMZ-resistant when MGMT was induced via doxycycline treatment. However, the pharmacological depletion of the dox-induced MGMT via O6BG restored TMZ sensitivity significantly (Figure 3.6B).

Our results confirmed that BETi largely sensitizes GBM cells expressing MGMT to TMZ and that MGMT plays a fundamental role in conferring resistance to TMZ.

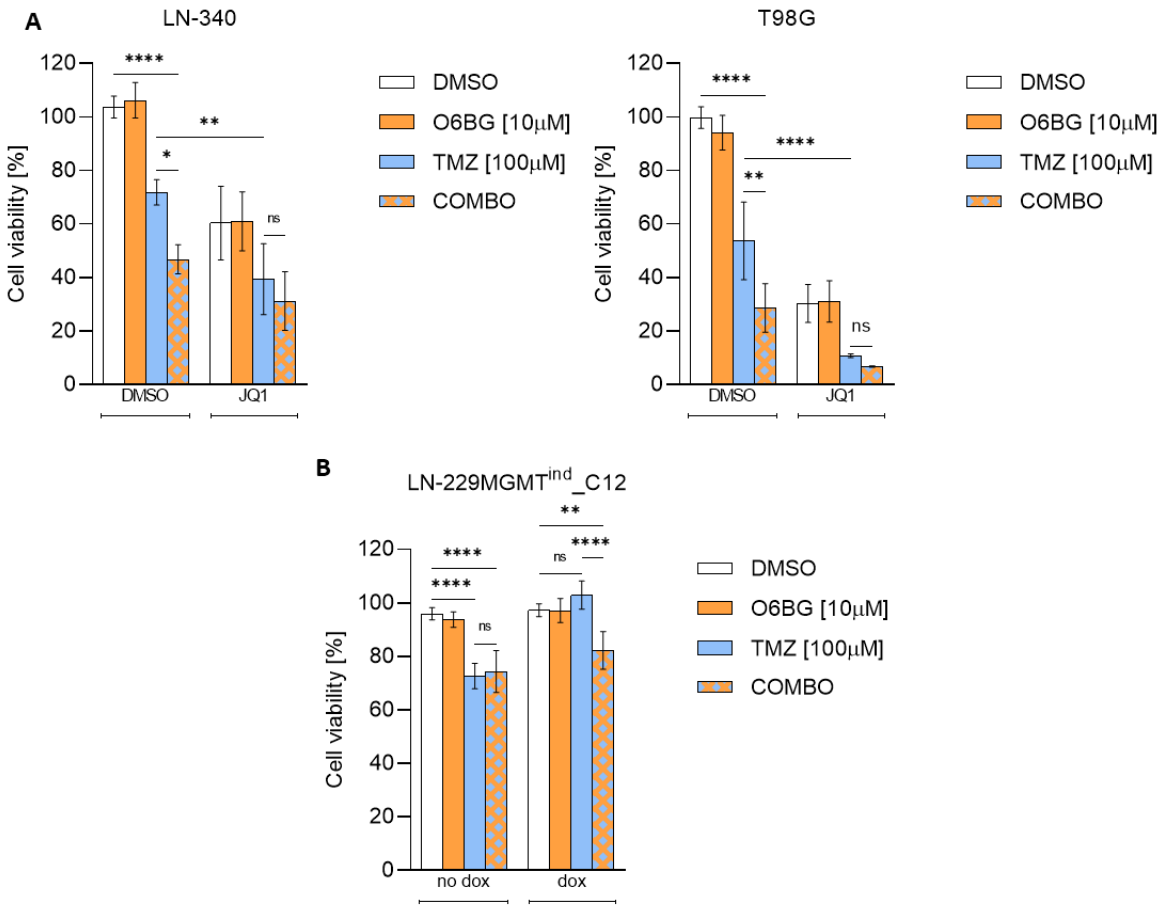

Figure 3. 6 BETi sensitizes GBM to TMZ. Percentage of cell viability analysis was performed on LN-340, T98G and LN-229MGMT^{ind}_C12. LN-340 cells were treated with JQ1 250nM, whereas T98G and LN-229MGMT^{ind}_C12 with JQ1 100nM, for 5 days. The latter was additionally treated with doxycycline 100ng/mL. On day 5, cells were treated with O6BG 10 µM together with TMZ 100µM. 2 additional TMZ treatments were given every 6 hours, for a total of 3 TMZ treatments on day 5. End-point was set at 96 hours after TMZ treatments. Data represent mean of 4 biological replicates. P-values were determined by two-way ANOVA test. Error bars are SD. * ($p \leq 0.05$), ** ($p \leq 0.01$), **** ($p < P \leq 0.0001$).

3.7 BET protein inhibition does not compromise the MMR system in glioblastoma

Given the pivotal role of the MMR system in the context of TMZ-mediated cytotoxicity, we aimed at investigating the effect of BETi on MSH6 and MSH2, two key components for the normal functioning of the MMR. A potential disruption in the MMR system would generate resistance to TMZ, even in the absence of MGMT. We observed that the use of BETi alone or in combination with TMZ did not significantly alter the protein expression levels of both MSH2 and MSH6 in LN-340 and T98G up to 5 days of treatment. The same was observed in GS lines (Figure S3.3A). Interestingly, we noticed the same specific response pattern upon BETi as the one from the RNA-seq previously reported in Figure 1, consisting of a modest initial decrease in expression, followed by a quick restoration to baseline. Thus, we concluded that BETi does not significantly impair the MMR pathway, avoiding unwanted TMZ resistance (Figure 3.7A).

To demonstrate the significant and substantial effect of a non-functional MMR pathway in conferring TMZ resistance, we developed in our primary experimental model LN-340 a dox-inducible Tet-On shRNA system targeting MSH6 and a non-targeting shRNA (Figure S3.3B). Accordingly, upon dox-mediated downregulation of MSH6, cells acquired strong resistance against TMZ treatment. Moreover, the depletion of MGMT via O6BG treatment did not significantly sensitize cells to TMZ, demonstrating that TMZ resistance is independent of MGMT in this scenario. On the contrary, dox-treated cells transduced with the non-targeting shRNA did not change behavior upon doxycycline (Figure 3.7B).

Finally, we demonstrated that the use of BETi in GBM does not negatively impact the MMR system, a potentially unwanted TMZ resistance mechanism.

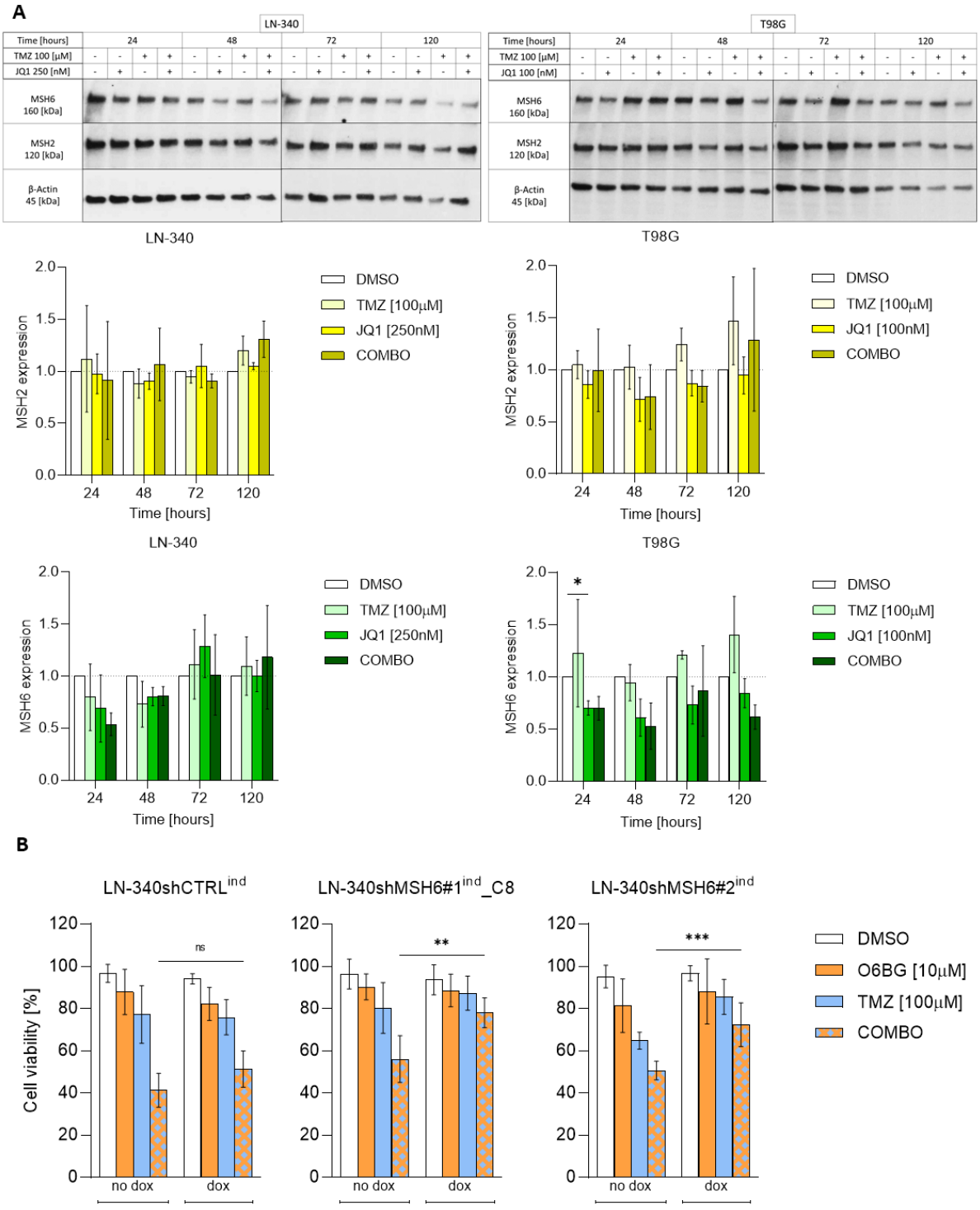

Figure 3. 7 BETi does not impair the MMR pathway in GBM. (A) Protein expression analysis of MSH6, MSH2 and β-Actin via WB at 24, 48, 72 and 120 hours after treatment. 1 of 3 biological replicates is shown as representative figure. Error bars are SD. * (p≤0.05). (B) Cell viability was performed on LN-340shCTRL^{ind} and LN-340shMSH6#1^{ind}_C8. Cells were treated with dox 500ng/mL for 5 days. On day 5, cells were treated with O6BG 10 μM together with TMZ 100μM. 2 additional TMZ treatments were given every 6 hours, for a total of 3 TMZ treatments on day 5. End-point was set at 96 hours after TMZ treatments. Data represent mean of 3 biological replicates.
P-values were determined by two-way ANOVA test. Error bars are SD. * (p≤0.05), *** (P≤ 0.001), **** (p< P ≤ 0.0001).

4. DISCUSSION & CONCLUSION

4.1 BETi modulation of the DDR signaling pathways

We observed that BETi dramatically and broadly shaped the DDR genes expression in GBM. Out of the 170 candidate DDR genes modulated by BETi in GBM, we focused on *MGMT* due to its essential clinical relevance in GBM patients. Surprisingly, *MGMT* was found significantly downregulated upon BETi, suggesting a potential novel therapeutic strategy to inhibit MGMT expression and sensitize patients to TMZ therapy, possibly extending survival. In addition to our study rationale focusing on MGMT, our data strongly suggests that BETi potentially generates additional vulnerabilities in GBM, as well as resistances worth exploring and exploiting.

We also reported that two key genes (*MSH6* and *MSH2*) in the MMR system were not compromised, suggesting that BETi does not impair the normal functioning of the MMR, an essential component in the context of MGMT-directed DNA repair. Of note, in addition to *MSH6* and *MSH2*, other components of the MMR pathway, such as *MLH1*, were also found in cluster 3. This suggests that BETi inhibition might have a similar effect on the entire MMR system, reinforcing the notion that BETi does not negatively impact the latter.

4.2 Modulation of MGMT upon BETi

Our results confirmed that MGMT expression is significantly downregulated upon BETi among multiple GBM lines, and its inhibitory effect was maintained in the presence of TMZ. To explain, the use of TMZ generally depleted MGMT in the first 24 to 48 hours. However, MGMT induction above baseline was quickly observed, particularly after 5 days post-treatment.

Interestingly, such upregulation or restoration of MGMT does not occur in BETi treated cells.

4.3 BRD4-directed downregulation of *MGMT*

Our data demonstrated that *MGMT* expression is directly regulated in part by BRD4 occupancy at the promoter region. Upon BETi, BRD4 gets displaced, and *MGMT* active transcription gets repressed. To further support this notion, we also reported that RNAP II occupancy is significantly reduced at the promoter region upon BETi.

Considering the vastness of the epigenome and the large regulatory mechanisms involved in gene expression, the role of additional marks could be studied to expand insights regarding the regulation of MGMT in the context of BETi. For example, H3K27ac is an epigenetic modification mark that indicates genomic regions associated with high activation of transcription; particularly, it is well recognized as a marker for active enhancers [206]. Distal enhancer regions regulating *MGMT* expression were reported by Chen and others in 2018, describing a novel enhancer region of MGMT located between the promoter of Ki67 and MGMT. Therefore, it would be of interest to investigate the role of BRD4 occupancy in this region. Moreover, other epigenetic marks such as H3K4me3, associated with transcriptionally active promoter regions, and H3K27me3, associated with transcriptionally silent promoter regions, could be studied. Performing ChIP-seq could be particularly useful in this context, to have a more global and informative view.

4.4 The effects of BETi on DNA DSBs, cell cycle profile and viability

BETi, in combination with TMZ, demonstrated enhanced DNA DSBs levels compared to single therapy via MGMT downregulation. Moreover, the induction of MGMT in a naturally MGMT-negative GBM line conferred strong TMZ resistance. The expression of MGMT in LN-229MGMT^{ind}_C12 is solely under the control of doxycycline due to the Tet-on system, therefore, the use of BETi did not re-sensitized those cells to TMZ.

Accordingly, the cell cycle profile of MGMT-positive cells is in line with the latter, showing an increased S and G2/M phase cell cycle arrest in BETi treated cells under TMZ, compared to TMZ alone. Interestingly, we noticed that the magnitude of TMZ effect is much greater in BETi treated cells compared to cells pre-treated with O6BG followed by TMZ only. This might suggest that other factors may positively play a role in modulating the cell cycle profile in addition to the MGMT-dependent effect. For

instance, it would be of interest to investigate more cell cycle-specific components, such as cyclins. Finally, we have shown that combinatorial therapy, including BETi and TMZ, significantly impaired cell viability compared to single-agent therapy. In addition to the sensitization of GBM cells expressing MGMT to TMZ via BETi treatment, we have also reported that the use of O6BG in the context of BETi did not further sensitize cells to TMZ, confirming that there was little to no MGMT left to deplete.

4.5 Experimental GBM models: 2D vs 3D

To better represent the disease, it is important to include multiple GBM models in the study. Accordingly, in this project, we selected various GBM adherent lines, and GBM GS lines. Generally, GS lines are considered an experimental model that retains several cancer stem-cells properties and supposedly comprise glioma-initiating cells, compared to regular adherent lines. First, GS lines are normally found to retain *EGFR* amplification, a common feature found in about 50% of GBM cases [207]. Moreover, recent studies [167] have monitored the expression of neuronal differentiation marker beta-III tubulin (TUJ1) upon BETi. Interestingly, BETi induces the upregulation of TUJ1, indicating a differentiation-like phenotype in GS lines. Secondly, GS lines are known to grow very invasively in the brain of orthotopically injected immunodeficient mice, mimicking most clinical scenarios. Last, GS lines better recapitulate the original molecular subtype of the tumor. In order to maintain those stem-cell properties, GS lines must be cultured in a neurobasal medium in the absence of FBS, typically used for adherent lines.

Interestingly, we observed that MGMT modulation upon BETi alone or in combination with TMZ is consistent with the results obtained in adherent lines, as well as the MMR pathway functionality. However, we experienced a generally lower basal MGMT expression in GS lines compared to adherent lines. Accordingly, we noticed significantly lower MGMT dependencies in the context of TMZ treatment. To illustrate, among multiple lines tested in the optimization phase of the project, we observed that the higher the MGMT is expressed, the more the cells depend on it. MGMT depletion via O6BG treatment in GBM cells highly positive for MGMT, such as T98G, have important sensitization features to TMZ. On the contrary, depletion of MGMT in GBM

cells with a low MGMT expression, typically GS lines, did not substantially sensitize cells to TMZ. Although mechanistic details in this context have yet to be investigated, studies [208] have suggested that the chromatin landscape of GS lines mostly correlates with their adherent counterparts; however, differences can still be detected. Considering the major differences in culture conditions between GS lines and adherent lines, chromatin regulatory mechanisms might in part be directed by media components rather than cell type-specific characteristics only.

Therefore, in light of MGMT expression variances among patients, preclinical models, and their distinct sensitivity to TMZ, MGMT expression levels cutoffs should be considered in the context of TMZ therapy. Accordingly, a 2019 study [209] has proposed a *MGMT* promoter methylation cutoff to select patients in the context of TMZ treatment.

4.6 Tailoring BETi therapeutic window

We reported that GBM sensitivity upon BETi varied considerably among the different models tested, denoting their very distinct nature. For this reason, it is crucial to determine the BETi working concentration for each model under investigation in order to avoid unwanted over toxicities from BETi *per se*. On the contrary, BETi should be enough to provide a significant positive therapeutic contribution in the context of TMZ chemotherapy via sufficient MGMT downregulation. Therefore, an accurate concentration adjustment for each GBM model is required in this particular experimental context.

4.7 Limitation of the current study

To answer the multiple experimental questions proposed in this project, we used the BET protein inhibitor JQ1. The latter is considered an adequate tool drug to investigate *in vitro* questions; however, it is not clinically relevant mainly due to its short half-life [137]. Moreover, most BETi available are not BET subfamily specific; therefore, it represents a limitation in the context of the specific role and importance of each BRD subfamily component in modulating gene expression. Considering that BETi act at the whole epigenome level, a large number of pathways and signatures get altered. Therefore, the nature of cells gets dramatically modulated. As a result, it might get challenging defining and quantifying MGMT-independent mechanisms that potentially contribute to additional vulnerabilities or resistances. Nevertheless, sequencing technologies are certainly of use in this context to unravel scientific difficulties or doubts.

As previously mentioned, the use of ChIP-qPCR to demonstrate the direct effect of BETi on MGMT expression provides an accurate yet limiting view on MGMT expression regulation. Accordingly, ChIP-seq on multiple GS lines would provide a broader, more informative, and more reliable read-out of MGMT modulation upon BETi.

In addition to that, we have demonstrated that the MMR system does not get compromised upon BETi by monitoring MSH6 and MSH2 expression, given their fundamental role in the pathway. However, the MMR is composed of many more elements that should considered to fully explore and elucidate the effect of BETi on the whole system.

Finally, the study lacks *in vivo* translation so far. Considering the high clinical relevance of the investigation, demonstrating MGMT downregulation and prolonged survival of immunodeficient mice bearing GBM upon combinatorial treatment versus single therapy would largely strengthen the study hypothesis.

4.8 Perspectives

4.8.1 Global epigenetic changes analysis upon BETi

A key relevant experiment in the context of MGMT regulation, but also to investigate the general effect of BETi on the GBM epigenome, would be performing ChIP-seq in multiple GS lines. Most importantly, the BET subfamily member BRD4 would be main investigated target, as it would provide specific information on which regions are directly regulated by BET proteins. Moreover, RNAPII would also provide relevant insights into the transcriptional status of regions of interest. In addition to the analysis of important transcription factors, several histone marks such as H3K27ac, H3K4me3, and H3K27me3 could also be tested in order to potentially expand the current knowledge with novel and useful insights. Moreover, the potential implementation of ATAC-seq would increase insights on the chromatin accessibility landscape of BETi treated GBM cells, providing global and substantial information on DNA accessible regions in the context of BETi versus normal cells. In particular, implementing ATAC-seq analysis with ChIP-seq data on the active transcription marker RNAPII would further support the identification of open chromatin and active transcription genome-wide regions directly modulated by BET proteins. In addition to that, chromosome conformation capture techniques might be adopted to analyze the spatial organization of chromatin in cells. Specifically, it would be of interest to integrate knowledge on the number of interactions between promoter-enhancer regions and how the 3D spatial conformation changes upon BETi. A high-throughput sequencing would be possible via Hi-C technologies, to detect novel, balanced and abnormal chromosomal rearrangements in GBM cells under BETi.

Altogether, biological conclusions derived from one single sequencing platform may be confirmed with alternative sequencing technologies, to assess the consistency of results and increase reliability.

4.8.2 Validation of key results in an *in vivo* setting

We demonstrated *in vitro* that BETi directly represses MGMT expression and sensitizes GBM to TMZ therapy. However, given the high translatability of this project into the clinical neuro-oncology field, a number of key experiments must be validated in a mouse model to strengthen the study hypothesis. To illustrate, the validation of MGMT downregulation upon BETi in immunocompromised mice bearing GBM intracranially would be the first fundamental question that needs to be addressed. Subsequently, it would be essential to demonstrate that combinatorial therapy, including BETi and TMZ, significantly improves overall survival compared to single-agent therapy. Ideally, a clinically relevant BETi, such as the above-mentioned CC-90010, would be implemented to potentially facilitate clinical translation and provide important preclinical efficacy data, as well as safety and toxicity profiles.

4.8.3 Discovery of MGMT-independent therapeutic avenues

The promiscuous features of BETi to modulate the expression of multiple cancer-relevant genes may also open new therapeutic avenues for GBM cancer patients, independent of MGMT status. Considering that a large number of determinants causes resistance to the current standard of care, the profound epigenetic dysregulation caused by BETi may reveal new potentially targetable vulnerabilities. For example, the expression of receptor tyrosine kinases (RTKs), such as EGFR and FGFR, have been found particularly altered upon BETi in our RNA-seq analysis. RTKs are frequently deregulated in GBM; therefore, they are considered a target of interest.

4.8.4 Effective epigenetic combination therapies

We have demonstrated that the implementation of BETi in combination with the alkylating agent TMZ sensitizes MGMT-positive GBM. However, it would be interesting to test BETi in combination with other epigenetic therapies. For instance, Gusyatiner and others [167] have demonstrated that BETi synergizes with HDAC inhibitors in GBM. Therefore, there is an excellent window of opportunities for rational combinatorial epigenetic therapies, considering the large number of different epigenetic drugs available.

4.8.5 Modulation of the GBM microenvironment upon BETi

Some previously described studies have reported that BETi have an essential effect on the GBM microenvironment. In particular, recent investigations [167] have shown repression of interferon-stimulated genes expression upon BETi, including *CD274* (PD-L1). Therefore, it would be relevant to study GBM cells co-cultured with relevant immune cells, such as macrophages and T cells, to explore the role of BETi in this context. Moreover, the use of immunocompetent mouse models bearing murine GBM could also provide additional insights into the effect of BETi on the microenvironment.

4.9 Conclusion

Altogether, we have demonstrated that TMZ resistance typically observed in GBM patients expressing MGMT can be counteracted with the use of BETi, which directly halt MGMT expression and induction. Therefore, novel small molecule inhibitors of BET proteins represent a promising tool to enhance response to TMZ treatment in GBM patients that express MGMT, potentially improving overall survival.

5. REFERENCES

1. Ji, W., et al., *Epigenetic silencing of O6-methylguanine DNA methyltransferase gene in NiS-transformed cells.* Carcinogenesis, 2008. **29**(6): p. 1267-75.

2. Capper, D., et al., *DNA methylation-based classification of central nervous system tumours.* Nature, 2018. **555**(7697): p. 469-474.

3. Wang, Q., et al., *Tumor evolution of glioma-intrinsic gene expression subtypes associates with immunological changes in the microenvironment.* Cancer Cell, 2017. **32**(1): p. 42-56 e6.

4. Wick, W., et al., *MGMT testing--the challenges for biomarker-based glioma treatment.* Nat Rev Neurol, 2014. **10**(7): p. 372-85.

5. Weller, M., et al., *EANO guidelines on the diagnosis and treatment of diffuse gliomas of adulthood.* Nat Rev Clin Oncol, 2021. **18**(3): p. 170-186.

6. Hegi, M.E., et al., *MGMT gene silencing and benefit from temozolomide in glioblastoma.* N Engl J Med, 2005. **352**(10): p. 997-1003.

7. Stathis, A. and F. Bertoni, *BET proteins as targets for anticancer treatment.* Cancer Discov, 2018. **8**(1): p. 24-36.

8. Gusyatiner, O. and M.E. Hegi, *Glioma epigenetics: From subclassification to novel treatment options.* Semin Cancer Biol, 2018. **51**: p. 50-58.

9. Ostrom, Q.T., et al., *CBTRUS statistical report: Primary brain and other central nervous system tumors diagnosed in the United States in 2012-2016.* Neuro Oncol, 2019. **21**(Supplement_5): p. v1-v100.

10. Louis, D.N., et al., eds. *WHO Classification of tumours of the central nervous system*. Revised 4th edition ed. World Health Organization classification of tumours, ed. F.T. Bosman, et al. 2016, IARC: Lyon.

11. Phillips, H.S., et al., *Molecular subclasses of high-grade glioma predict prognosis, delineate a pattern of disease progression, and resemble stages in neurogenesis.* Cancer Cell, 2006. **9**(3): p. 157-73.

12. Louis, D.N., et al., *The 2021 WHO classification of tumors of the central nervous system: a summary.* Neuro Oncol, 2021. **23**(8): p. 1231-1251.

13. Dang, L., et al., *Cancer-associated IDH1 mutations produce 2-hydroxyglutarate.* Nature, 2009. **462**(7274): p. 739-44.

14. Christians, A., et al., *The prognostic role of IDH mutations in homogeneously treated patients with anaplastic astrocytomas and glioblastomas.* Acta Neuropathologica Communications, 2019. **7**(1): p. 156.

15. Verhaak, R.G., et al., *Integrated genomic analysis identifies clinically relevant subtypes of glioblastoma characterized by abnormalities in PDGFRA, IDH1, EGFR, and NF1.* Cancer Cell, 2010. **17**(1): p. 98-110.

16. Lee, J.K., et al., *Spatiotemporal genomic architecture informs precision oncology in glioblastoma.* Nat Genet, 2017. **49**(4): p. 594-599.

17. Patel, A.P., et al., *Single-cell RNA-seq highlights intratumoral heterogeneity in primary glioblastoma.* Science, 2014. **344**(6190): p. 1396-401.

18. Wang, J., et al., *Clonal evolution of glioblastoma under therapy.* Nat Genet, 2016. **48**(7): p. 768-76.

19. Stupp, R., et al., *Radiotherapy plus concomitant and adjuvant temozolomide for glioblastoma.* N Engl J Med, 2005. **352**(10): p. 987-996.

20. Kirkpatrick, D.B., *The first primary brain-tumor operation.* J Neurosurg, 1984. **61**(5): p. 809-13.

21. Chaichana, K.L., et al., *Establishing percent resection and residual volume thresholds affecting survival and recurrence for patients with newly diagnosed intracranial glioblastoma.* Neuro Oncol, 2014. **16**(1): p. 113-22.

22. Brown, T.J., et al., *Association of the Extent of Resection With Survival in Glioblastoma: A Systematic Review and Meta-analysis.* JAMA Oncol, 2016. **2**(11): p. 1460-1469.

23. Molinaro, A.M., et al., *Association of Maximal Extent of Resection of Contrast-Enhanced and Non-Contrast-Enhanced Tumor With Survival Within Molecular Subgroups of Patients With Newly Diagnosed Glioblastoma.* JAMA Oncol, 2020.

24. Stummer, W., et al., *Fluorescence-guided surgery with 5-aminolevulinic acid for resection of malignant glioma: a randomised controlled multicentre phase III trial.* The Lancet Oncology, 2006. **7**(5): p. 392-401.

25. Ringel, F., et al., *Clinical benefit from resection of recurrent glioblastomas: results of a multicenter study including 503 patients with recurrent glioblastomas undergoing surgical resection.* Neuro Oncol, 2016. **18**(1): p. 96-104.

26. Suchorska, B., et al., *Complete resection of contrast-enhancing tumor volume is associated with improved survival in recurrent glioblastoma-results from the DIRECTOR trial.* Neuro Oncol, 2016. **18**(4): p. 549-56.

27. Chaichana, K.L., et al., *Multiple resections for patients with glioblastoma: prolonging survival.* J Neurosurg, 2013. **118**(4): p. 812-20.

28. Nava, F., et al., *Survival effect of first- and second-line treatments for patients with primary glioblastoma: a cohort study from a prospective registry, 1997-2010.* Neuro Oncol, 2014. **16**(5): p. 719-27.

29. Gorlia, T., et al., *New prognostic factors and calculators for outcome prediction in patients with recurrent glioblastoma: A pooled analysis of EORTC Brain Tumour Group phase I and II clinical trials.* Eur J Cancer, 2012. **48**(8): p. 1176-84.

30. Tan, A.C., et al., *Management of glioblastoma: State of the art and future directions.* CA: A Cancer Journal for Clinicians, 2020. **70**(4): p. 299-312.

31. Cabrera, A.R., et al., *Radiation therapy for glioblastoma: Executive summary of an American Society for Radiation Oncology Evidence-Based Clinical Practice Guideline.* Pract Radiat Oncol, 2016. **6**(4): p. 217-225.

32. Stupp, R., et al., *Effects of radiotherapy with concomitant and adjuvant temozolomide versus radiotherapy alone on survival in glioblastoma in a randomised phase III study: 5-year analysis of the EORTC-NCIC trial.* Lancet Oncol, 2009. **10**(5): p. 459-66.

33. Stupp, R., et al., *Effect of tumor-treating fields plus maintenance temozolomide vs maintenance temozolomide alone on survival in patients with glioblastoma: A randomized clinical trial.* JAMA, 2017. **318**(23): p. 2306-2316.

34. van Breemen, M.S., et al., *Efficacy of anti-epileptic drugs in patients with gliomas and seizures.* J Neurol, 2009. **256**(9): p. 1519-26.

35. Schiff, D., et al., *Medical management of brain tumors and the sequelae of treatment.* Neuro Oncol, 2015. **17**(4): p. 488-504.

36. Le Rhun, E., et al., *Molecular targeted therapy of glioblastoma.* Cancer Treat Rev, 2019. **80**: p. 101896.

37. Lim, M., et al., *Current state of immunotherapy for glioblastoma.* Nature Reviews Clinical Oncology, 2018. **15**(7): p. 422-442.

38. Wick, W., et al., *Lomustine and Bevacizumab in Progressive Glioblastoma.* N Engl J Med, 2017. **377**(20): p. 1954-1963.

39. Gilbert, M.R., E.P. Sulman, and M.P. Mehta, *Bevacizumab for newly diagnosed glioblastoma.* N Engl J Med, 2014. **370**(21): p. 2048-9.

40. Chinot, O.L., et al., *Bevacizumab plus radiotherapy-temozolomide for newly diagnosed glioblastoma.* N Engl J Med, 2014. **370**(8): p. 709-22.

41. Reardon, D.A., et al., *Randomized phase 3 study evaluating the efficacy and safety of nivolumab vs bevacizumab in patients with recurrent glioblastoma: CheckMate 143.* Neuro Oncol, 2017. **19**(Suppl. 3).

42. Sampson, J.H., et al., *Preliminary safety and activity of nivolumab and its combination with ipilimumab in recurrent glioblastoma (GBM): CHECKMATE-143.* Journal of Clinical Oncology, 2015. **33**(15_suppl): p. 3010-3010.

43. Reardon, D.A., et al., *Effect of Nivolumab vs Bevacizumab in Patients With Recurrent Glioblastoma: The CheckMate 143 Phase 3 Randomized Clinical Trial.* JAMA Oncol, 2020. **6**(7): p. 1003-1010.

44. Lim, M., et al., *Nivolumab (nivo) in combination with radiotherapy (RT) ± temozolomide (TMZ): Updated safety results from CheckMate 143 in pts with methylated or unmethylated newly diagnosed glioblastoma (GBM).* Annals of Oncology, 2017. **28**: p. v109.

45. Huang, B., et al., *Current Immunotherapies for Glioblastoma Multiforme.* Frontiers in Immunology, 2021. **11**(3890).

46. Goth, R. and M.F. Rajewsky, *Persistence of O6-ethylguanine in rat-brain DNA: correlation with nervous system-specific carcinogenesis by ethylnitrosourea.* Proc Natl Acad Sci U S A, 1974. **71**(3): p. 639-43.

47. Goth-Goldstein, R., *Inability of Chinese hamster ovary cells to excise O6-alkylguanine.* Cancer Res, 1980. **40**(7): p. 2623-4.

48. Srivenugopal, K.S., et al., *Ubiquitination-dependent proteolysis of O6-methylguanine-DNA methyltransferase in human and murine tumor cells following inactivation with O6-benzylguanine or 1,3-bis(2-chloroethyl)-1-nitrosourea.* Biochemistry, 1996. **35**(4): p. 1328-34.

49. Esteller, M., et al., *Inactivation of the DNA repair gene O6-methylguanine-DNA methyltransferase by promoter hypermethylation is a common event in primary human neoplasia.* Cancer Res, 1999. **59**(4): p. 793-7.

50. Sciuscio, D., et al., *Extent and patterns of MGMT promoter methylation in glioblastoma- and respective glioblastoma-derived spheres.* Clin Cancer Res, 2011. **17**(2): p. 255-66.

51. Weller, M., et al., *MGMT promoter methylation in malignant gliomas: ready for personalized medicine?* Nat Rev Neurol, 2010. **6**(1): p. 39-51.

52. Wick, W., et al., *MGMT testing—the challenges for biomarker-based glioma treatment.* Nature Reviews Neurology, 2014. **10**(7): p. 372-385.

53. Moen, E.L., et al., *The role of gene body cytosine modifications in MGMT expression and sensitivity to temozolomide.* Mol Cancer Ther, 2014. **13**(5): p. 1334-44.

54. Nakagawachi, T., et al., *Silencing effect of CpG island hypermethylation and histone modifications on O6-methylguanine-DNA methyltransferase (MGMT) gene expression in human cancer.* Oncogene, 2003. **22**(55): p. 8835-44.

55. Zhao, W., et al., *The essential role of histone H3 Lys9 di-methylation and MeCP2 binding in MGMT silencing with poor DNA methylation of the promoter CpG island.* J Biochem, 2005. **137**(3): p. 431-40.

56. Filipowicz, W., et al., *Post-transcriptional gene silencing by siRNAs and miRNAs.* Curr Opin Struct Biol, 2005. **15**(3): p. 331-41.

57. Wang, J., et al., *miR-181b modulates glioma cell sensitivity to temozolomide by targeting MEK1.* Cancer Chemother Pharmacol, 2013. **72**(1): p. 147-58.

58. Zhang, W., et al., *miR-181d: a predictive glioblastoma biomarker that downregulates MGMT expression.* Neuro Oncol, 2012. **14**(6): p. 712-9.

59. Quintavalle, C., et al., *miR-221/222 Target the DNA Methyltransferase MGMT in Glioma Cells.* PLOS ONE, 2013. **8**(9): p. e74466.

60. Kreth, S., et al., *In human glioblastomas transcript elongation by alternative polyadenylation and miRNA targeting is a potent mechanism of MGMT silencing.* Acta Neuropathol, 2013. **125**(5): p. 671-81.

61. Everhard, S., et al., *Identification of regions correlating MGMT promoter methylation and gene expression in glioblastomas.* Neuro Oncol, 2009. **11**: p. 348-56.

62. Park, C.-K., et al., *The Changes in MGMT Promoter Methylation Status in Initial and Recurrent Glioblastomas.* Translational oncology, 2012. **5**(5): p. 393-397.

63. Chen, X., et al., *A novel enhancer regulates MGMT expression and promotes temozolomide resistance in glioblastoma.* Nat Commun, 2018. **9**(1): p. 2949.

64. Moody, C.L. and R.T. Wheelhouse, *The medicinal chemistry of imidazotetrazine prodrugs.* Pharmaceuticals (Basel), 2014. **7**(7): p. 797-838.

65. Reid, J.M., et al., *Pharmacokinetics of 3-methyl-(triazen-1-yl)imidazole-4-carboximide following administration of temozolomide to patients with advanced cancer.* Clin Cancer Res, 1997. **3**(12 Pt 1): p. 2393-8.

66. Friedman, H.S., T. Kerby, and H. Calvert, *Temozolomide and treatment of malignant glioma.* Clin Cancer Res, 2000. **6**(7): p. 2585-97.

67. Beranek, D.T., *Distribution of methyl and ethyl adducts following alkylation with monofunctional alkylating agents.* Mutation Research/Fundamental and Molecular Mechanisms of Mutagenesis, 1990. **231**(1): p. 11-30.

68. Tang, J.B., et al., *N-methylpurine DNA glycosylase and DNA polymerase beta modulate BER inhibitor potentiation of glioma cells to temozolomide.* Neuro Oncol, 2011. **13**(5): p. 471-86.

69. Thanasupawat, T., et al., *Dovitinib enhances temozolomide efficacy in glioblastoma cells.* Mol Oncol, 2017. **11**(8): p. 1078-1098.

70. Agnihotri, S., et al., *Alkylpurine-DNA-N-glycosylase confers resistance to temozolomide in xenograft models of glioblastoma multiforme and is associated with poor survival in patients.* J Clin Invest, 2012. **122**(1): p. 253-66.

71. Lim, A. and B.F. Li, *The nuclear targeting and nuclear retention properties of a human DNA repair protein O6-methylguanine-DNA methyltransferase are both required for its nuclear localization: the possible implications.* EMBO J, 1996. **15**(15): p. 4050-60.

72. Day, R.S., 3rd, et al., *Defective repair of alkylated DNA by human tumour and SV40-transformed human cell strains.* Nature, 1980. **288**(5792): p. 724-7.

73. Yarosh, D.B., et al., *Repair of O6-methylguanine in DNA by demethylation is lacking in Mer- human tumor cell strains.* Carcinogenesis, 1983. **4**(2): p. 199-205.

74. Kitange, G.J., et al., *Induction of MGMT expression is associated with temozolomide resistance in glioblastoma xenografts.* Neuro Oncol, 2009. **11**(3): p. 281-91.

75. Karran, P. and M. Bignami, *DNA damage tolerance, mismatch repair and genome instability.* Bioessays, 1994. **16**(11): p. 833-9.

76. Modrich, P. and R. Lahue, *Mismatch repair in replication fidelity, genetic recombination, and cancer biology.* Annu Rev Biochem, 1996. **65**: p. 101-33.

77. Duckett, D.R., et al., *Human MutSalpha recognizes damaged DNA base pairs containing O6-methylguanine, O4-methylthymine, or the cisplatin-d(GpG) adduct.* Proc Natl Acad Sci U S A, 1996. **93**(13): p. 6443-7.

78. Kaina, B., *Critical steps in alkylation-induced aberration formation.* Mutation Research/Fundamental and Molecular Mechanisms of Mutagenesis, 1998. **404**(1): p. 119-124.

79. Kaina, B. and M. Christmann, *DNA repair in personalized brain cancer therapy with temozolomide and nitrosoureas.* DNA Repair (Amst), 2019. **78**: p. 128-141.

80. Quiros, S., W.P. Roos, and B. Kaina, *Processing of O6-methylguanine into DNA double-strand breaks requires two rounds of replication whereas apoptosis is also induced in subsequent cell cycles.* Cell Cycle, 2010. **9**(1): p. 168-78.

81. Yip, S., et al., *MSH6 mutations arise in glioblastomas during temozolomide therapy and mediate temozolomide resistance.* Clin Cancer Res, 2009. **15**(14): p. 4622-9.

82. Felsberg, J., et al., *Promoter methylation and expression of MGMT and the DNA mismatch repair genes MLH1, MSH2, MSH6 and PMS2 in paired primary and recurrent glioblastomas.* International Journal of Cancer, 2011. **129**(3): p. 659-670.

83. McFaline-Figueroa, J.L., et al., *Minor Changes in Expression of the Mismatch Repair Protein MSH2 Exert a Major Impact on Glioblastoma Response to Temozolomide.* Cancer Res, 2015. **75**(15): p. 3127-38.

84. Cahill, D.P., et al., *Loss of the mismatch repair protein MSH6 in human glioblastomas is associated with tumor progression during temozolomide treatment.* Clin Cancer Res, 2007. **13**(7): p. 2038-45.

85. Gilbert, M.R., et al., *Dose-dense temozolomide for newly diagnosed glioblastoma: A randomized phase iii clinical trial.* J Clin Oncol, 2013. **31**(32): p. 4085-91.

86. Quinn, J.A., et al., *Phase II trial of temozolomide plus o6-benzylguanine in adults with recurrent, temozolomide-resistant malignant glioma.* J Clin Oncol, 2009. **27**(8): p. 1262-7.

87. Jansen, M., et al., *Hematoprotection and enrichment of transduced cells in vivo after gene transfer of MGMT(P140K) into hematopoietic stem cells.* Cancer Gene Ther, 2002. **9**(9): p. 737-46.

88. Adair, J.E., et al., *Extended Survival of Glioblastoma Patients After Chemoprotective HSC Gene Therapy.* Science Translational Medicine, 2012. **4**(133): p. 133ra57-133ra57.

89. Allis, C.D. and T. Jenuwein, *The molecular hallmarks of epigenetic control.* Nat Rev Genet, 2016. **17**(8): p. 487-500.

90. Meaney, M.J., *Epigenetics and the Biological Definition of Gene × Environment Interactions.* Child Development, 2010. **81**(1): p. 41-79.

91. Meaney, M.J. and A.C. Ferguson-Smith, *Epigenetic regulation of the neural transcriptome: the meaning of the marks.* Nature Neuroscience, 2010. **13**(11): p. 1313-1318.

92. Esteller, M., *Epigenetics in evolution and disease.* The Lancet, 2008. **372**: p. S90-S96.

93. Kouzarides, T., *Chromatin modifications and their function.* Cell, 2007. **128**(4): p. 693-705.

94. Audia, J.E. and R.M. Campbell, *Histone Modifications and Cancer.* Cold Spring Harbor perspectives in biology, 2016. **8**(4): p. a019521-a019521.

95. Arrowsmith, C.H., et al., *Epigenetic protein families: a new frontier for drug discovery.* Nat Rev Drug Discov, 2012. **11**(5): p. 384-400.

96. Baylin, S.B. and P.A. Jones, *A decade of exploring the cancer epigenome - biological and translational implications.* Nat Rev Cancer, 2011. **11**(10): p. 726-34.

97. Jones, P.A. and S.B. Baylin, *The epigenomics of cancer.* Cell, 2007. **128**(4): p. 683-92.

98. Paz, M.F., et al., *A systematic profile of DNA methylation in human cancer cell lines.* Cancer Res, 2003. **63**(5): p. 1114-21.

99. Kulis, M. and M. Esteller, *DNA methylation and cancer.* Adv Genet, 2010. **70**: p. 27-56.

100. Kusaba, H., et al., *Association of 5' CpG demethylation and altered chromatin structure in the promoter region with transcriptional activation of the multidrug resistance 1 gene in human cancer cells.* Eur J Biochem, 1999. **262**(3): p. 924-32.

101. Tada, Y., et al., *MDR1 Gene Overexpression and Altered Degree of Methylation at the Promoter Region in Bladder Cancer during Chemotherapeutic Treatment.* Clinical Cancer Research, 2000. **6**(12): p. 4618-4627.

102. Sharma, G., et al., *CpG hypomethylation of MDR1 gene in tumor and serum of invasive ductal breast carcinoma patients.* Clin Biochem, 2010. **43**(4-5): p. 373-9.

103. Hanahan, D. and Robert A. Weinberg, *Hallmarks of Cancer: The next generation.* Cell, 2011. **144**(5): p. 646-674.

104. Greger, V., et al., *Epigenetic changes may contribute to the formation and spontaneous regression of retinoblastoma.* Hum Genet, 1989. **83**: p. 155-158.

105. Bannister, A.J. and T. Kouzarides, *Regulation of chromatin by histone modifications.* Cell Res, 2011. **21**(3): p. 381-95.

106. Garraway, Levi A. and Eric S. Lander, *Lessons from the Cancer Genome.* Cell, 2013. **153**(1): p. 17-37.

107. Noushmehr, H., et al., *Identification of a CpG island methylator phenotype that defines a distinct subgroup of glioma.* Cancer Cell, 2010. **17**(5): p. 510-22.

108. Sturm, D., S.M. Pfister, and D.T.W. Jones, *Pediatric Gliomas: Current Concepts on Diagnosis, Biology, and Clinical Management.* J Clin Oncol, 2017. **35**(21): p. 2370-2377.

109. Ropero, S. and M. Esteller, *The role of histone deacetylases (HDACs) in human cancer.* Mol Oncol, 2007. **1**(1): p. 19-25.

110. Chinnaiyan, P., et al., *Modulation of radiation response by histone deacetylase inhibition.* International Journal of Radiation Oncology*Biology*Physics, 2005. **62**(1): p. 223-229.

111. Kim, M.S., et al., *Inhibition of histone deacetylase increases cytotoxicity to anticancer drugs targeting DNA.* Cancer Res, 2003. **63**(21): p. 7291-300.

112. Galanis, E., et al., *Phase II trial of vorinostat in recurrent glioblastoma multiforme: a north central cancer treatment group study.* J Clin Oncol, 2009. **27**(12): p. 2052-8.

113. Friday, B.B., et al., *Phase II trial of vorinostat in combination with bortezomib in recurrent glioblastoma: a north central cancer treatment group study.* Neuro Oncol, 2012. **14**(2): p. 215-21.

114. Galanis, E., et al., *Phase I/II trial of vorinostat combined with temozolomide and radiation therapy for newly diagnosed glioblastoma: results of Alliance N0874/ABTC 02.* Neuro Oncol, 2018. **20**(4): p. 546-556.

115. Kim, K.H. and C.W.M. Roberts, *Targeting EZH2 in cancer.* Nature Medicine, 2016. **22**(2): p. 128-134.

116. Zhang, J., et al., *EZH2 is a negative prognostic factor and exhibits pro-oncogenic activity in glioblastoma.* Cancer Lett, 2015. **356**(2 Pt B): p. 929-36.

117. Yin, Y., S. Qiu, and Y. Peng, *Functional roles of enhancer of zeste homolog 2 in gliomas.* Gene, 2016. **576**(1 Pt 2): p. 189-94.

118. Lewis, P.W., et al., *Inhibition of PRC2 activity by a gain-of-function H3 mutation found in pediatric glioblastoma.* Science, 2013. **340**(6134): p. 857-61.

119. Stazi, G., et al., *Dissecting the role of novel EZH2 inhibitors in primary glioblastoma cell cultures: effects on proliferation, epithelial-mesenchymal transition, migration, and on the pro-inflammatory phenotype.* Clinical Epigenetics, 2019. **11**(1): p. 173.

120. Turcan, S., et al., *Efficient induction of differentiation and growth inhibition in IDH1 mutant glioma cells by the DNMT Inhibitor Decitabine.* Oncotarget, 2013. **4**(10): p. 1729-36.

121. Borodovsky, A., et al., *5-azacytidine reduces methylation, promotes differentiation and induces tumor regression in a patient-derived IDH1 mutant glioma xenograft.* Oncotarget, 2013. **4**(10): p. 1737-47.

122. Kantarjian, H.M., et al., *Guadecitabine (SGI-110) in treatment-naive patients with acute myeloid leukaemia: phase 2 results from a multicentre, randomised, phase 1/2 trial.* Lancet Oncol, 2017. **18**(10): p. 1317-1326.

123. Zwergel, C., et al., *Identification of a novel quinoline-based DNA demethylating compound highly potent in cancer cells.* Clinical Epigenetics, 2019. **11**(1): p. 68.

124. Rohle, D., et al., *An inhibitor of mutant IDH1 delays growth and promotes differentiation of glioma cells.* Science, 2013. **340**(6132): p. 626-30.

125. Tateishi, K., et al., *Extreme vulnerability of IDH1 mutant cancers to nad+ depletion.* Cancer Cell, 2015. **28**(6): p. 773-84.

126. Tejera, D., et al., *Ivosidenib, an IDH1 inhibitor, in a patient with recurrent, IDH1-mutant glioblastoma: a case report from a Phase I study.* CNS Oncology, 2020. **9**(3): p. CNS62.

127. Mellinghoff, I.K., et al., *A phase I, open label, perioperative study of AG-120 and AG-881 in recurrent IDH1 mutant, low-grade glioma: Results from cohort 1.* Journal of Clinical Oncology, 2019. **37**(15_suppl): p. 2003-2003.

128. Natsume, A., et al., *Phase I study of a brain penetrant mutant IDH1 inhibitor DS-1001b in patients with recurrent or progressive IDH1 mutant gliomas.* Journal of Clinical Oncology, 2019. **37**(15_suppl): p. 2004-2004.

129. Fan, B., et al., *Clinical pharmacokinetics and pharmacodynamics of ivosidenib, an oral, targeted inhibitor of mutant IDH1, in patients with advanced solid tumors.* Investigational New Drugs, 2020. **38**(2): p. 433-444.

130. Dawson, M.A., T. Kouzarides, and B.J.P. Huntly, *Targeting Epigenetic Readers in Cancer.* New England Journal of Medicine, 2012. **367**(7): p. 647-657.

131. Belkina, A.C. and G.V. Denis, *BET domain co-regulators in obesity, inflammation and cancer.* Nature Reviews Cancer, 2012. **12**(7): p. 465-477.

132. Devaiah, B.N. and D.S. Singer, *Two faces of BRD4.* Transcription, 2013. **4**(1): p. 13-17.

133. Whyte, W.A., et al., *Master transcription factors and mediator establish super-enhancers at key cell identity genes.* Cell, 2013. **153**(2): p. 307-19.

134. Hnisz, D., et al., *Super-enhancers in the control of cell identity and disease.* Cell, 2013. **155**(4): p. 934-47.

135. Malik, S. and R.G. Roeder, *The metazoan Mediator co-activator complex as an integrative hub for transcriptional regulation.* Nature Reviews Genetics, 2010. **11**(11): p. 761-772.

136. Yang, Z., et al., *Recruitment of P-TEFb for Stimulation of Transcriptional Elongation by the Bromodomain Protein Brd4.* Molecular Cell, 2005. **19**(4): p. 535-545.

137. Filippakopoulos, P., et al., *Selective inhibition of BET bromodomains.* Nature, 2010. **468**(7327): p. 1067-73.

138. Spriano, F., A. Stathis, and F. Bertoni, *Targeting BET bromodomain proteins in cancer: The example of lymphomas.* Pharmacol Ther, 2020. **215**: p. 107631.

139. Cromm, P.M. and C.M. Crews, *Targeted Protein Degradation: from Chemical Biology to Drug Discovery.* Cell Chem Biol, 2017. **24**(9): p. 1181-1190.

140. Duan, Y., et al., *Targeting Brd4 for cancer therapy: inhibitors and degraders.* Medchemcomm, 2018. **9**(11): p. 1779-1802.

141. Jiang, F., et al., *Discovery of novel small molecule induced selective degradation of the bromodomain and extra-terminal (BET) bromodomain protein BRD4 and BRD2 with cellular potencies.* Bioorganic & Medicinal Chemistry, 2020. **28**(1): p. 115181.

142. Yang, H., et al., *BRD4: An emerging prospective therapeutic target in glioma.* Molecular Therapy - Oncolytics, 2021. **21**: p. 1-14.

143. Marcotte, R., et al., *Functional Genomic Landscape of Human Breast Cancer Drivers, Vulnerabilities, and Resistance.* Cell, 2016. **164**(1-2): p. 293-309.

144. Delmore, J.E., et al., *BET bromodomain inhibition as a therapeutic strategy to target c-Myc.* Cell, 2011. **146**(6): p. 904-17.

145. French, C.A., et al., *BRD4-NUT fusion oncogene: a novel mechanism in aggressive carcinoma.* Cancer Res, 2003. **63**(2): p. 304-7.

146. Yang, Z., N. He, and Q. Zhou, *Brd4 recruits P-TEFb to chromosomes at late mitosis to promote G1 gene expression and cell cycle progression.* Mol Cell Biol, 2008. **28**(3): p. 967-76.

147. Sinha, A., D.V. Faller, and G.V. Denis, *Bromodomain analysis of Brd2-dependent transcriptional activation of cyclin A.* Biochem J, 2005. **387**(Pt 1): p. 257-69.

148. Mochizuki, K., et al., *The bromodomain protein Brd4 stimulates G1 gene transcription and promotes progression to S phase.* J Biol Chem, 2008. **283**(14): p. 9040-8.

149. Lu, L., et al., *Inhibition of BRD4 suppresses the malignancy of breast cancer cells via regulation of Snail.* Cell Death & Differentiation, 2020. **27**(1): p. 255-268.

150. Dawson, M.A., et al., *Inhibition of BET recruitment to chromatin as an effective treatment for MLL-fusion leukaemia.* Nature, 2011. **478**(7370): p. 529-33.

151. Miller, A.L., et al., *The BET inhibitor JQ1 attenuates double-strand break repair and sensitizes models of pancreatic ductal adenocarcinoma to PARP inhibitors.* EBioMedicine, 2019. **44**: p. 419-430.

152. Hogg, S.J., et al., *BET-Bromodomain inhibitors engage the host immune system and regulate expression of the immune checkpoint ligand PD-L1.* Cell Rep, 2017. **18**(9): p. 2162-2174.

153. Dey, A., et al., *BRD4 directs hematopoietic stem cell development and modulates macrophage inflammatory responses.* The EMBO journal, 2019. **38**(7): p. e100293.

154. Gilan, O., et al., *Selective targeting of BD1 and BD2 of the BET proteins in cancer and immunoinflammation.* Science, 2020. **368**(6489): p. 387-394.

155. Kagoya, Y., et al., *BET bromodomain inhibition enhances T cell persistence and function in adoptive immunotherapy models.* J Clin Invest, 2016. **126**(9): p. 3479-94.

156. Adeegbe, D.O., et al., *Synergistic Immunostimulatory Effects and Therapeutic Benefit of Combined Histone Deacetylase and Bromodomain Inhibition in Non-Small Cell Lung Cancer.* Cancer Discov, 2017. **7**(8): p. 852-867.

157. Wang, H., et al., *JQ 1, a Selective Bromodomain Inhibitor, Decreased the Expression of the Tolerogenic Molecule PDL1 in Antigen-Presenting Cells (APCs) and Restores the Responsiveness of Anergic CD4+ T Cells.* Blood, 2014. **124**(21): p. 2749-2749.

158. Shorstova, T., W.D. Foulkes, and M. Witcher, *Achieving clinical success with BET inhibitors as anti-cancer agents.* British Journal of Cancer, 2021. **124**(9): p. 1478-1490.

159. Veneziani, I., et al., *The BET-bromodomain inhibitor JQ1 renders neuroblastoma cells more resistant to NK cell-mediated recognition and killing by downregulating ligands for NKG2D and DNAM-1 receptors.* Oncotarget, 2019. **10**(22): p. 2151-2160.

160. Berenguer-Daize, C., et al., *OTX015 (MK-8628), a novel BET inhibitor, displays in vitro and in vivo antitumor effects alone and in combination with conventional therapies in glioblastoma models.* Int J Cancer, 2016. **139**(9): p. 2047-55.

161. Lam, F.C., et al., *Enhanced efficacy of combined temozolomide and bromodomain inhibitor therapy for gliomas using targeted nanoparticles.* Nat Commun, 2018. **9**(1): p. 1991.

162. Cheng, Z., et al., *Inhibition of BET bromodomain targets genetically diverse glioblastoma.* Clin Cancer Res, 2013. **19**(7): p. 1748-59.

163. Wen, N., et al., *Bromodomain inhibitor jq1 induces cell cycle arrest and apoptosis of glioma stem cells through the VEGF/PI3K/AKT signaling pathway.* Int J Oncol, 2019. **55**(4): p. 879-895.

164. Zhang, Y., et al., *Combined HDAC and bromodomain protein inhibition reprograms tumor cell metabolism and elicits synthetic lethality in glioblastoma.* Clin Cancer Res, 2018. **24**(16): p. 3941-3954.

165. Cancer, M., et al., *BET and Aurora Kinase A inhibitors synergize against MYCN-positive human glioblastoma cells.* Cell Death Dis, 2019. **10**(12): p. 881.

166. Yao, Z., et al., *BET inhibitor I-BET151 sensitizes GBM cells to temozolomide via PUMA induction.* Cancer Gene Ther, 2019.

167. Gusyatiner, O., et al., *BET inhibitors repress expression of interferon-stimulated genes and synergize with HDAC inhibitors in glioblastoma.* Neuro Oncol, 2021. **23**(10): p. 1680-1692.

168. Amorim, S., et al., *Bromodomain inhibitor OTX015 in patients with lymphoma or multiple myeloma: a dose-escalation, open-label, pharmacokinetic, phase 1 study.* Lancet Haematol, 2016. **3**(4): p. e196-204.

169. Berthon, C., et al., *Bromodomain inhibitor OTX015 in patients with acute leukaemia: a dose-escalation, phase 1 study.* Lancet Haematol, 2016. **3**(4): p. e186-95.

170. Abramson, J.S., et al., *BET Inhibitor CPI-0610 Is Well Tolerated and Induces Responses in Diffuse Large B-Cell Lymphoma and Follicular Lymphoma: Preliminary Analysis of an Ongoing Phase 1 Study.* Blood, 2015. **126**(23).

171. Falchook, G., et al., *Development of 2 Bromodomain and Extraterminal Inhibitors With Distinct Pharmacokinetic and Pharmacodynamic Profiles for the Treatment of Advanced Malignancies.* Clinical Cancer Research, 2020. **26**(6): p. 1247-1257.

172. Stathis, A., et al., *Clinical Response of Carcinomas Harboring the BRD4-NUT Oncoprotein to the Targeted Bromodomain Inhibitor OTX015/MK-8628.* Cancer Discov, 2016. **6**(5): p. 492-500.

173. Lewin, J., et al., *Phase Ib Trial With Birabresib, a Small-Molecule Inhibitor of Bromodomain and Extraterminal Proteins, in Patients With Selected Advanced Solid Tumors.* Journal of Clinical Oncology, 2018. **36**(30): p. 3007-3014.

174. Piha-Paul, S.A., et al., *First-in-Human Study of Mivebresib (ABBV-075), an Oral Pan-Inhibitor of Bromodomain and Extra Terminal Proteins, in Patients with Relapsed/Refractory Solid Tumors.* Clin Cancer Res, 2019. **25**(21): p. 6309-6319.

175. Piha-Paul, S.A., et al., *Phase 1 Study of Molibresib (GSK525762), a Bromodomain and Extra-Terminal Domain Protein Inhibitor, in NUT Carcinoma and Other Solid Tumors.* JNCI Cancer Spectr, 2020. **4**(2): p. pkz093.

176. Moreno, V., et al., *Phase I study of CC-90010, a reversible, oral BET inhibitor in patients with advanced solid tumors and relapsed/refractory non-Hodgkin's lymphoma.* Ann Oncol, 2020.

177. Hottinger, A.F., et al., *Dose optimization of MK-8628 (OTX015), a small molecule inhibitor of bromodomain and extra-terminal (BET) proteins, in patients (pts) with recurrent glioblastoma (GB).* Journal of Clinical Oncology, 2016. **34**(15): p. e14123-e14123.

178. Postel-Vinay, S., et al., *First-in-human phase I study of the bromodomain and extraterminal motif inhibitor BAY 1238097: emerging pharmacokinetic/pharmacodynamic relationship and early termination due to unexpected toxicity.* Eur J Cancer, 2019. **109**: p. 103-110.

179. Lin, X., et al., *HEXIM1 as a robust pharmacodynamic marker for monitoring target engagement of BET family bromodomain inhibitors in tumors and surrogate tissues.* Mol Cancer Ther, 2017. **16**(2): p. 388-396.

180. Yeh, T.C., et al., *Identification of CCR2 and CD180 as robust pharmacodynamic tumor and blood biomarkers for clinical use with BRD4/BET inhibitors.* Clinical Cancer Research, 2017. **23**(4): p. 1025-1035.

181. Settleman, J., *Bet on drug resistance.* Nature, 2016. **529**(7586): p. 289-290.

182. Rathert, P., et al., *Transcriptional plasticity promotes primary and acquired resistance to BET inhibition.* Nature, 2015. **525**(7570): p. 543-547.

183. Fong, C.Y., et al., *BET inhibitor resistance emerges from leukaemia stem cells.* Nature, 2015. **525**(7570): p. 538-42.

184. Kumar, K., et al., *GLI2-dependent c-MYC upregulation mediates resistance of pancreatic cancer cells to the BET bromodomain inhibitor JQ1.* Scientific Reports, 2015. **5**(1): p. 9489.

185. Shu, S., et al., *Response and resistance to BET bromodomain inhibitors in triple-negative breast cancer.* Nature, 2016. **529**(7586): p. 413-417.

186. Calder, J., et al., *Resistance to BET inhibitors in lung adenocarcinoma is mediated by casein kinase phosphorylation of BRD4.* Oncogenesis, 2021. **10**(3): p. 27.

187. Hogg, S.J., et al., *BET Inhibition Induces Apoptosis in Aggressive B-Cell Lymphoma via Epigenetic Regulation of BCL-2 Family Members.* Mol Cancer Ther, 2016. **15**(9): p. 2030-41.

188. Zhao, Y., et al., *High-Resolution Mapping of RNA Polymerases Identifies Mechanisms of Sensitivity and Resistance to BET Inhibitors in t(8;21) AML.* Cell Rep, 2016. **16**(7): p. 2003-16.

189. Jang, J.E., et al., *AMPK-ULK1-Mediated Autophagy Confers Resistance to BET Inhibitor JQ1 in Acute Myeloid Leukemia Stem Cells.* Clin Cancer Res, 2017. **23**(11): p. 2781-2794.

190. Saenz, D.T., et al., *Mechanistic basis and efficacy of targeting the β-catenin-TCF7L2-JMJD6-c-Myc axis to overcome resistance to BET inhibitors.* Blood, 2020. **135**(15): p. 1255-1269.

191. Bowry, A., et al., *BET Inhibition Induces HEXIM1- and RAD51-Dependent Conflicts between Transcription and Replication.* Cell Rep, 2018. **25**(8): p. 2061-2069.e4.

192. Devaraj, S.G., et al., *HEXIM1 induction is mechanistically involved in mediating anti-AML activity of BET protein bromodomain antagonist.* Leukemia, 2016. **30**(2): p. 504-8.

193. Bady, P., et al., *DNA fingerprinting of glioma cell lines and considerations on similarity measurements.* Neuro Oncol, 2012. **14**(6): p. 701-11.

194. Kurscheid, S., et al., *Chromosome 7 gain and DNA hypermethylation at the HOXA10 locus are associated with expression of a stem cell related HOX-signature in glioblastoma.* Genome Biol, 2015. **16**(1): p. 16.

195. Ishii, N., et al., *Frequent co-alterations of TP53, p16/CDKN2A, p14ARF, PTEN tumor suppressor genes in human glioma cell lines.* Brain Pathol, 1999. **9**(3): p. 469-79.

196. Glousker, G., et al., *Human shelterin protein POT1 prevents severe telomere instability induced by homology-directed DNA repair.* EMBO J, 2020. **39**(23): p. e104500.

197. Kaina, B., et al., *Transfection and expression of human O6-methylguanine-DNA methyltransferase (MGMT) cDNA in Chinese hamster cells: the role of MGMT in protection against the genotoxic effects of alkylating agents.* Carcinogenesis, 1991. **12**(10): p. 1857-67.

198. Barretina, J., et al., *The Cancer Cell Line Encyclopedia enables predictive modelling of anticancer drug sensitivity.* Nature, 2012. **483**(7391): p. 603-7.

199. Doroshow, D.B., J.P. Eder, and P.M. LoRusso, *BET inhibitors: a novel epigenetic approach.* Ann Oncol, 2017. **28**(8): p. 1776-1787.

200. Puissant, A., et al., *Targeting MYCN in neuroblastoma by BET bromodomain inhibition.* Cancer Discov, 2013. **3**(3): p. 308-23.

201. Chapuy, B., et al., *Discovery and characterization of super-enhancer-associated dependencies in diffuse large B cell lymphoma.* Cancer Cell, 2013. **24**(6): p. 777-90.

202. KUO, L.J. and L.-X. YANG, *γ-H2AX - A novel biomarker for DNA double-strand breaks.* In Vivo, 2008. **22**(3): p. 305-309.

203. Hermisson, M., et al., *O6-methylguanine DNA methyltransferase and p53 status predict temozolomide sensitivity in human malignant glioma cells.* J Neurochem, 2006. **96**(3): p. 766-76.

204. Happold, C., et al., *Distinct molecular mechanisms of acquired resistance to temozolomide in glioblastoma cells.* J Neurochem, 2012. **122**(2): p. 444-55.

205. St-Coeur, P.D., et al., *Investigating a signature of temozolomide resistance in GBM cell lines using metabolomics.* J Neurooncol, 2015. **125**(1): p. 91-102.

206. Creyghton, M.P., et al., *Histone H3K27ac separates active from poised enhancers and predicts developmental state.* Proceedings of the National Academy of Sciences, 2010. **107**(50): p. 21931-21936.

207. Balvers, R.K., et al., *Serum-free culture success of glial tumors is related to specific molecular profiles and expression of extracellular matrix-associated gene modules.* Neuro Oncol, 2013. **15**(12): p. 1684-95.

208. Suva, M.L., et al., *Reconstructing and Reprogramming the Tumor-Propagating Potential of Glioblastoma Stem-like Cells.* Cell, 2014. **9**(14): p. 00229-3.

209. Hegi, M.E., et al., *MGMT Promoter methylation cutoff with safety margin for selecting glioblastoma patients into trials omitting temozolomide. A pooled analysis of four clinical trials.* Clin Cancer Res, 2019. **25**(6): p. 1809-1816.

6. SUPPLEMENTARY DATA

Table 1 qPCR primers

Gene	Forward primer (5'-3')	Reverse primer (5'-3')
GAPDH	AGGTGAAGGTCGGAGTCAACG	CGTTCTCAGCCTTGACGGTG
HEXIM1	AAGGACTAGCTAAAGGCGTCAC	TGGCTAGTAGAGTCCTCGAAGTTT
MGMT	GCTGCGGTTCTCGGAGGTC	CTGCCAGGGCTGCTAATTGC
MSH6	CACCAGGAGATTTGGTTTGG	TGTTGGGCTGTCATCAAAAA
MSH2	GACCGGGGCGACTTCTATAC	GCCCCATGTACTTGATCACC

Table 2 ChIP-qPCR primers

Gene	Forward primer (5'-3')	Reverse primer (5'-3')
MGMT_F2	AAAAGGTACGGGCCATTTG	CAGTCTGCGCATCCTCG
MGMT_F3	GCGCTCTCTTGCTTTTCTCA	GACACTCACCAAGTCGCAAA
H19	Undisclosed – Diagenode Kit	Undisclosed – Diagenode Kit
Myoglobin exon 2	Undisclosed – Diagenode Kit	Undisclosed – Diagenode Kit

A

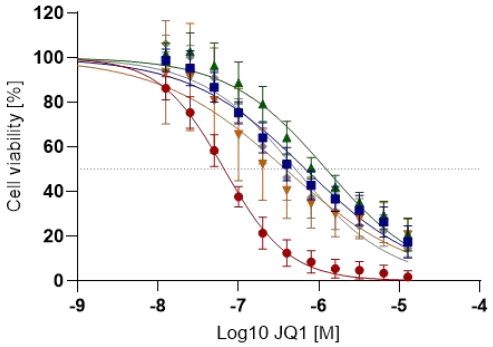

GBM line	JQ1 IC_{50}
LN-18	66nM
T98G	684nM
LN-340	1'234nM
LN-382	384nM
LN-229	514nM

B

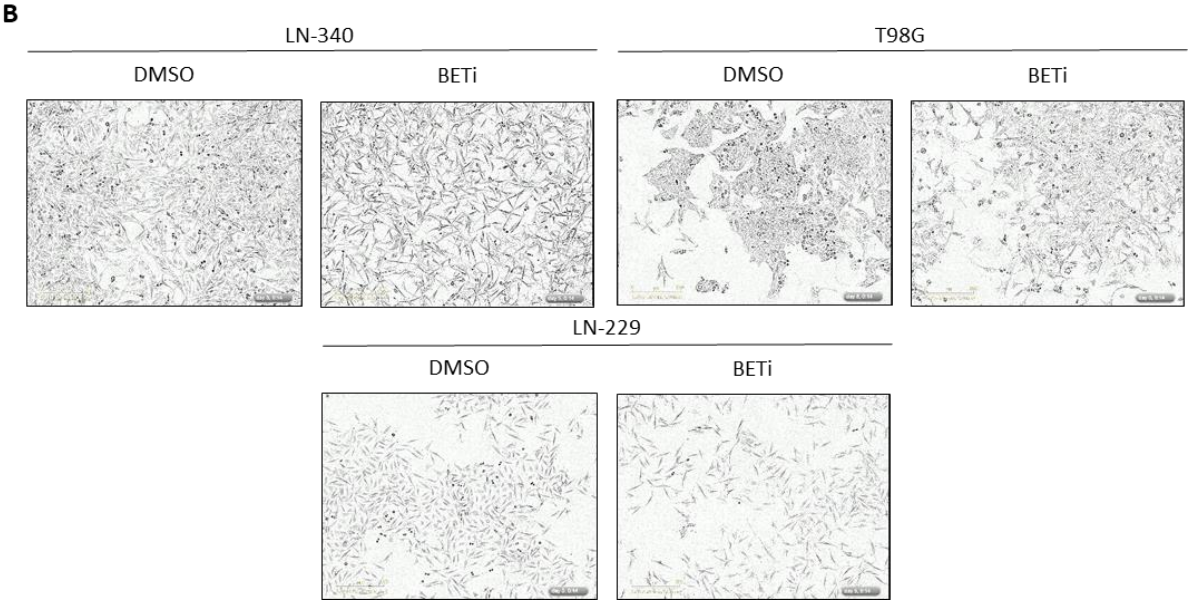

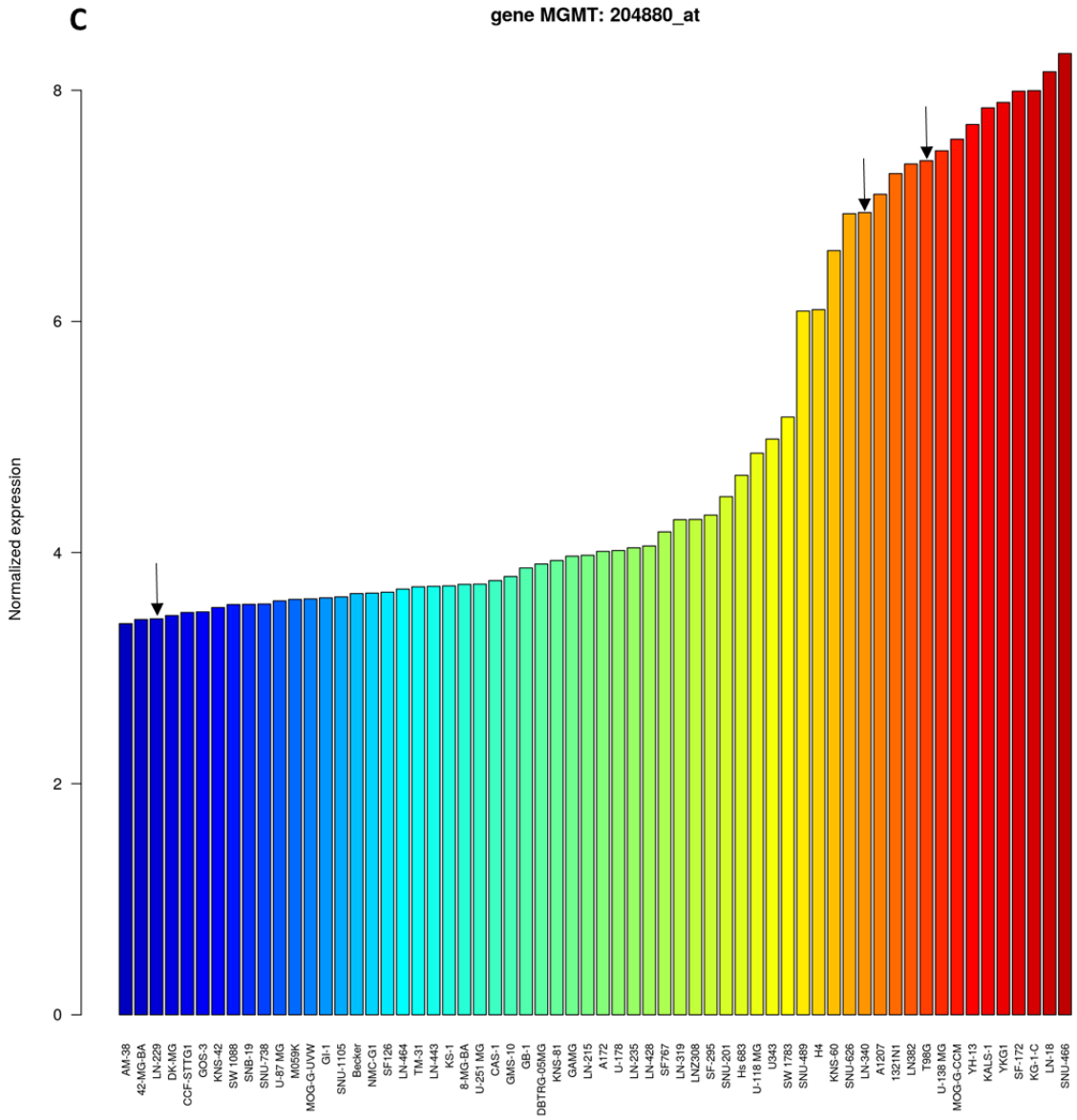
C
gene MGMT: 204880_at
Normalized expression
0
2
4
6
8
AM-38
42-MG-BA
LN-229
DK-MG
CCF-STTG1
GOS-3
KNS-42
SW 1088
SNB-19
SNU-738
U-87 MG
M059K
MOG-G-UVW
GI-1
SNU-1105
Becker
NMC-G1
SF126
LN-464
TM-31
LN-443
KS-1
8-MG-BA
U-251 MG
CAS-1
GMS-10
GB-1
DBTRG-05MG
KNS-81
GAMG
LN-215
A172
U-178
LN-235
LN-428
SF767
LN-319
LNZ308
SF-295
SNU-201
Hs 683
U-118 MG
U343
SW 1783
SNU-489
H4
KNS-60
SNU-626
LN-340
A1207
1321N1
LN382
T98G
U-138 MG
MOG-G-CCM
YH-13
KALS-1
YKG1
SF-172
KG-1-C
LN-18
SNU-466

D

LN-340

Time [hours]	24				48				72				120			
JQ1 [µM]	0	0.25	0.5	1	0	0.25	0.5	1	0	0.25	0.5	1	0	0.25	0.5	1
MGMT 24 [kDa]	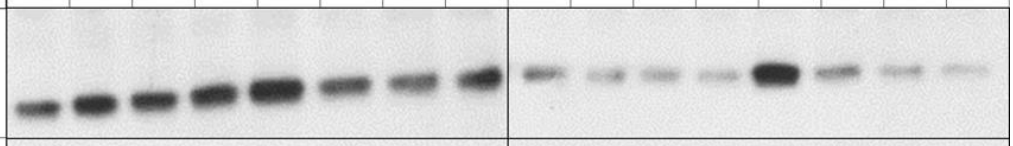															
β-Actin 45 [kDa]	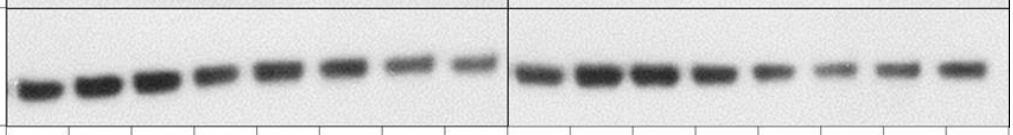															
Ratio	1	1.04	0.82	1.09	1	0.41	0.48	1.09	1	0.25	0.14	0.03	1	0.31	0.17	0.08

T98G

Time [hours]	24				48				72				120			
JQ1 [µM]	0	0.25	0.5	1	0	0.25	0.5	1	0	0.25	0.5	1	0	0.25	0.5	1
MGMT 24 [kDa]	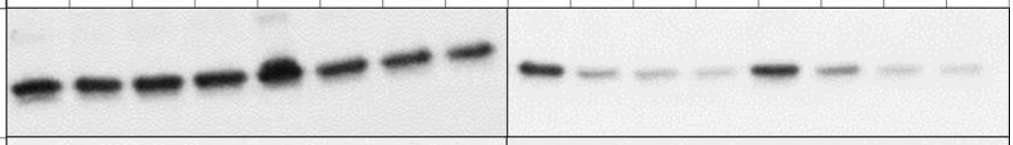															
β-Actin 45 [kDa]	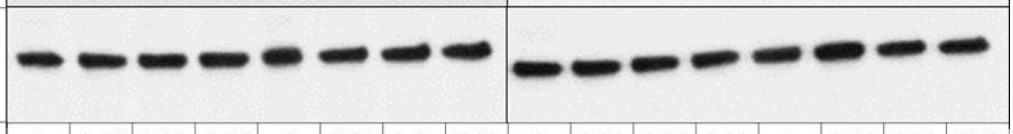															
Ratio	1	0.78	0.86	0.80	1	0.65	0.61	0.53	1	0.39	0.34	0.23	1	0.34	0.23	0.18

GSC-23luc

Time [hours]	24				48				72				120			
JQ1 [µM]	0	0.25	0.5	1	0	0.25	0.5	1	0	0.25	0.5	1	0	0.25	0.5	1
MGMT 24 [kDa]	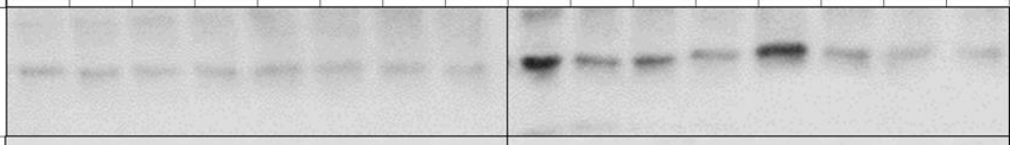															
β-Actin 45 [kDa]	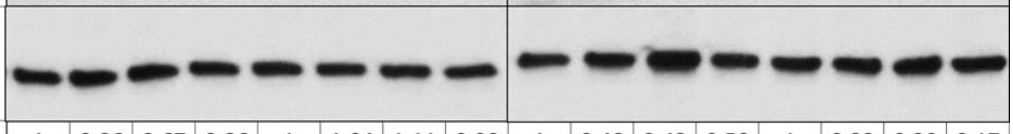															
Ratio	1	0.86	0.67	0.86	1	1.04	1.11	0.90	1	0.48	0.43	0.50	1	0.33	0.20	0.17

LN-2683GS

Time [hours]	24				48				72				120			
JQ1 [µM]	0	0.25	0.5	1	0	0.25	0.5	1	0	0.25	0.5	1	0	0.25	0.5	1
MGMT 24 [kDa]	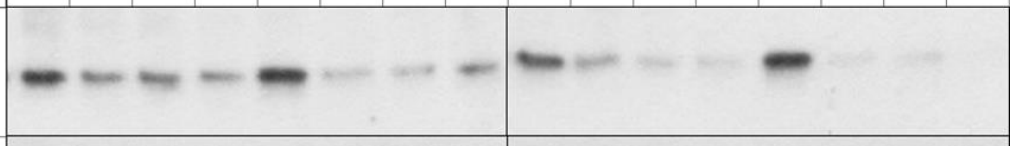															
α-Tubulin 52 [kDa]																
Ratio	1	0.84	1.18	0.49	1	0.31	0.38	0.37	1	0.35	0.27	0.25	1	0.16	0.30	0.04

E

GSC-23luc

Time [hours]	24				48				72				120			
TMZ 100 [µM]	-	-	+	+	-	-	+	+	-	-	+	+	-	-	+	+
JQ1 250 [nM]	-	+	-	+	-	+	-	+	-	+	-	+	-	+	-	+
MGMT 24 [kDa]																
β-Actin 45 [kDa]																
Ratio	1	1.22	0.58	0.36	1	0.86	0.52	0.40	1	0.80	0.61	0.29	1	0.38	1.50	0.69

LN-2683GS

Time [hours]	24				48				72				120			
TMZ 100 [µM]	-	-	+	+	-	-	+	+	-	-	+	+	-	-	+	+
JQ1 1000 [nM]	-	+	-	+	-	+	-	+	-	+	-	+	-	+	-	+
MGMT 24 [kDa]																
α-Tubulin 52 [kDa]																
Ratio	1	0.54	1.07	1.02	1	0.43	0.25	0.13	1	0.52	0.39	0.30	1	0.90	1.45	0.32

LN-4372GS

Time [hours]	24				48				72				120			
TMZ 100 [µM]	-	-	+	+	-	-	+	+	-	-	+	+	-	-	+	+
JQ1 1000 [nM]	-	+	-	+	-	+	-	+	-	+	-	+	-	+	-	+
MGMT 24 [kDa]																
α-Tubulin 52 [kDa]																
Ratio	1	0.59	0.21	0.11	1	0.41	0.38	0.22	1	0.31	1.21	0.40	1	0.15	0.65	0.08

Figure S3. 1 BET protein inhibition reduces MGMT expression and halts its induction upon temozolomide treatment. (A) IC_{50} was calculated from a panel of GBM lines were treated with JQ1 for 72 hours making a 2-point fold dilution starting from a concentration of 12.8µM. Data represent mean of 3 independent biological replicates. Data was normalized to DMSO. Error bars are SD. (B) Visual representation of morphological changes for 3 GBM lines treated with JQ1 for 5 days. LN-340 cells were treated at 250nM, whereas T98G and LN-229 were treated at 100nM. (C) Normalized *MGMT* expression across GBM lines. (D) MGMT protein expression upon multiple JQ1 concentrations over 5 days in adherent lines LN-340 and T98G, as well as patient-derived lines GSC-23luc and LN-2683GS. Protein expression analysis was performed via Western Blot using β-actin or α-Tubulin as housekeeping. (E) MGMT protein modulation upon BETi alone or in combination with TMZ in patient-derived GBM lines. Protein expression analysis was performed via Western Blot using β-Actin or α-Tubulin as housekeeping.

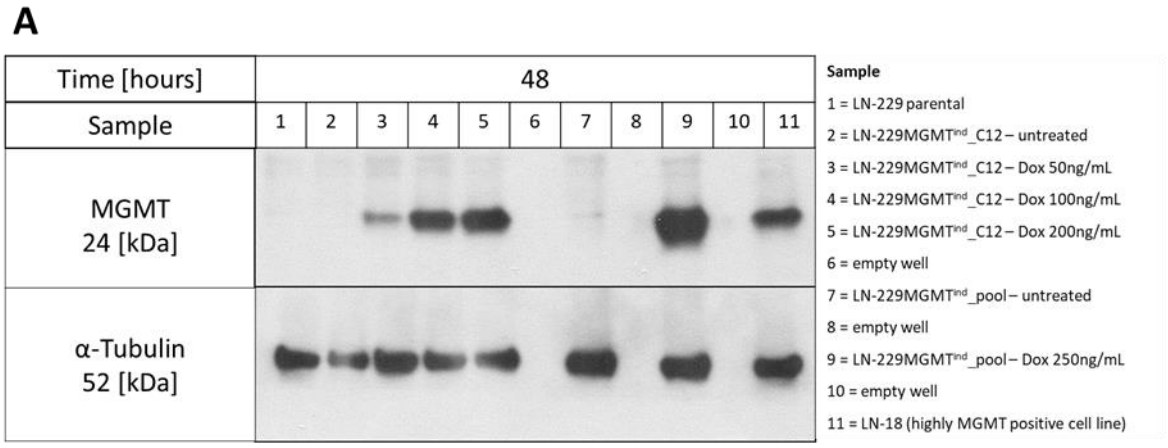

Figure S3. 2 Doxycycline (dox)-inducible Tet-On system for MGMT in LN-229. (A) Parental LN-229, LN-229MGMT^{ind}_pool and LN-229MGMT^{ind}_C12 were treated for 48H with different doses of doxycycline. Protein expression analysis was performed via Western Blot using α-Tubulin as house-keeping.

A

GSC-23luc

Time [hours]	24				48				72				120			
TMZ 100 [µM]	-	-	+	+	-	-	+	+	-	-	+	+	-	-	+	+
JQ1 250 [nM]	-	+	-	+	-	+	-	+	-	+	-	+	-	+	-	+
MSH6 160 [kDa]																
MSH2 120 [kDa]																
β-Actin 45 [kDa]																
Ratio MSH6	1	0.93	1.36	1.32	1	0.77	0.78	0.54	1	1.35	0.78	0.79	1	1.1	0.80	1.07
Ratio MSH2	1	0.87	1.20	1.15	1	0.93	1.02	1.04	1	1.12	0.71	0.78	1	1.14	0.92	1.76

B

Time [hours]	48					
LN-340shRNA^{ind}	shCTRL^{ind}		shMSH6#1_C8		shMSH6#2	
Dox 500 [ng/mL]	-	+	-	+	-	+
MSH6 160 [kDa]						
β-Actin 45 [kDa]						
Ratio	1.00	0.93	1.00	0.39	1.00	0.38

Figure S3. 3 BET protein inhibition does not compromise the MMR system in GBM. (A) MSH6 and MSH2 protein modulation upon BETi alone or in combination with TMZ in patient-derived GBM line GSC-23luc. Protein expression analysis was performed via Western Blot using β-Actin as housekeeping. (B) Doxycycline (dox)-inducible Tet-On system shRNA system targeting MSH6 and a non-targeting shRNA validation. Protein expression analysis was performed via Western Blot using β-Actin as housekeeping.